

Liquid-Liquid Extraction Operations and Equipment

Lanny A. Robbins, Ph.D., *Research Fellow, Dow Chemical Company; Member, American Institute of Chemical Engineers*

Roger W. Cusack, Vice President, *Glitsch Process Systems, Inc.; Member, American Institute of Chemical Engineers*

LIQUID-LIQUID EXTRACTION OPERATIONS

Uses for Liquid-Liquid Extraction	15-4
Definitions	15-5

PHASE EQUILIBRIA

Equilibrium Partition Ratios	15-6
Phase Diagrams	15-6
Thermodynamic Basis of Liquid-Liquid Equilibria	15-8
Example 1: Partition Ratios	15-8
Hydrogen-Bonding Interactions	15-8
Experimental Equilibrium Data	15-9
Desirable Solvent Properties	15-9

CALCULATION METHODS

Single Stage	15-16
Crosscurrent Theoretical Stages	15-16
Countercurrent Theoretical Stages	15-16
Right-Triangular Method	15-16
Example 2: Stage and Composition Calculation	15-17
Shortcut Methods	15-17
Example 3: Shortcut Calculation, Case A	15-18
Example 4: Shortcut Calculation, Case B	15-19
Countercurrent Mass-Transfer-Unit Calculations	15-19
Example 5: Number of Transfer Units	15-20
Stage Efficiency and Height of a Theoretical Stage or Transfer Unit	15-20
Fractionation Stages	15-20
Countercurrent Liquid-Liquid Heat Transfer	15-22

LIQUID-LIQUID EXTRACTION EQUIPMENT

Stagewise Equipment (Mixer-Settlers)	15-22
--	-------

Rates of Mass Transfer	15-22
Continuous-Phase Coefficients	15-22
Dispersed-Phase Coefficients	15-23
Overall Coefficients and Stage Efficiency	15-23
Scale-Up of Mixers	15-24
Settlers	15-25
Emulsions and Dispersions	15-25
Sedimentation	15-26
Coalescence	15-26
Gravity Settlers; Decanters	15-26
Cyclones	15-27
Centrifuges	15-27
Settler Auxiliaries	15-27
Coalescers	15-27
Separating Membranes	15-27
Electrical Devices	15-28
Mixer-Settler Combinations	15-28
Overall Stage Efficiencies	15-29
Continuous (Differential) Contact Equipment	15-29
General Characteristics	15-30
Axial Dispersion	15-30
Equipment Classification	15-30
Spray Towers	15-30
Packed Towers	15-32
Perforated-Plate (Sieve-Plate) Towers	15-34
Mechanically Agitated Gravity Devices	15-37
Rotary-Disk Contactors (RDC)	15-37
Lightnin Mixer (Oldshue-Rushton) Tower	15-38
Scheibel Extraction Towers	15-40
Kühni Tower	15-42
Treybal Tower	15-42
Karr Reciprocating Plate Tower	15-42
Pulsed Columns	15-44
Centrifugal Extractors	15-46

Nomenclature

Symbol	Definition	SI units	U.S. customary units	Symbol	Definition	SI units	U.S. customary units
A°	Activity of solute	—	—	H_{to}	Overall height of a transfer unit	m	ft
A_p	Area of a drop	m ²	ft ²	HETS	Height equivalent to a theoretical stage	m	ft
A_t	Cross-sectional area of tower	m ²	ft ²	h	Head loss due to friction	m	ft
a	Specific interfacial surface between liquids	m ² /m ³	ft ² /ft ³	A°	Activity of solute	—	—
a_p	Specific packing surface	m ² /m ³	ft ² /ft ³	h_C	Contribution to h due to continuous phase	m	ft
B	Ratio of total length to characteristic length			h_D	Contribution to h due to dispersed phase	m	ft
b	Constant			h_o	Contribution to h_D due to orifice	m	ft
C	Constant			h_σ	Contribution to h_D due to interfacial tension	m	ft
C_O	Orifice coefficient	Dimensionless	Dimensionless	K	Overall mass-transfer coefficient	kmol/(s·m ²) (kmol/m ³)	(lb·mol)/(h·ft ²) [(lb·mol)/ft ³]
c	Concentration	kmol/m ³	(lb·mol)/ft ³	K	Partition coefficient in weight fractions	Dimensionless	Dimensionless
c_p	Heat capacity			K°	Partition coefficient in mole fractions	Dimensionless	Dimensionless
D	Solute diffusivity	m ² /s	ft ² /h	K'	Partition coefficient in Bancroft (weight-ratio) coordinates	Dimensionless	Dimensionless
D'	Enhanced diffusivity	m ² /s	ft ² /h	K_C	Mass transfer coefficient for overall driving force in continuous phase concentration units	kmol/(s·m ²) (kmol/m ³)	(lb·mol)/(h·ft ²) [(lb·mol)/ft ³]
d	Differential operator			K_D	Mass transfer coefficient for overall driving force in dispersed phase concentration units	kmol/(s·m ²) (kmol/m ³)	(lb·mol)/(h·ft ²) [(lb·mol)/ft ³]
d_F	Packing size	m	ft	k	Individual-phase mass-transfer coefficient	kmol/(s·m ²) (kmol/m ³)	(lb·mol)/(h·ft ²) [(lb·mol)/ft ³]
d_{FC}	Critical packing size	m	ft	k_t	Thermal conductivity	W/(m·K)	Btu/[h·ft ² ·°F/ft]
d_i	Impeller diameter	m	ft	L	Superficial mass velocity	kg/(s·m ²)	lbm/(h·ft ²)
d_O	Nozzle, perforation, orifice diameter	m	ft	L'	Superficial molar mass velocity	kmol/(s·m ²)	(lb·mol)/(h·ft ²)
d_p	Drop diameter, diameter of sphere of same volume per surface	m	ft	m	Slope of equilibrium distribution curve, dy/dx		
d_{pj}	Drop diameter at jetting if no jet forms	m	ft	m	Slope of equilibrium line in Bancroft coordinates	Dimensionless	Dimensionless
d_r	Diameter of rotor	m	ft	m^*	Slope of equilibrium line in mole fractions	Dimensionless	Dimensionless
d_s	Diameter of stator-ring opening	m	ft	m_{CD}	Slope of equilibrium line continuous/dispersed phase	Dimensionless	Dimensionless
d_t	Tube or tank diameter	m	ft	m'	Slope of equilibrium distribution curve, dc_E/dc_R	(kmol/m ³)/(kmol/m ³)	[(lb·mol)/ft ³]/[(lb·mol)/ft ³]
E	Weight (or mass flow rate) of extract	kg (or kg/s)	lb (or lb/h)	m'	Slope of equilibrium line in concentration, c, units	Dimensionless	Dimensionless
E'	Weight (or mass flow rate) of extraction solvent alone in extract	kg (or kg/s)	lb (or lb/h)	m'_{CD}	Slope of equilibrium curve, dc_C/dc_D	(kmol/m ³)/(kmol/m ³)	[(lb·mol)/ft ³]/[(lb·mol)/ft ³]
E_f	Fractional efficiency of a single stage (mixer-settlers)			N_s	Impeller speed	r/s	r/h
E_d	Longitudinal dispersion coefficient (differential extractors)	m ² /s	ft ² /h	N_f	Flux of mass transfer	kmol/(s·m ²)	(lb·mol)/(h·ft ²)
E_{MD}	Murphree dispersed-phase stage efficiency, fractional			N_{oh}	Number of heat transfer units based on hot phase	Dimensionless	Dimensionless
E_O	Overall stage efficiency of a cascade, fractional			N_{or}	Number of mass transfer units based on overall driving force in raffinate concentration	Dimensionless	Dimensionless
e	2.7183 (napierian logarithm base)			N_{Pe}	Péclet number for axial dispersion, Vd_F/E_d for packing	Dimensionless	Dimensionless
e	Extraction factor (slope of equilibrium line/slope of operating line)			N_{Po}	Power number, $P_g/\rho N^3 d_i^5$	Dimensionless	Dimensionless
F	Weight (or mass flow rate) of feed	kg (or kg/s)	lb (or lb/h)	N_{Re}	Reynolds number; for pipe flow, $d_i V \rho_{av}/u_{av}$; for an impeller, $d_i^2 N \rho_{av}/u_{av}$; for drops, $d_p V_i u_c/\rho c$	Dimensionless	Dimensionless
F'	Weight (or mass flow rate) of feed solvent alone in feed	kg (or kg/s)	lb (or lb/h)				
f_e	Weighting factor						
f_r	Weighting factor						
g	Local acceleration due to gravity	9.83 m/s ²	4.18 E08 ft/h ²				
g_c	Gravitational conversion factor	1(kg·m)/(N·s)	4.18 E08 (lbm·ft)/(lbf·h ²)				
H_e	Height of a transfer unit attributed to driving force in extract phase	m	ft				
H_{or}	Height of a transfer unit based on overall driving force in raffinate concentrations	m	ft				
H_r	Height of a transfer unit attributed to driving force in raffinate phase	m	ft				

Nomenclature (Concluded)

Symbol	Definition	SI units	U.S. customary units	Symbol	Definition	SI units	U.S. customary units
N_{Sc}	Schmidt number, $u/\rho D$	Dimensionless	Dimensionless	Z_H	Height of the heavy phase in decanter	m	ft
N_{to}	Number of overall transfer units	Dimensionless	Dimensionless	Z_i	Height of the interface in decanter	ft m	
$N_{We,f}$	Impeller Weber number, $\rho d_i^3 N^2 / \sigma g_c$	Dimensionless	Dimensionless	Z_L	Height of the light phase in decanter	m	ft
$N_{We,t}$	Pipe Weber number, $\rho d_i V^2 / \sigma g_c$	Dimensionless	Dimensionless	Z_t	Distance between trays	m	ft
NTS	Number of theoretical i (equilibrium) stages	Dimensionless	Dimensionless	Z'_t	Distance between trays	m	in
n	Number of orifices or perforations per plate			z	Distance	m	ft
n_d	Number of drops			z	Weight-fraction solute in mixture	Dimensionless	Dimensionless
P	Power for one real stage	W	(ft·lbf)/h	Greek symbols			
Q	Total flow rate	m ³ /s	ft ³ /h	α	Relative separation factor (selectivity)		
R	Weight (or mass flow rate) of raffinate	kg (or kg/s)	lb (or lb/h)	γ	Activity coefficient of solute		
R'	Weight (or mass flow rate) of feed solvent alone in raffinate	kg (or kg/s)	lb (or lb/h)	Δ	Delta (or difference) mixture		
S	Weight (or mass flow rate) of extraction-solvent stream	kg (or kg/s)	lb (or lb/h)	Δp	Pressure drop	Pa	lbf/ft ²
S'	Weight (or mass flow rate) of extraction-solvent alone	kg (or kg/s)	lb (or lb/h)	$\Delta \rho$	Difference in density	kg/m ³	lbm/ft ³
SPM	Reciprocating speed, strokes/minute			δ	Dimensionless amplitude for oscillating drops		
T	Diameter of mixing vessel or extraction tower	m	ft	ϵ	Fraction void volume in packed section		
T	Temperature in hot (raffinate) phase			θ	Time of contact	s	h
t	Temperature in cold (extract) phase			θ_C	Time between coalescences	s	h
U_o	Overall heat-transfer coefficient	W/(m ² ·K)	Btu/(h·ft ² ·°F)	θ_F	Time of drop formation	s	h
V	Superficial velocity	m/s = m ³ /(s·m ²)	ft/h = ft ³ /(h·ft ²)	λ	Eigenvalue		
V_d	Velocity in a down spout	m/s	ft/h	μ	Viscosity	Pa·s	lbm/(ft·h)
V_K	Characteristic velocity	m/s	ft/h	μ'	Viscosity	Pa·s	cP
V_O	Velocity through an orifice or nozzle	m/s	ft/h	ν	Coalescence frequency, fraction of drops coalescing per time	L/s	L/h
V'_O	Velocity through an orifice or nozzle	m/s	ft/h	π	3.1416		
V'_{Oj}	Jetting velocity	m/s	ft/h	ρ	Density	kg/m ³	lbm/ft ³
V_s	Slip velocity	m/s	ft/h	Σ	Summation		
V_t	Terminal settling velocity	m/s	ft/h	σ	Interfacial tension	N/m	lbf/ft
v	Liquid volume	m ³	ft ³	σ'	Interfacial tension	N/m	dyn/cm
v_p	Drop volume	m ³	ft ³	ϕ	Volume fraction of a liquid in a vessel or extractor's void volume		
W	Weight (or mass flow rate) of wash phase or stream	kg (or kg/s)	lb (or lb/h)	ω	Vibration frequency for oscillating drops	L/s	L/h
W'	Weight (or mass flow rate) of wash solvent alone	kg (or kg/s)	lb (or lb/h)	Additional subscripts			
X	Weight solute/weight feed solvent in feed (raffinate) phase	Dimensionless	Dimensionless	av	Average		
x	Weight-fraction solute in feed (raffinate) phase	Dimensionless	Dimensionless	C	Continuous phase		
x°	Mole-fraction solute in feed (raffinate) phase	Dimensionless	Dimensionless	D	Dispersed phase		
Y	Weight solute/weight extraction solvent in extract	Dimensionless	Dimensionless	E	Extract		
y	Weight-fraction solute in extract phase	Dimensionless	Dimensionless	e	Extract phase or stream		
y°	Mole-fraction solute in extract phase	Dimensionless	Dimensionless	F	Flooding		
Z	Height of liquid in vessel or mixer; for towers, height of packed section	m	ft	f	Feed phase or stream		
				H	Heavy liquid		
				L	Light liquid		
				M	Mixture		
				max	Maximum		
				o	Organic		
				plug	Plug flow		
				R	Raffinate		
				r	Raffinate phase or stream		
				s	Extraction solvent phase or stream		
				w	Water or aqueous liquid		
				1,2,etc.	Stream leaving stage 1,2,etc.		
				1	Concentrated end		
				2	Dilute end		

GENERAL REFERENCES: Foust, Wenzel, Clump, Maus, and Anderson, *Principles of Unit Operations*, 2d ed., Wiley, New York, 1980. Schweitzer (ed.), *Handbook of Separation Techniques for Chemical Engineers*, 2d ed., McGraw-Hill, New York, 1988. Sorenson and Arlt, "Liquid-Liquid Equilibrium Data Collection," DECHEMA, Frankfurt, Germany, *Binary Systems* vol V, part 1, 1979, *Ternary Systems* vol V, part 2, 1980, *Ternary & Quaternary Systems*, vol 5, part 3, 1980, Macedo and Rasmussen, *Supplement 1*, vol V, part 4, 1987. Treybal, *Liquid Extraction*, 2d ed., McGraw-Hill, New York, 1963. Treybal, *Mass-Transfer Operations*, 3d ed., McGraw-Hill, New York, 1980. Wisniak and Tamir, *Liquid-Liquid Equilibrium and Extraction: A Literature Source Book*, part A, Elsevier, Amsterdam, 1981. Lo, Baird, and Hanson, *Handbook of Solvent Extraction*, Wiley, New York, 1983. Astarita, *Mass Transfer with Chemical Reactions*, Elsevier, New York, 1967. Calderbank, "Mass Transfer," in Uhl and Gray (eds.), *Mixing*, vol. 2, Academic, New York, 1967. Cremer and Davies, *Chemical Engineering Practice*, vol. 5, Academic, New York, 1958. Davies, "Mass Transfer and Interfacial Phenomena," in Drew, Hoopes, and Vermeulen (eds.), *Advances in Chemical Engineering*, vol. 4, Academic, New York, 1963. Hanson (ed.), *Recent Advances in Liquid-Liquid Extraction*, Pergamon, New York, 1971. Hyman, *Mixing and Agitation*, *ibid.*, vol. 3, 1962. Kalichevsky and Kobe, *Petroleum Refining with Chemicals*, Van Nostrand, Princeton, N.J., 1965. Kintner,

"Drop Phenomena Affecting Liquid Extraction," in Drew et al. (eds.), *Advances in Chemical Engineering*, vol. 4, Academic, New York, 1963. Molyneux, *Chemical Plant Design*, vol. 1, Butterworth, Washington, 1965. Olney and Miller, "Liquid Extraction," in Acrivos (ed.) *Modern Chemical Engineering*, vol 1, Reinhold, New York, 1963. Olson and Stout, "Mixing and Chemical Reactions," in Uhl and Gray (eds.), *Mixing*, vol. 2, Academic, New York, 1967. Reitma, "Segregation in Liquid-Liquid Dispersions," in Drew et al. (eds.), *Advances in Chemical Engineering*, vol. 5, Academic, New York, 1964. Rod, Misek, and Sterbacek, *Liquid Extraction*, Statne Nakladatelstvi Techniki Literatury, Prague, 1964. Sideman, "Direct-Contact Heat Transfer between Immiscible Liquids," in Drew et al. (eds.), *Advances in Chemical Engineering*, vol. 6, Academic, New York, 1966. Treybal, *Mechanically Aided Liquid Extraction*, *ibid.*, vol. 1, 1956. Ziolkowski, *Liquid Extraction in the Chemical Industry*, Gos. Nauchn. Tekhn. Izd. Khim. Lit, Leningrad, 1963. Cusack, Fremeaux, and Glatz, "A Fresh Look at Liquid-Liquid Extraction," part 1, *Extraction Systems, Chemical Engineering*, vol. 98, no. 2, p. 66-67, Feb. 1991. Cusack, and Fremeaux, part 2, "Inside the Extractor," *Chemical Engineering*, vol. 98, no. 3, p. 132-138, Mar. 1991. Cusack and Karr, part 3, "Extractor Design and Specification," *Chemical Engineering*, vol. 98, no. 4, p. 112-120, Apr. 1991.

LIQUID-LIQUID EXTRACTION OPERATIONS

Liquid-liquid extraction is a process for separating components in solution by their distribution between two immiscible liquid phases. Such a process can also be simply referred to as **liquid extraction** or **solvent extraction**; however, the latter term may be confusing because it also applies to the leaching of a soluble substance from a solid.

Since liquid-liquid extraction involves the transfer of mass from one liquid phase into a second immiscible liquid phase, the process can be carried out in many different ways. The simplest example involves the transfer of one component from a binary mixture into a second immiscible liquid phase. One example is liquid-liquid extraction of an impurity from wastewater into an organic solvent. This is analogous to stripping or absorption in which mass is transferred from one phase to another. Transfer of the dissolved component (solute) may be enhanced by the addition of "salting out" agents to the feed mixture or by adding "complexing" agents to the extraction solvent. Or in some cases a chemical reaction can be used to enhance the transfer, an example being the use of an aqueous caustic solution to remove phenolics from a hydrocarbon stream. A more sophisticated concept of liquid-liquid fractionation can be used in a process to separate two solutes completely. A primary extraction solvent is used to extract one of the solutes from a mixture (similar to stripping in distillation), and a wash solvent is used to scrub the extract free from the second solute (similar to rectification in distillation).

USES FOR LIQUID-LIQUID EXTRACTION

Liquid-liquid extraction is used primarily when distillation is impractical or too costly to use. It may be more practical than distillation when the relative volatility for two components falls between 1.0 and 1.2. Likewise, liquid-liquid extraction may be more economical than distillation or steam-stripping a dissolved impurity from wastewater when the relative volatility of the solute to water is less than 4. In one case discussed by Robbins [*Chem. Eng. Prog.*, **76** (10), 58 (1980)], liquid-liquid extraction was economically more attractive than carbon-bed or resin-bed adsorption as a pretreatment process for wastewater detoxification before biotreatment.

In other cases the components to be separated may be heat-

sensitive, like antibiotics, or relatively nonvolatile, like mineral salts, and liquid-liquid extraction may provide the most cost-effective separation process. However, the potential use of distillation should generally be evaluated carefully before considering liquid-liquid extraction. An extraction process usually requires (1) liquid-liquid extraction, (2) solvent recovery, and (3) raffinate desolventizing.

Several examples of cost-effective liquid-liquid extraction processes include the recovery of acetic acid from water (Fig. 15-1), using ethyl ether or ethyl acetate as described by Brown [*Chem. Eng. Prog.*, **59**(10), 65 (1963)], or the recovery of phenolics from water as described by Lauer, Littlewood, and Butler [*Iron Steel Eng.*, **46**(5), 99 (1969)] with butyl acetate, or with isopropyl ether as described by Wurm [*Glückauf*, **12**, 517 (1968)], or with methyl isobutyl ketone as described by Scheibel ["Liquid-Liquid Extraction," in Perry & Weiss-

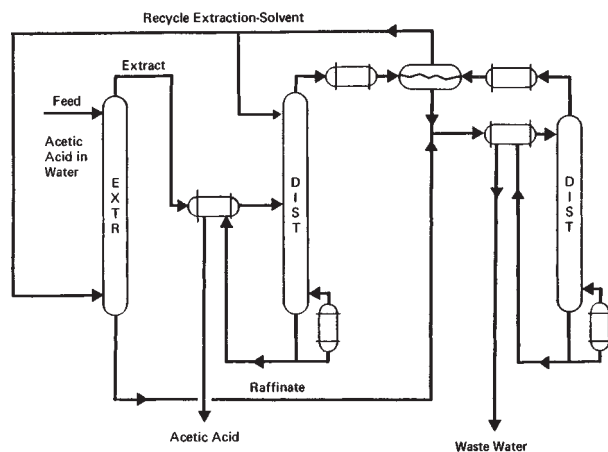


FIG. 15-1 Solvent extraction of acetic acid from water.

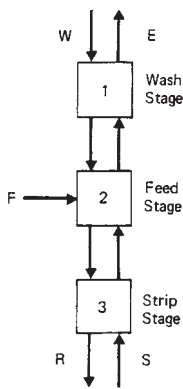


FIG. 15-6 Liquid-liquid fractionation.

W scrubs the extract free from the unwanted second solute. The second solute leaves the contactor in the raffinate stream.

Dissociation extraction is the process of using chemical reaction to force a solute to transfer from one liquid phase to another. One example is the use of a sodium hydroxide solution to extract phenolics, acids, or mercaptans from a hydrocarbon stream. The opposite transfer can be forced by adding an acid to a sodium phenate stream to **spring** the phenolic back to a **free phenol** that can be extracted into an organic solvent. Similarly, primary, secondary, and tertiary amines can be protonated with a strong acid to transfer the amine into a water solution, for example, as an amine hydrochloride salt. Conversely, a strong base can be added to convert the amine salt back to **free base**, which can be extracted into a solvent. This procedure is quite common in pharmaceutical production.

Fractionation dissociation extraction involves both the chemical reaction and the fractionation scheme for the separation of components by their difference in dissociation constants as described by Colby [in Hanson (ed.), *Recent Advances in Liquid-Liquid Extraction*, Pergamon, New York, 1971, chap. 4].

PHASE EQUILIBRIA

The separation of components by liquid-liquid extraction depends primarily on the thermodynamic equilibrium partition of those components between the two liquid phases. Knowledge of these partition relationships is essential for selecting the ratio of extraction solvent to feed that enters an extraction process and for evaluating the mass-transfer rates or theoretical stage efficiencies achieved in process equipment. Since two liquid phases that are immiscible are used, the thermodynamic equilibrium involves considerable evaluation of non-ideal solutions. In the simplest case a feed solvent *F* contains a solute that is to be transferred into an extraction solvent *S*.

EQUILIBRIUM PARTITION RATIOS

The weight fraction of solute in the extract phase *y* divided by the weight fraction of solute in the raffinate phase *x* at equilibrium is called the partition ratio, *K* [Eq. (15-1)].

$$K = y/x \tag{15-1}$$

Thermodynamically the partition ratio *K*^o is derived in mole fractions *y*^o and *x*^o [Eq. (15-2)].

$$K^o = y^o/x^o \tag{15-2}$$

For shortcut calculations the partition ratio *K'* in Bancroft [*Phys. Rev.*, **3**, 120 (1895)] coordinates using the weight ratio of solute to extraction solvent in the extract phase *Y* and the weight ratio of solute to feed solvent in the raffinate phase *X* is preferred [Eq. (15-3)].

$$K' = Y/X \tag{15-3}$$

In shortcut calculations the slope of the equilibrium line in Bancroft (weight-ratio) coordinates *m* is also used [Eq. (15-4)].

$$m = dY/dX \tag{15-4}$$

For low concentrations in which the equilibrium line is linear the value of *K'* is equal to *m*.

The value of *K'* is one of the main parameters used to establish the minimum ratio of extraction solvent to feed solvent that can be employed in an extraction process. For example, if the partition ratio *K'* is 4, then a countercurrent extractor would require 0.25 kg or more of extraction-solvent flow to remove all the solute from 1 kg of feed-solvent flow.

The **relative separation**, or **selectivity**, *α* between two components, *b* and *c*, can be described by the ratio of the two partition ratios [Eq. (15-5)].

$$\alpha(b/c) = K_b^o/K_c^o = K_b/K_c = K'_b/K'_c \tag{15-5}$$

This is analogous to relative volatility in distillation.

PHASE DIAGRAMS

Ternary-phase equilibrium data can be tabulated as in Table 15-1 and then worked into an electronic spreadsheet as in Table 15-2 to be presented as a **right-triangular diagram** as shown in Fig. 15-7. The weight-fraction solute is on the horizontal axis and the weight-fraction extraction-solvent is on the vertical axis. The tie-lines connect the points that are in equilibrium. For low-solute concentrations the horizontal scale can be expanded. The water-acetic acid-methylisobutylketone ternary is a **Type I** system where only one of the binary pairs, water-MIBK, is immiscible. In a **Type II** system two of the binary pairs are immiscible, i.e. the solute is not totally miscible in one of the liquids.

Many immiscible-liquid systems exhibit a **critical solution temperature** beyond which the system no longer separates into two liquid phases. This is shown in Fig. 15-8, in which an increase in temperature can change a Type II system to a Type I system above the

TABLE 15-1 Water-Acetic Acid-Methyl Isobutyl Ketone, 25°C*

Weight % in raffinate			X	Weight % in extract			Y
Water	Acetic acid	MIBK		Water	Acetic acid	MIBK	
98.45	0	1.55	0	2.12	0	97.88	0
95.46	2.85	1.7	0.0299	2.80	1.87	95.33	0.0196
85.8	11.7	2.5	0.1364	5.4	8.9	85.7	0.1039
75.7	20.5	3.8	0.2708	9.2	17.3	73.5	0.2354
67.8	26.2	6.0	0.3864	14.5	24.6	60.9	0.4039
55.0	32.8	12.2	0.5964	22.0	30.8	47.2	0.6525
42.9	34.6	22.5	0.8065	31.0	33.6	35.4	0.9492

*From Sherwood, Evans, and Longcor [*Ind. Eng. Chem.*, **31**, 599 (1939)].

TABLE 15-2 Spreadsheet for Right Triangular Ternary Diagram of Water/Acetic Acid/MIBK Liquid-Liquid-Equilibrium Data at 25°C in Fig. 15-7

Wt. fraction Variable	Acetic acid X	MIBK Y1	MIBK Y2	1 - wf AA Y3
Water	0.0000	0.0155		1.0000
Phase	0.0285	0.0170		0.9715
Line	0.1170	0.0250		0.8830
and	0.2050	0.0380		0.7950
Top of	0.2620	0.0600		0.7380
Triangle	0.3280	0.1220		0.6720
	0.3460	0.2250		0.6540
	1.0000			0.0000
MIBK	0.0000		0.9788	
Phase	0.0187		0.9533	
Line	0.0890		0.8570	
	0.1730		0.7350	
	0.2460		0.6090	
	0.3080		0.4720	
	0.3360		0.3540	
Tie-line 1	0.0285	0.0170		
	0.0187	0.9533		
Tie-line 2	0.1170		0.0250	
	0.0890		0.8570	
Tie-line 3	0.2050	0.0380		
	0.1730	0.7350		
Tie-line 4	0.2620		0.0600	
	0.2460		0.6090	
Tie-line 5	0.3280	0.1220		
	0.3080	0.4720		
Tie-line 6	0.3460		0.2250	
	0.3360		0.3540	

Data from Sherwood, Evans, and Longcor [*Ind. Eng. Chem.*, **31**, 599 (1939)].

critical temperature of the solute and extraction-solvent binary system T_{BS} . The system becomes totally miscible above the critical temperature of the feed solvent and extraction-solvent binary T_{AS} . Occasionally a system can also have a lower critical solution temperature below which the system will be totally miscible. The methyl ethyl ketone-water binary system provides one example. Changes in pressure ordinarily have a negligible effect on liquid-liquid equilibrium.

For graphical calculation of the number of theoretical stages in a ternary system the **right-triangular diagram** is more convenient to use than an equilateral triangle. The ternary equilibrium data are simply plotted on ordinary rectangular-coordinate graph paper with the weight fraction of the solute on the horizontal axis and the weight fraction of the extraction solvent on the vertical axis. For low-solute concentrations the horizontal scale can be expanded.

For the McCabe-Thiele type of graphical calculations and shortcut methods, the Bancroft (weight-ratio) concentrations can be used on

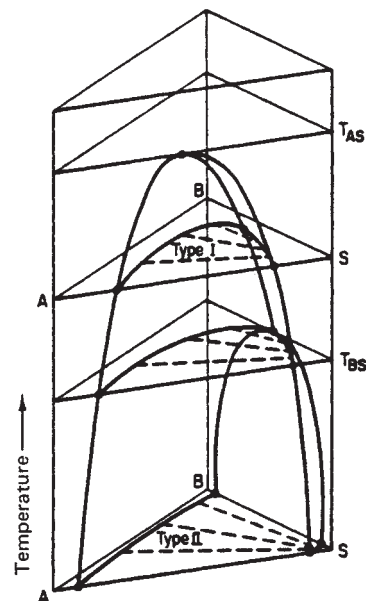


FIG. 15-8 Effect of temperature on ternary liquid-liquid equilibrium. A = feed solvent, B = solute, and S = extraction solvent.

ordinary rectangular-coordinate graph paper. The entire ternary system can be plotted in Bancroft (weight-ratio) concentrations on log-log graph paper as shown by Hand [*J. Phys. Chem.*, **34**, 1961 (1930)], and the equilibrium line can often be correlated by three straight-line segments (Fig. 15-9 and Table 15-3). The plait-point composition for a Type I system can easily be found by using this Hand plot as shown by Treybal, Weber, and Daley [*Ind. Eng. Chem.*, **38**, 817 (1946)]. This type of plot is also helpful for extrapolation and interpolation when data are scarce.

Multicomponent systems containing four or more components become difficult to display graphically. However, process-design calculations can often be made for the extraction of the component with the lowest partition ratio K' and treated as a ternary system. The components with higher K' values may be extracted more thoroughly from the raffinate than the solute chosen for design. Or computer calculations can be used to reduce the tedium of multicomponent, multistage calculations.

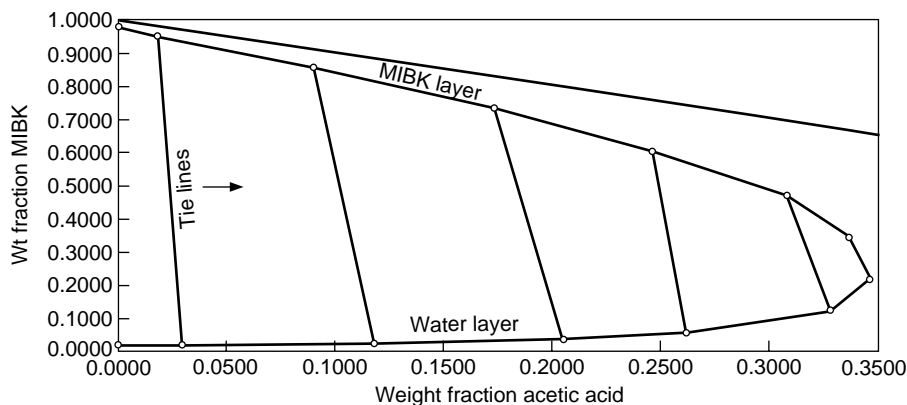


FIG. 15-7 Type I ternary diagram (water-acetic acid-MIBK).

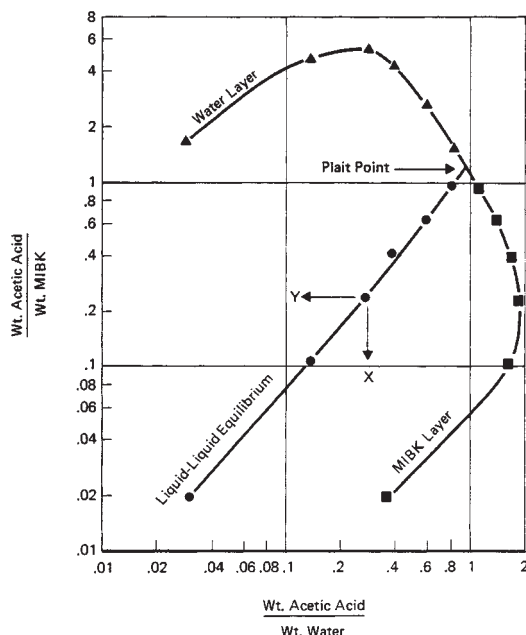


FIG. 15-9 Hand-type ternary diagram for water-acetic acid-methyl isobutyl ketone.

TABLE 15-3 Correlation of Liquid-Liquid Equilibrium Data for Water-Acetic Acid-MIBK

X	Y	$0.93 \cdot X^{1.10}$	$1.27 \cdot X^{1.29}$
0.0299	0.0196	0.0195	
0.1364	0.1039	0.1039	
0.2708	0.2354	0.2210	0.2355
0.3864	0.4039		0.3725
0.5964	0.6525		0.6519
0.8065	0.9492		0.9624

THERMODYNAMIC BASIS OF LIQUID-LIQUID EQUILIBRIA

In a ternary liquid-liquid system, such as the acetic acid–water–MIBK system, all three components are present in both liquid phases. At equilibrium the activity A° of any component is the same in both phases by definition [Eq. (15-6)].

$$A^\circ = \gamma_r x^\circ = A^\circ_e = \gamma_e y^\circ \quad (15-6)$$

where A° = activity of solute
 γ = activity coefficient of solute
 r = raffinate phase
 e = extract phase

Consequently, the partition ratio in mole-fraction units K° is a result of the ratio of activity coefficients in the two layers [Eq. (15-7)].

$$K^\circ = y^\circ/x^\circ = \gamma_r/\gamma_e \quad (15-7)$$

The **activity coefficient** γ can be defined as the escaping tendency of a component relative to Raoult's law in vapor-liquid equilibrium (see Sec. 4 in this handbook or Null, *Phase Equilibrium in Process Design*, Wiley-Interscience, 1970).

Gmehling and Onken (*Vapor-Liquid Equilibrium Data Collection*, DECHEMA, Frankfurt, Germany, 1979) have reported a large collection of vapor-liquid equilibrium data along with correlations of the resulting activity coefficients. This can be used to predict liquid-liquid equilibrium partition ratios as shown in Example 1.

Example 1: Partition Ratios Let us estimate the partition ratio in weight fractions K for extracting low concentrations of acetone from water into chloroform. The solute is acetone, the feed solvent is water, and the extraction solvent is chloroform in this case.

Gmehling and Onken (op. cit.) give the activity coefficient of acetone in water at infinite dilution γ^∞ as 6.74 at 25°C, depending on which set of vapor-liquid equilibrium data is correlated. From Eqs. (15-1) and (15-7) the partition ratio at infinite dilution of solute can be calculated as follows:

$$K = \frac{\gamma_r}{\gamma_e} \frac{\text{molecular weight of feed solvent}}{\text{molecular weight of extraction solvent}} = \frac{6.74}{0.30} \frac{(18)}{(119.4)} = 3.4$$

Sorenson and Arlt (*Liquid-Liquid Equilibrium Data Collection*, DECHEMA, Frankfurt, Germany, 1979) report several sets of liquid-liquid equilibrium data for the system acetone–water–chloroform, but the lowest solute concentrations reported at 25°C were 3 weight percent acetone in the water layer in equilibrium with 9 weight percent acetone in the chloroform layer. This gives a partition ratio K of 3.0.

This example clearly shows good distribution because of a negative deviation from Raoult's law in the extract layer. The activity coefficient of acetone is less than 1.0 in the chloroform layer. However, there is another problem because acetone and chloroform reach a maximum-boiling-point azeotrope composition and cannot be separated completely by distillation at atmospheric pressure.

A higher-boiling solvent, e.g., 1,1,2-trichloroethane, can be used which still gives acetone a negative deviation from Raoult's law ($\gamma_e = 0.732$ at 2 mole percent acetone) but does not form a maximum-boiling-point azeotrope according to Treybal, Weber, and Daley [*Ind. Eng. Chem.*, **38**, 817 (1946)].

An activity coefficient greater than 1.0 for a solute in solution is generally considered to be a **positive deviation** from Raoult's law; i.e., the escaping tendency is higher than predicted by Raoult's law. Likewise, an activity coefficient less than 1.0 is considered to be a **negative deviation** from Raoult's law; i.e., the escaping tendency is lower than predicted by ideal-solution behavior. "Positive" and "negative" thus refer to the sign of the logarithm of the activity coefficient.

HYDROGEN-BONDING INTERACTIONS

Deviations from Raoult's law in solution behavior have been attributed to many characteristics such as molecular size and shape, but the strongest deviations appear to be due to hydrogen bonding and electron donor-acceptor interactions. Robbins [*Chem. Eng. Prog.*, **76** (10), 58 (1980)] presented a table of these interactions, Table 15-4, that provides a qualitative guide to solvent selection for liquid-liquid extraction, extractive distillation, azeotropic distillation, or even solvent crystallization. The activity coefficient in the liquid phase is common to all these separation processes.

In Example 1 the solute, acetone, contains a ketone carbonyl group which is a hydrogen acceptor, i.e., solute class 5 according to Table 15-4. This solute is to be extracted from water with chloroform solvent which contains a hydrogen donor group, i.e., solvent class 4. The solute class 5 and solvent class 4 interaction in Table 15-4 is shown to give a negative deviation from Raoult's law.

A negative deviation reduces the activity of the solute in the solvent, which enhances the liquid-liquid partition ratio but also leads to maximum-boiling-point azeotropes. Among other classes of solvents shown in Table 15-4 that suppress the escaping tendency of a ketone are classes 1 and 2, i.e., phenolics and acids.

Other ketones, i.e., solvent class 5, are shown to be compatible with acetone, i.e., solute class 5, and tend to give activity coefficients near 1.0, i.e., nearly zero deviation from Raoult's law, and tend to be non-azeotropic. The solvent classes 6 through 12 tend to provide a hostile environment for acetone which increases the escaping tendency, i.e., give activity coefficients greater than 1.0 and tend to form minimum-boiling-point azeotropes. Whenever positive deviations give activity coefficients greater than 7.4, then phase separation, i.e., two liquid phases, can result, as shown by Martin [*Hydrocarbon Process.*, 241 (November 1975)].

Most of the classes in Table 15-4 are self-explanatory, but some can use additional definition. Class 4 includes halogenated solvents that have highly active hydrogens as described by Ewell, Harrison, and Berg [*Ind. Eng. Chem.*, **36**, 871 (1944)]. These are molecules that

TABLE 15-4 Organic-Group Interactions Based on 900 Binary Systems*

Solute class		Solvent class											
		1	2	3	4	5	6	7	8	9	10	11	12
H donor groups													
1	Phenol	0	0	—	0	—	—	—	—	—	—	+	+
2	Acid, thiol	0	0	—	0	—	—	0	0	—	0	+	+
3	Alcohol, water	—	—	0	+	+	0	—	—	+	+	+	+
4	Active H on multihalogen paraffin	0	0	+	0	—	—	—	—	—	—	0	+
H acceptor groups													
5	Ketone, amide with no H on N, sulfone, phosphine oxide	—	—	+	—	0	+	+	+	+	+	+	+
6	Tertiary amine	—	—	0	—	+	0	+	+	0	+	0	0
7	Secondary amine	—	0	—	—	+	+	0	0	0	0	0	+
8	Primary amine, ammonia, amide with 2H on N	—	0	—	—	+	+	0	0	+	+	+	+
9	Ether, oxide, sulfoxide	—	0	+	—	+	0	0	+	0	+	0	+
10	Ester, aldehyde, carbonate, phosphate, nitrate, nitrite, nitrile, intramolecular bonding, e.g., <i>o</i> -nitrophenol	—	0	+	—	+	+	0	+	+	0	+	+
11	Aromatic, olefin, halogen aromatic, multihalogen paraffin without active H, monohalogen paraffin	+	+	+	0	+	0	0	+	0	+	0	0
Non-H-bonding groups													
12	Paraffin, carbon disulfide	+	+	+	+	+	0	+	+	+	+	0	0

*From Robbins, *Chem. Eng. Prog.*, **76**(10), 58–61 (1980), by permission.

have two or three halogen atoms on the same carbon as a hydrogen atom, such as methylene chloride, chloroform, 1,1-dichloroethane and 1,1,2,2-tetrachloroethane. Class 4 also includes molecules that have one halogen on the same carbon atom as a hydrogen atom and one or more halogen atoms on an adjacent carbon atom, such as 1,2-dichloroethane and 1,1,2-trichloroethane. Apparently the halogens interact intramolecularly to leave the hydrogen atom highly active.

Monohalogen paraffins like methyl chloride and ethyl chloride are in class 11 along with multihalogen paraffins and olefins without active hydrogen such as carbon tetrachloride and perchloroethylene. Chlorinated benzenes are also in class 11 because they do not have halogens on the same carbon as a hydrogen atom.

Intramolecular bonding on aromatics is another fascinating interaction which gives a net result that behaves much like an ester group, class 10. Examples of this include *ortho*-nitrophenol and *ortho*-hydroxybenzaldehyde (salicylaldehyde). The intramolecular hydrogen bonding is so strong between the hydrogen donor group (phenol) and the hydrogen acceptor group (nitrate or aldehyde) that the molecule ends up by acting as an ester. One result is its low solubility in hot water. By contrast, the *para* derivative is highly soluble in hot water.

Table 15-4 gives a qualitative indication of interactions between classes of molecules but does not give quantitative differences within each class. Taft et al. [*J. Am. Chem. Soc.*, **91**, 4801 (1969)] have quantified the strength of hydrogen acceptors. The quantitative prediction of activity coefficients for solutions is reviewed by Reid, Prausnitz, and Sherwood (*The Properties of Gases and Liquids*, 3d ed., McGraw-Hill, New York, 1977) for the UNIFAC method, the Perotti, Deal, and Derr [*Ind. Eng. Chem.*, **51**, 95 (1959)] method, and the analytical-solution-of-groups (ASOG) method. Leo, Hansch, and Elkins [*Chem. Rev.*, **71**(6), 525 (1971)] also provide methods for predicting partition ratios for solutes between water and many solvents. Magnussen, Rasmussen, and Fredenslund [*Ind. Eng. Chem. Process Des. Dev.*, **20**(2), 331 (1981)] have presented a UNIFAC parameter table specifically for predicting liquid-liquid equilibrium.

EXPERIMENTAL EQUILIBRIUM DATA

Several large collections of experimental equilibrium data are now available for liquid-liquid systems. Sorenson and Arlt (*Liquid-Liquid*

Equilibrium Data Collection, DECHEMA, Frankfurt, Germany, 1979) have reported several volumes of data that have been correlated with activity-coefficient equations.

Wisniak and Tamir (*Liquid-Liquid Equilibrium and Extraction: A Literature Source Book*, Elsevier, Amsterdam, 1980) have listed many references. Leo, Hansch, and Elkins [*Chem. Rev.*, **71**(6), 525 (1971)] have tabulated partition ratios for a large number of solutes between water and solvents. Table 15-5 gives a selected list of partition ratios.

DESIRABLE SOLVENT PROPERTIES

The following properties of a potential solvent should be considered before use in a liquid-liquid extraction process.

1. *Selectivity.* The relative separation, or selectivity, α of a solvent is the ratio of two components in the extraction-solvent phase divided by the ratio of the same components in the feed-solvent phase. The separation power of a liquid-liquid system is governed by the deviation of α from unity, analogous to relative volatility in distillation. A relative separation α of 1.0 gives no separation of the components between the two liquid phases. Dilute solute concentrations generally give the highest relative separation factors.

2. *Recoverability.* The extraction solvent must usually be recovered from the extract stream and also from the raffinate stream in an extraction process. Since distillation is often used, the relative volatility of the extraction-solvent to nonsolvent components should be significantly greater or less than unity. A low latent heat of vaporization is desirable for a volatile solvent.

3. *Partition ratio.* The partition ratio for a solute should preferably be large so that a low ratio of extraction solvent to feed can be used.

4. *Capacity.* This property refers to the loading of solute per weight of extraction solvent that can be achieved in an extract layer at the plait point in a Type I system or at the solubility limit in a Type II system.

5. *Solvent solubility.* A low solubility of extraction solvent in the raffinate generally leads to a high relative volatility in a raffinate stripper or a low solvent loss if the raffinate is not desolventized. A low solubility of feed solvent in the extract leads to a high relative separation and, generally, to low solute-recovery costs.

TABLE 15-5 Selected List of Ternary Systems

Component A = feed solvent, component B = solute, and component S = extraction solvent. K_1 is the partition ratio in weight-fraction solute y/x for the tie line of lowest solute concentration reported. Ordinarily, K will approach unity as the solute concentration is increased.

Component B	Component S	Temp., °C.	K_1	Ref.
A = cetane				
Benzene	Aniline	25	1.290	47
<i>n</i> -Heptane	Aniline	25	0.0784	47
A = cottonseed oil				
Oleic acid	Propane	85	0.150	46
		98.5	0.1272	46
A = cyclohexane				
Benzene	Furfural	25	0.680	44
Benzene	Nitromethane	25	0.397	127
A = docosane				
1,6-Diphenylhexane	Furfural	45	0.980	11
		80	1.100	11
		115	1.062	11
A = dodecane				
Methylnaphthalene	β,β' -Iminodipropionitrile	ca. 25	0.625	92
Methylnaphthalene	β,β' -Oxydipropionitrile	ca. 25	0.377	92
A = ethylbenzene				
Styrene	Ethylene glycol	25	0.190	10
A = ethylene glycol				
Acetone	Amyl acetate	31	1.838	86
Acetone	<i>n</i> -Butyl acetate	31	1.940	86
Acetone	Cyclohexane	27	0.508	86
Acetone	Ethyl acetate	31	1.850	86
Acetone	Ethyl butyrate	31	1.903	86
Acetone	Ethyl propionate	31	2.32	86
A = furfural				
Trilinolein	<i>n</i> -Heptane	30	47.5	15
		50	21.4	15
		70	19.5	15
Triolein	<i>n</i> -Heptane	30	95	15
		50	108	15
		70	41.5	15
A = glycerol				
Ethanol	Benzene	25	0.159	62
Ethanol	Carbon tetrachloride	25	0.0667	63
A = <i>n</i> -heptane				
Benzene	Ethylene glycol	25	0.300	50
		125	0.316	50
Benzene	β,β' -thiodipropionitrile	25	0.350	92
Benzene	Triethylene glycol	25	0.351	89
Cyclohexane	Aniline	25	0.0815	47
Cyclohexane	Benzyl alcohol	0	0.107	29
		15	0.267	29
Cyclohexane	Dimethylformamide	20	0.1320	28
Cyclohexane	Furfural	30	0.0635	78
Ethylbenzene	Dipropylene glycol	25	0.329	90
Ethylbenzene	β,β' -Oxydipropionitrile	25	0.180	101
Ethylbenzene	β,β' -Thiodipropionitrile	25	0.100	101
Ethylbenzene	Triethylene glycol	25	0.140	89
Methylcyclohexane	Aniline	25	0.087	116
Toluene	Aniline	0	0.577	27
		13	0.477	27
		20	0.457	27
		40	0.425	27
Toluene	Benzyl alcohol	0	0.694	29
Toluene	Dimethylformamide	0	0.667	28
		20	0.514	28
Toluene	Dipropylene glycol	25	0.331	90
Toluene	Ethylene glycol	25	0.150	101
Toluene	Propylene carbonate	20	0.732	39
Toluene	β,β' -Thiodipropionitrile	25	0.150	101
Toluene	Triethylene glycol	25	0.289	89
<i>m</i> -Xylene	β,β' -Thiodipropionitrile	25	0.050	101
<i>o</i> -Xylene	β,β' -Thiodipropionitrile	25	0.150	101
<i>p</i> -Xylene	β,β' -Thiodipropionitrile	25	0.080	101
A = <i>n</i> -hexane				
Benzene	Ethylenediamine	20	4.14	23
A = <i>neo</i> -hexane				
Cyclopentane	Aniline	15	0.1259	96
		25	0.311	96
A = methylcyclohexane				
Toluene	Methylperfluorooctanoate	10	0.1297	58
		25	0.200	58

TABLE 15-5 Selected List of Ternary Systems (Continued)

Component B	Component S	Temp., °C.	K_1	Ref.
A = <i>iso</i> -octane				
Benzene	Furfural	25	0.833	44
Cyclohexane	Furfural	25	0.1076	44
<i>n</i> -Hexane	Furfural	30	0.083	78
A = perfluoroheptane				
Perfluorocyclic oxide	Carbon tetrachloride	30	0.1370	58
Perfluorocyclic oxide	<i>n</i> -Heptane	30	0.329	58
A = perfluoro- <i>n</i> -hexane				
<i>n</i> -Hexane	Benzene	30	6.22	80
<i>n</i> -Hexane	Carbon disulfide	25	6.50	80
A = perfluorotri- <i>n</i> -butylamine				
Iso-octane	Nitroethane	25	3.59	119
		31.5	2.36	119
		33.7	4.56	119
A = toluene				
Acetone	Ethylene glycol	0	0.286	100
		24	0.326	100
A = triethylene glycol				
α -Picoline	Methylcyclohexane	20	3.87	14
α -Picoline	Diisobutylene	20	0.445	14
α -Picoline	Mixed heptanes	20	0.317	14
A = triolein				
Oleic acid	Propane	85	0.138	46
A = water				
Acetaldehyde	<i>n</i> -Amyl alcohol	18	1.43	74
Acetaldehyde	Benzene	18	1.119	74
Acetaldehyde	Furfural	16	0.967	74
Acetaldehyde	Toluene	17	0.478	74
Acetaldehyde	Vinyl acetate	20	0.560	81
Acetic acid	Benzene	25	0.0328	43
		30	0.0984	38
		40	0.1022	38
		50	0.0558	38
		60	0.0637	38
Acetic acid	1-Butanol	26.7	1.613	102
Acetic acid	Butyl acetate	30	0.705	45
			0.391	67
Acetic acid	Caproic acid	25	0.349	73
Acetic acid	Carbon tetrachloride	27	0.1920	91
		27.5	0.0549	54
Acetic acid	Chloroform	ca. 25	0.178	70
		25	0.0865	72
		56.8	0.1573	17
Acetic acid	Creosote oil	34	0.706	91
Acetic acid	Cyclohexanol	26.7	1.325	102
Acetic acid	Diisobutyl ketone	25–26	0.284	75
Acetic acid	Di- <i>n</i> -butyl ketone	25–26	0.379	75
Acetic acid	Diisopropyl carbinol	25–26	0.800	75
Acetic acid	Ethyl acetate	30	0.907	30
Acetic acid	2-Ethylbutyric acid	25	0.323	73
Acetic acid	2-Ethylhexoic acid	25	0.286	73
Acetic acid	Ethylidene diacetate	25	0.85	104
Acetic acid	Ethyl propionate	28	0.510	87
Acetic acid	Fenchone	25–26	0.310	75
Acetic acid	Furfural	26.7	0.787	102
Acetic acid	Heptadecanol	25	0.312	114
		50	0.1623	114
Acetic acid	3-Heptanol	25	0.828	76
Acetic acid	Hexalin acetate	25–26	0.520	75
Acetic acid	Hexane	31	0.0167	85
Acetic acid	Isoamyl acetate	25–26	0.343	75
Acetic acid	Isophorone	25–26	0.858	75
Acetic acid	Isopropyl ether	20	0.248	31
		25–26	0.429	75
Acetic acid	Methyl acetate		1.273	67
Acetic acid	Methyl butyrate	30	0.690	66
Acetic acid	Methyl cyclohexanone	25–26	0.930	75
Acetic acid	Methylisobutyl carbinol	30	1.058	83
Acetic acid	Methylisobutyl ketone	25	0.657	97
		25–26	0.755	75
Acetic acid	Monochlorobenzene	25	0.0435	77
Acetic acid	Octyl acetate	25–26	0.1805	75
Acetic acid	<i>n</i> -Propyl acetate		0.638	67
Acetic acid	Toluene	25	0.0644	131
Acetic acid	Trichloroethylene	27	0.140	91
		30	0.0549	54

TABLE 15-5 Selected List of Ternary Systems (Continued)

Component B	Component S	Temp., °C.	K_1	Ref.
Acetic acid	Vinyl acetate	28	0.294	103
Acetone	Amyl acetate	30	1.228	117
Acetone	Benzene	15	0.940	11
		30	0.862	11
		45	0.725	11
Acetone	<i>n</i> -Butyl acetate		1.127	67
Acetone	Carbon tetrachloride	30	0.238	12
Acetone	Chloroform	25	1.830	43
		25	1.720	3
Acetone	Dibutyl ether	25–26	1.941	75
Acetone	Diethyl ether	30	1.00	54
Acetone	Ethyl acetate	30	1.500	117
Acetone	Ethyl butyrate	30	1.278	117
Acetone	Ethyl propionate	30	1.385	117
Acetone	<i>n</i> -Heptane	25	0.274	112
Acetone	<i>n</i> -Hexane	25	0.343	114
Acetone	Methyl acetate	30	1.153	117
Acetone	Methylisobutyl ketone	25–26	1.910	75
Acetone	Monochlorobenzene	25–26	1.000	75
Acetone	Propyl acetate	30	0.243	117
Acetone	Tetrachloroethane	25–26	2.37	57
Acetone	Tetrachloroethylene	30	0.237	88
Acetone	1,1,2-Trichloroethane	25	1.467	113
Acetone	Toluene	25–26	0.835	75
Acetone	Vinyl acetate	20	1.237	81
		25	3.63	104
Acetone	Xylene	25–26	0.659	75
Allyl alcohol	Diallyl ether	22	0.572	32
Aniline	Benzene	25	14.40	40
		50	15.50	40
Aniline	<i>n</i> -Heptane	25	1.425	40
		50	2.20	40
Aniline	Methylcyclohexane	25	2.05	40
		50	3.41	40
Aniline	Nitrobenzene	25	18.89	108
Aniline	Toluene	25	12.91	107
Aniline hydrochloride	Aniline	25	0.0540	98
Benzoic acid	Methylisobutyl ketone	26.7	76.9°	49
<i>iso</i> -Butanol	Benzene	25	0.989	1
<i>iso</i> -Butanol	1,1,2,2-Tetrachloroethane	25	1.80	36
<i>iso</i> -Butanol	Tetrachloroethylene	25	0.0460	7
<i>n</i> -Butanol	Benzene	25	1.263	126
		35	2.12	126
<i>n</i> -Butanol	Toluene	30	1.176	37
<i>tert</i> -Butanol	Benzene	25	0.401	99
<i>tert</i> -Butanol	<i>tert</i> -Butyl hypochlorite	0	0.1393	130
		20	0.1487	130
		40	0.200	129
		60	0.539	129
<i>tert</i> -Butanol	Ethyl acetate	20	1.74	5
2-Butoxyethanol	Methylethyl ketone	25	3.05	68
2,3-Butylene glycol	<i>n</i> -Butanol	26	0.597	71
		50	0.893	71
2,3-Butylene glycol	Butyl acetate	26	0.0222	71
		50	0.0326	71
2,3-Butylene glycol	Butylene glycol diacetate	26	0.1328	71
		75	0.565	71
2,3-Butylene glycol	Methylvinyl carbinol acetate	26	0.237	71
		50	0.351	71
		75	0.247	71
<i>n</i> -Butylamine	Monochlorobenzene	25	1.391	77
1-Butyraldehyde	Ethyl acetate	37.8	41.3	52
Butyric acid	Methyl butyrate	30	6.75	66
Butyric acid	Methylisobutyl carbinol	30	12.12	83
Cobaltous chloride	Dioxane	25	0.0052	93
Cupric sulfate	<i>n</i> -Butanol	30	0.000501	9
Cupric sulfate	<i>sec</i> -Butanol	30	0.00702	9
Cupric sulfate	Mixed pentanols	30	0.000225	9
<i>p</i> -Cresol	Methylnaphthalene	35	9.89	82
Diacetone alcohol	Ethylbenzene	25	0.335	22
Diacetone alcohol	Styrene	25	0.445	22
Dichloroacetic acid	Monochlorobenzene	25	0.0690	77
1,4-Dioxane	Benzene	25	1.020	8
Ethanol	<i>n</i> -Amyl alcohol	25–26	0.598	75
Ethanol	Benzene	25	0.1191	13
		25	0.0536	115
Ethanol	<i>n</i> -Butanol	20	3.00	26

TABLE 15-5 Selected List of Ternary Systems (Continued)

Component B	Component S	Temp., °C.	K ₁	Ref.
Ethanol	Cyclohexane	25	0.0157	118
Ethanol	Cyclohexene	25	0.0244	124
Ethanol	Dibutyl ether	25–26	0.1458	75
Ethanol	Di- <i>n</i> -propyl ketone	25–26	0.592	75
Ethanol	Ethyl acetate	0	0.0263	5
		20	0.500	5
		70	0.455	41
Ethanol	Ethyl isovalerate	25	0.392	13
Ethanol	Heptadecanol	25	0.270	114
Ethanol	<i>n</i> -Heptane	30	0.274	94
Ethanol	3-Heptanol	25	0.783	76
Ethanol	<i>n</i> -Hexane	25	0.00212	111
Ethanol	<i>n</i> -Hexanol	28	1.00	56
Ethanol	<i>sec</i> -Octanol	28	0.825	56
Ethanol	Toluene	25	0.01816	122
Ethanol	Trichloroethylene	25	0.0682	16
Ethylene glycol	<i>n</i> -Amyl alcohol	20	0.1159	59
Ethylene glycol	<i>n</i> -Butanol	27	0.412	85
Ethylene glycol	Furfural	25	0.315	18
Ethylene glycol	<i>n</i> -Hexanol	20	0.275	59
Ethylene glycol	Methylethyl ketone	30	0.0527	85
Formic acid	Chloroform	25	0.00445	72
		56.9	0.0192	17
Formic acid	Methylisobutyl carbinol	30	1.218	83
Furfural	<i>n</i> -Butane	51.5	0.712	42
		79.5	0.930	42
Furfural	Methylisobutyl ketone	25	7.10	19
Furfural	Toluene	25	5.64	53
Hydrogen chloride	<i>iso</i> -Amyl alcohol	25	0.170	21
Hydrogen chloride	2,6-Dimethyl-4-heptanol	25	0.266	21
Hydrogen chloride	2-Ethyl-1-butanol	25	0.534	21
Hydrogen chloride	Ethylbutyl ketone	25	0.01515	79
Hydrogen chloride	3-Heptanol	25	0.0250	21
Hydrogen chloride	1-Hexanol	25	0.345	21
Hydrogen chloride	2-Methyl-1-butanol	25	0.470	21
Hydrogen chloride	Methylisobutyl ketone	25	0.0273	79
Hydrogen chloride	2-Methyl-1-pentanol	25	0.502	21
Hydrogen chloride	2-Methyl-2-pentanol	25	0.411	21
Hydrogen chloride	Methylisopropyl ketone	25	0.0814	79
Hydrogen chloride	1-Octanol	25	0.424	21
Hydrogen chloride	2-Octanol	25	0.380	21
Hydrogen chloride	1-Pentanol	25	0.257	21
Hydrogen chloride	Pentanol (mixed)	25	0.271	21
Hydrogen fluoride	Methylisobutyl ketone	25	0.370	79
Lactic acid	<i>iso</i> -Amyl alcohol	25	0.352	128
Methanol	Benzene	25	0.01022	4
Methanol	<i>n</i> -Butanol	0	0.600	65
		15	0.479	65
		30	0.510	65
		45	1.260	65
		60	0.682	65
Methanol	<i>p</i> -Cresol	35	0.313	82
Methanol	Cyclohexane	25	0.0156	125
Methanol	Cyclohexene	25	0.01043	124
Methanol	Ethyl acetate	0	0.0589	5
		20	0.238	5
Methanol	<i>n</i> -Hexanol	28	0.565	55
Methanol	Methylnaphthalene	25	0.025	82
		35	0.0223	82
Methanol	<i>sec</i> -Octanol	28	0.584	55
Methanol	Phenol	25	1.333	82
Methanol	Toluene	25	0.0099	60
Methanol	Trichloroethylene	27.5	0.0167	54
Methyl- <i>n</i> -butyl ketone	<i>n</i> -Butanol	37.8	53.4	52
Methylethyl ketone	Cyclohexane	25	1.775	48
		30	3.60	85
Methylethyl ketone	Gasoline	25	1.686	64
Methylethyl ketone	<i>n</i> -Heptane	25	1.548	112
Methylethyl ketone	<i>n</i> -Hexane	25	1.775	112
		37.8	2.22	52
Methylethyl ketone	2-Methyl furan	25	84.0	109
Methylethyl ketone	Monochlorobenzene	25	2.36	68
Methylethyl ketone	Naphtha	26.7	0.885†	6
Methylethyl ketone	1,1,2-Trichloroethane	25	3.44	68
Methylethyl ketone	Trichloroethylene	25	3.27	68
Methylethyl ketone	2,2,4-Trimethylpentane	25	1.572	64
Nickelous chloride	Dioxane	25	0.0017	93

TABLE 15-5 Selected List of Ternary Systems (Continued)

Component B	Component S	Temp., °C.	K_1	Ref.
Nicotine	Carbon tetrachloride	25	9.50	34
Phenol	Methylnaphthalene	25	7.06	82
α -Picoline	Benzene	20	8.75	14
α -Picoline	Diisobutylene	20	1.360	14
α -Picoline	Heptanes (mixed)	20	1.378	14
α -Picoline	Methylcyclohexane	20	1.00	14
<i>iso</i> -Propanol	Benzene	25	0.276	69
<i>iso</i> -Propanol	Carbon tetrachloride	20	1.405	25
<i>iso</i> -Propanol	Cyclohexane	25	0.0282	123
<i>iso</i> -Propanol	Cyclohexene	15	0.0583	124
		25	0.0682	124
		35	0.1875	124
<i>iso</i> -Propanol	Diisopropyl ether	25	0.406	35
<i>iso</i> -Propanol	Ethyl acetate	0	0.200	5
		20	1.205	5
<i>iso</i> -Propanol	Tetrachloroethylene	25	0.388	7
<i>iso</i> -Propanol	Toluene	25	0.1296	121
<i>n</i> -Propanol	<i>iso</i> -Amyl alcohol	25	3.34	20
<i>n</i> -Propanol	Benzene	37.8	0.650	61
<i>n</i> -Propanol	<i>n</i> -Butanol	37.8	3.61	61
<i>n</i> -Propanol	Cyclohexane	25	0.1553	123
		35	0.1775	123
<i>n</i> -Propanol	Ethyl acetate	0	1.419	5
		20	1.542	5
<i>n</i> -Propanol	<i>n</i> -Heptane	37.8	0.540	61
<i>n</i> -Propanol	<i>n</i> -Hexane	37.8	0.326	61
<i>n</i> -Propanol	<i>n</i> -Propyl acetate	20	1.55	106
		35	2.14	106
<i>n</i> -Propanol	Toluene	25	0.299	2
Propionic acid	Benzene	30	0.598	57
Propionic acid	Cyclohexane	31	0.1955	84
Propionic acid	Cyclohexene	31	0.303	84
Propionic acid	Ethyl acetate	30	2.77	87
Propionic acid	Ethyl butyrate	26	1.470	87
Propionic acid	Ethyl propionate	28	0.510	87
Propionic acid	Hexanes (mixed)	31	0.186	84
Propionic acid	Methyl butyrate	30	2.15	66
Propionic acid	Methylisobutyl carbinol	30	3.52	83
Propionic acid	Methylisobutyl ketone	26.7	1.949*	49
Propionic acid	Monochlorobenzene	30	0.513	57
Propionic acid	Tetrachloroethylene	31	0.167	84
Propionic acid	Toluene	31	0.515	84
Propionic acid	Trichloroethylene	30	0.496	57
Pyridine	Benzene	15	2.19	110
		25	3.00	105
		25	2.73	120
		45	2.49	110
		60	2.10	110
Pyridine	Monochlorobenzene	25	2.10	77
Pyridine	Toluene	25	1.900	120
Pyridine	Xylene	25	1.260	120
Sodium chloride	<i>iso</i> -Butanol	25	0.0182	36
Sodium chloride	<i>n</i> -Ethyl- <i>sec</i> -butyl amine	32	0.0563	24
Sodium chloride	<i>n</i> -Ethyl- <i>tert</i> -butyl amine	40	0.1792	24
Sodium chloride	2-Ethylhexyl amine	30	0.187	24
Sodium chloride	1-Methyldiethyl amine	39.1	0.0597	24
Sodium chloride	1-Methyldodecyl amine	30	0.693	24
Sodium chloride	<i>n</i> -Methyl-1,3-dimethylbutyl amine	30	0.0537	24
Sodium chloride	1-Methyloctyl amine	30	0.589	24
Sodium chloride	<i>tert</i> -Nonyl amine	30	0.0318	24
Sodium chloride	1,1,3,3-Tetramethyl butyl amine	30	0.072	24
Sodium hydroxide	<i>iso</i> -Butanol	25	0.00857	36
Sodium nitrate	Dioxane	25	0.0246	95
Succinic acid	Ethyl ether	15	0.220	33
		20	0.198	33
		25	0.1805	33
Trimethyl amine	Benzene	25	0.857	51
		70	2.36	51

*Concentrations in lb.-moles/cu. ft.

†Concentrations in volume fraction.

References:

1. Alberty and Washburn, *J. Phys. Chem.*, **49**, 4 (1945).
2. Baker, *J. Phys. Chem.*, **59**, 1182 (1955).
3. Bancroft and Hubbard, *J. Am. Chem. Soc.*, **64**, 347 (1942).
4. Barbaudy, *Compt. rend.*, **182**, 1279 (1926).
5. Beech and Glasstone, *J. Chem. Soc.*, **1938**, 67.
6. Berg, Manders, and Switzer, *Chem. Eng. Progr.*, **47**, 11 (1951).
7. Bergelin, Lockhart, and Brown, *Trans. Am. Inst. Chem. Engrs.*, **39**, 173 (1943).
8. Berndt and Lynch, *J. Am. Chem. Soc.*, **66**, 282 (1944).
9. Blumberg, Cejtin, and Fuchs, *J. Appl. Chem.*, **10**, 407 (1960).

TABLE 15-5 Selected List of Ternary Systems (Concluded)

10. Boobar *et al.*, *Ind. Eng. Chem.*, **43**, 2922 (1951).
11. Briggs and Comings, *Ind. Eng. Chem.*, **35**, 411 (1943).
12. Buchanan, *Ind. Eng. Chem.*, **44**, 2449 (1952).
13. Chang and Moulton, *Ind. Eng. Chem.*, **45**, 2350 (1953).
14. Charles and Morton, *J. Appl. Chem.*, **7**, 39 (1957).
15. Church and Briggs, *J. Chem. Eng. Data*, **9**, 207 (1964).
16. Colburn and Phillips, *Trans. Am. Inst. Chem. Engrs.*, **40**, 333 (1944).
17. Conti, Othmer, and Gilmont, *J. Chem. Eng. Data*, **5**, 301 (1960).
18. Conway and Norton, *Ind. Eng. Chem.*, **43**, 1433 (1951).
19. Conway and Phillips, *Ind. Eng. Chem.*, **46**, 1474 (1954).
20. Coull and Hope, *J. Phys. Chem.*, **39**, 967 (1935).
21. Crittenden and Hixson, *Ind. Eng. Chem.*, **46**, 265 (1954).
22. Crook and Van Winkle, *Ind. Eng. Chem.*, **46**, 1474 (1954).
23. Cumming and Morton, *J. Appl. Chem.*, **3**, 358 (1953).
24. Davison, Smith, and Hood, *J. Chem. Eng. Data*, **11**, 304 (1966).
25. Denzler, *J. Phys. Chem.*, **49**, 358 (1945).
26. Drouillon, *J. chim. phys.*, **22**, 149 (1925).
27. Durandet and Gladel, *Rev. Inst. Franc. Pétrole*, **9**, 296 (1954).
28. Durandet and Gladel, *Rev. Inst. Franc. Pétrole*, **11**, 811 (1956).
29. Durandet, Gladel, and Graziani, *Rev. Inst. Franc. Pétrole*, **10**, 585 (1955).
30. Eaglesfield, Kelly, and Short, *Ind. Chemist*, **29**, 147, 243 (1953).
31. Elgin and Browning, *Trans. Am. Inst. Chem. Engrs.*, **31**, 639 (1935).
32. Fairburn, Cheney, and Chernovsky, *Chem. Eng. Progr.*, **43**, 280 (1947).
33. Forbes and Coolidge, *J. Am. Chem. Soc.*, **41**, 150 (1919).
34. Fowler and Noble, *J. Appl. Chem.*, **4**, 546 (1954).
35. Frere, *Ind. Eng. Chem.*, **41**, 2365 (1949).
36. Fritzsche and Stockton, *Ind. Eng. Chem.*, **38**, 737 (1946).
37. Fuoss, *J. Am. Chem. Soc.*, **62**, 3183 (1940).
38. Garner, Ellis, and Roy, *Chem. Eng. Sci.*, **2**, 14 (1953).
39. Gladel and Lablaude, *Rev. Inst. Franc. Pétrole*, **12**, 1236 (1957).
40. Griswold, Chew, and Klecka, *Ind. Eng. Chem.*, **42**, 1246 (1950).
41. Griswold, Chu, and Winsauer, *Ind. Eng. Chem.*, **41**, 2352 (1949).
42. Griswold, Klecka, and West, *Chem. Eng. Progr.*, **44**, 839 (1948).
43. Hand, *J. Phys. Chem.*, **34**, 1961 (1930).
44. Henty, McManamey, and Price, *J. Appl. Chem.*, **14**, 148 (1964).
45. Hirata and Hirose, *Kagaku Kogaku*, **27**, 407 (1963).
46. Hixon and Bockelmann, *Trans. Am. Inst. Chem. Engrs.*, **38**, 891 (1942).
47. Hunter and Brown, *Ind. Eng. Chem.*, **39**, 1343 (1947).
48. Jeffreys, *J. Chem. Eng. Data*, **8**, 320 (1963).
49. Johnson and Bliss, *Trans. Am. Inst. Chem. Engrs.*, **42**, 331 (1946).
50. Johnson and Francis, *Ind. Eng. Chem.*, **46**, 1662 (1954).
51. Jones and Grigsby, *Ind. Eng. Chem.*, **44**, 378 (1952).
52. Jones and McCants, *Ind. Eng. Chem.*, **46**, 1956 (1954).
53. Knight, *Trans. Am. Inst. Chem. Engrs.*, **39**, 439 (1943).
54. Krishnamurty, Murti, and Rao, *J. Sci. Ind. Res.*, **12B**, 583 (1953).
55. Krishnamurty and Rao, *J. Sci. Ind. Res.*, **14B**, 614 (1955).
56. Krishnamurty and Rao, *Trans. Indian Inst. Chem. Engrs.*, **6**, 153 (1954).
57. Krishnamurty, Rao, and Rao, *Trans. Indian Inst. Chem. Engrs.*, **6**, 161 (1954).
58. Kyle and Reed, *J. Chem. Eng. Data*, **5**, 266 (1960).
59. Laddha and Smith, *Ind. Eng. Chem.*, **40**, 494 (1948).
60. Mason and Washburn, *J. Am. Chem. Soc.*, **59**, 2076 (1937).
61. McCants, Jones, and Hopson, *Ind. Eng. Chem.*, **45**, 454 (1953).
62. McDonald, *J. Am. Chem. Soc.*, **62**, 3183 (1940).
63. McDonald, Kluender, and Lane, *J. Phys. Chem.*, **46**, 946 (1942).
64. Moulton and Walkey, *Trans. Am. Inst. Chem. Engrs.*, **40**, 695 (1944).
65. Mueller, Pugsley, and Ferguson, *J. Phys. Chem.*, **35**, 1314 (1931).
66. Murty, Murty, and Subrahmanyam, *J. Chem. Eng. Data*, **11**, 335 (1966).
67. Murti, Venkataratnam, and Rao, *J. Sci. Ind. Res.*, **13B**, 392 (1954).
68. Newman, Hayworth, and Treybal, *Ind. Eng. Chem.*, **41**, 2039 (1949).
69. Olsen and Washburn, *J. Am. Chem. Soc.*, **57**, 303 (1935).
70. Othmer, *Chem. Met. Eng.*, **43**, 325 (1936).
71. Othmer, Bergen, Schlechter, and Bruins, *Ind. Eng. Chem.*, **37**, 890 (1945).
72. Othmer and Ku, *J. Chem. Eng. Data*, **4**, 42 (1959).
73. Othmer and Serrano, *Ind. Eng. Chem.*, **41**, 1030 (1949).
74. Othmer and Tobias, *Ind. Eng. Chem.*, **34**, 690 (1942).
75. Othmer, White, and Treuger, *Ind. Eng. Chem.*, **33**, 1240 (1941).
76. Oualline and Van Winkle, *Ind. Eng. Chem.*, **44**, 1668 (1952).
77. Peake and Thompson, *Ind. Eng. Chem.*, **44**, 2439 (1952).
78. Pennington and Marwill, *Ind. Eng. Chem.*, **45**, 1371 (1953).
79. Pilloton, *A.S.T.M. Spec. Tech. Publ.*, **238**, 5 (1958).
80. Pliskin and Treybal, *J. Chem. Eng. Data*, **11**, 49 (1966).
81. Pratt and Glover, *Trans. Inst. Chem. Engrs. (London)*, **24**, 52 (1946).
82. Prutton, Walsh, and Desar, *Ind. Eng. Chem.*, **42**, 1210 (1950).
83. Rao, Ramamurty, and Rao, *Chem. Eng. Sci.*, **8**, 265 (1958).
84. Rao and Rao, *J. Appl. Chem.*, **6**, 270 (1956).
85. Rao and Rao, *J. Appl. Chem.*, **7**, 659 (1957).
86. Rao and Rao, *J. Sci. Ind. Res.*, **14B**, 204 (1955).
87. Rao and Rao, *J. Sci. Ind. Res.*, **14B**, 444 (1955).
88. Rao and Rao, *Trans. Indian Inst. Chem. Engrs.*, **7**, 78 (1954–1955).
89. Rifai, *Riv. Combust.*, **11**, 811 (1957).
90. Rifai, *Riv. Combust.*, **11**, 829 (1957).
91. Saletore, Mene, and Warhadpande, *Trans. Indian Inst. Chem. Engrs.*, **2**, 16 (1950).
92. Saunders, *Ind. Eng. Chem.*, **43**, 121 (1951).
93. Schott and Lynch, *J. Chem. Eng. Data*, **11**, 215 (1966).
94. Schweppe and Lorah, *Ind. Eng. Chem.*, **46**, 2391 (1954).
95. Selikson and Ricci, *J. Am. Chem. Soc.*, **64**, 2474 (1942).
96. Serjian, Spurr, and Gibbons, *J. Am. Chem. Soc.*, **68**, 1763 (1946).
97. Sherwood, Evans, and Longcor, *Ind. Eng. Chem.*, **31**, 1144 (1939).
98. Sidgwick, Pickford, and Wilsdon, *J. Chem. Soc.*, **99**, 1122 (1911).
99. Simonsen and Washburn, *J. Am. Chem. Soc.*, **68**, 235 (1946).
100. Sims and Bolme, *J. Chem. Eng. Data*, **10**, 111 (1965).
101. Skinner, *Ind. Eng. Chem.*, **47**, 222 (1955).
102. Skrzec and Murphy, *Ind. Eng. Chem.*, **46**, 2245 (1954).
103. Smith, *J. Phys. Chem.*, **45**, 1301 (1941).
104. Smith, *J. Phys. Chem.*, **46**, 229 (1942).
105. Smith, *J. Phys. Chem.*, **46**, 376 (1942).
106. Smith and Bonner, *Ind. Eng. Chem.*, **42**, 896 (1950).
107. Smith and Drexel, *Ind. Eng. Chem.*, **37**, 601 (1945).
108. Smith, Foecking, and Barber, *Ind. Eng. Chem.*, **41**, 2289 (1949).
109. Smith and La Bonte, *Ind. Eng. Chem.*, **44**, 2740 (1952).
110. Smith, Stibolt, and Day, *Ind. Eng. Chem.*, **43**, 190 (1951).
111. Taresenkov and Paulsen, *J. Gen. Chem. (U.S.S.R.)*, **7**, 2143 (1937).
112. Treybal and Vondrak, *Ind. Eng. Chem.*, **41**, 1761 (1949).
113. Treybal, Weber, and Daley, *Ind. Eng. Chem.*, **38**, 817 (1946).
114. Upchurch and Van Winkle, *Ind. Eng. Chem.*, **44**, 618 (1952).
115. Varteressian and Fenske, *Ind. Eng. Chem.*, **28**, 928 (1936).
116. Varteressian and Fenske, *Ind. Eng. Chem.*, **29**, 270 (1937).
117. Venkataratnam, Rao, and Rao, *Chem. Eng. Sci.*, **7**, 102 (1957).
118. Vold and Washburn, *J. Am. Chem. Soc.*, **54**, 4217 (1932).
119. Vreeland and Dunlap, *J. Phys. Chem.*, **61**, 329 (1957).
120. Vriens and Medcalf, *Ind. Eng. Chem.*, **45**, 1098 (1953).
121. Washburn and Beguin, *J. Am. Chem. Soc.*, **62**, 579 (1940).
122. Washburn, Beguin, and Beckord, *J. Am. Chem. Soc.*, **61**, 1694 (1939).
123. Washburn, Brockway, Graham, and Deming, *J. Am. Chem. Soc.*, **64**, 1886 (1942).
124. Washburn, Graham, Arnold, and Transue, *J. Am. Chem. Soc.*, **62**, 1454 (1940).
125. Washburn and Spencer, *J. Am. Chem. Soc.*, **56**, 361 (1934).
126. Washburn and Strandkov, *J. Phys. Chem.*, **48**, 241 (1944).
127. Weck and Hunt, *Ind. Eng. Chem.*, **46**, 2521 (1954).
128. Weiser and Geankoplis, *Ind. Eng. Chem.*, **47**, 858 (1955).
129. Westwater, *Ind. Eng. Chem.*, **47**, 451 (1955).
130. Westwater and Audieth, *Ind. Eng. Chem.*, **46**, 1281 (1954).
131. Woodman, *J. Phys. Chem.*, **30**, 1283 (1926).

6. **Density.** The difference in density between the two liquid phases in equilibrium affects the countercurrent flow rates that can be achieved in extraction equipment as well as the coalescence rates. The density difference decreases to zero at a plait point, but in some systems it can become zero at an intermediate solute concentration (isopycnic, or twin-density, tie line) and can invert the phases at higher concentrations. Differential types of extractors cannot cross such a solute concentration, but mixer-settlers can.

7. **Interfacial tension.** A high interfacial tension promotes rapid coalescence and generally requires high mechanical agitation to produce small droplets. A low interfacial tension allows drop breakup with low agitation intensity but also leads to slow coalescence rates. Interfacial tension usually decreases as solubility and solute concentration increase and falls to zero at the plait point (Fig. 15-10).

8. **Toxicity.** Low toxicity from solvent-vapor inhalation or skin contact is preferred because of potential exposure during repair of equipment or while connections are being broken after a solvent transfer. Also, low toxicity to fish and bioorganisms is preferred when extraction is used as a pretreatment for wastewater before it enters a biotreatment plant and with final effluent discharge to a stream or lake. Often solvent toxicity is low if water solubility is high.

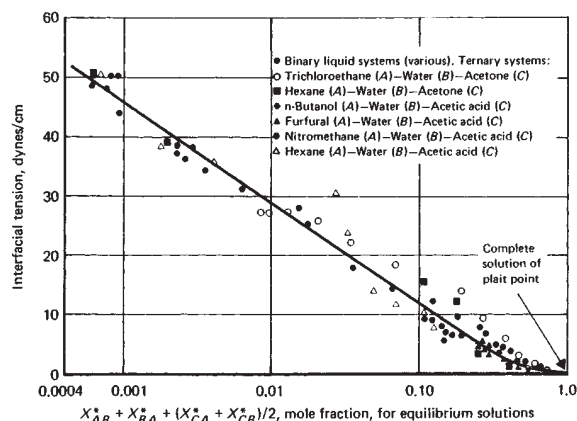


FIG. 15-10 Correlation of interfacial tension with mutual solubility for binary and ternary liquid mixtures. (From Treybal, *Liquid Extraction*, 2d ed., McGraw-Hill, New York, 1963.)

CALCULATION METHODS

SINGLE STAGE

An equilibrium, or theoretical, stage in liquid-liquid extraction as defined earlier is routinely utilized in laboratory procedures. A feed solution is contacted with an immiscible solvent to remove one or more of the solutes from the feed. This can be carried out in a separating funnel, or, preferably, in an agitated vessel that can produce droplets of about 1 mm in diameter. After agitation has stopped and the phases separate, the two clear liquid layers are isolated by decantation.

The equilibrium distribution coefficient can be calculated by material balance, using the weight of the feed F , raffinate R , and extract E , plus the weight-fraction solute in the feed x_f and raffinate x_r , when the weight-fraction solute in the extraction solvent y_s is zero [Eq. (15-8)].

$$K = \frac{y_e}{x_r} = \frac{R}{E} \left[\frac{F}{R} \frac{x_f}{x_r} - 1 \right] \quad (15-8)$$

However, an actual analysis of the weight-fraction solute in the extract y_e and raffinate x_r is preferred.

CROSSCURRENT THEORETICAL STAGES

After a single-stage liquid-liquid contact the phase remaining from the feed solution (raffinate) can be contacted with another quantity of fresh extraction solvent. This **crosscurrent extraction scheme** (Fig. 15-4) is an excellent laboratory procedure because the extract and raffinate phases can be analyzed after each stage to generate equilibrium data. Also, the feasibility of solute removal to low levels can be demonstrated.

The number of crosscurrent stages N that are required to reach a specified raffinate composition, in Bancroft coordinates X_n , can be calculated directly if K' is constant, the ratio of extraction solvent to feed solvent S'/F' is kept constant, and fresh extraction solvent $Y_s = 0$ (pre-saturated with feed solvent) is used in each stage [Eq. (15-9)].

$$N = \frac{\log(X_f/X_n)}{\log(K'S'/F' + 1)} \quad (15-9)$$

The crosscurrent scheme is not generally economically attractive for large commercial processes because solvent usage is high and solute concentration in the combined extract is low.

COUNTERCURRENT THEORETICAL STAGES

The main objective for calculating the number of theoretical stages (or mass-transfer units) in the design of a liquid-liquid extraction process is to evaluate the compromise between the size of the equipment, or number of contactors required, and the ratio of extraction solvent to feed flow rates required to achieve the desired transfer of mass from one phase to the other. In any mass-transfer process there can be an infinite number of combinations of flow rates, number of stages, and degrees of solute transfer. The optimum is governed by economic considerations.

The number of stages that are required can be kept to a minimum by selecting a solvent with a high partition ratio or by operating with a high ratio of extraction solvent to feed. However, a high solvent flow rate usually requires a high operating cost because of the cost of recovering the solvent. A high solvent flow rate should be carefully compared with an increase in capital cost for taller or more equipment to achieve more theoretical stages (or mass-transfer units) and reduce the required flow of solvent. The operating cost of an extractor is generally quite low in comparison with the operating cost of the solvent-recovery distillation column.

The other common objective for calculating the number of countercurrent theoretical stages (or mass-transfer units) is to evaluate the performance of liquid-liquid extraction test equipment in a pilot plant or to evaluate production equipment in an industrial plant. Most liquid-liquid extraction equipment in common use can be designed to achieve the equivalent of 1 to 8 theoretical countercurrent stages, with some designed to achieve 10 to 12 stages.

Right-Triangular Method This method is a rigorous Ponchon-Savarit type of graphical technique for determining the number of countercurrent theoretical stages of a ternary system (Fig. 15-11). The horizontal axis is the concentration of solute in weight fractions x or y . The vertical axis is the weight fraction of extraction solvent. The weight fraction of feed solvent is simply the amount remaining so that all three weight fractions add up to 1.0.

For the system water-acetic acid-MIBK in Fig. 15-11 the raffinate (water) layer is the solubility curve with low concentrations of MIBK, and the extract (MIBK) layer is the solubility curve with high concentrations of MIBK. The dashed lines are **tie lines** which connect the two layers in equilibrium as given in Table 15-1. Example 2 describes the right-triangular method of calculating the number of theoretical stages required.

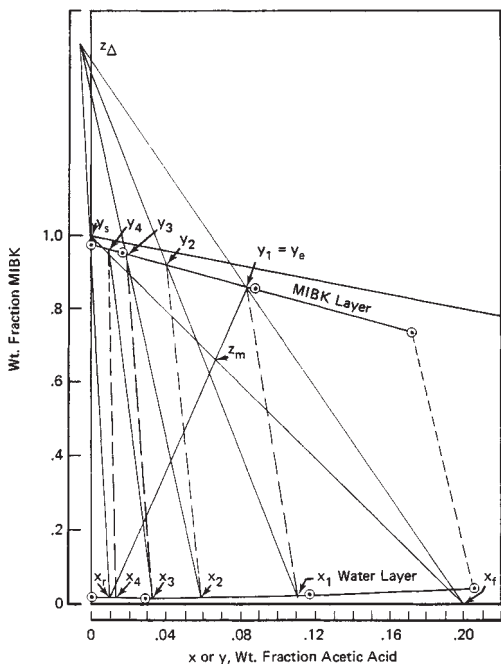


FIG. 15-11 Right-triangular graphical stages.

Example 2: Stage and Composition Calculation A 100-kg/h feed stream containing 20 weight percent acetic acid in water is to be extracted with 200 kg/h of recycle MIBK that contains 0.1 percent acetic acid and 0.01 percent water. The aqueous raffinate is to be extracted down to 1 percent acetic acid. How many theoretical stages will be required and what will the extract composition be?

The solute concentration in the feed, $x_f = 0.20$, in the raffinate, $x_r = 0.01$, and in the extraction solvent, $y_e = 0.001$, can be located on the diagram. Then the mix point z_m can be calculated from the feed, $F = 100$ kg/h, and the solvent, $S = 200$ kg/h, entering the extractor [Eq. (15-10)].

$$z_m = (Fx_f + Sy_s)/(F + S) \quad (15-10)$$

The mix point, $z_m = 0.0673$, falls on a straight line connecting x_f and y_e . The extract composition is then determined by drawing a straight line from x_r through z_m until the line intersects the extract line at the final extract composition, $y_e = 0.084$. The delta point z_Δ is then found at the intersection of two lines. One line connects the feed and extract compositions x_f and y_e . The other line connects the raffinate and solvent compositions x_r and y_s .

The graphical stepping off of theoretical stages starts at the extract composition y_e , and a tie line is drawn (parallel to the nearest one) to the raffinate composition leaving stage 1, $x_1 = y_e/K = 0.084/(0.117/0.089) = 0.1104$. The size of the extract stream can be calculated by the material balance $E = (F + S)(z_m - x_r)/(y_e - x_r)$. A straight line is drawn between x_1 and z_Δ to find the extract composition leaving stage 2, $y_2 = 0.0415$. Another tie line is drawn to find the raffinate composition leaving stage 2, x_2 , and the stepwise procedure continues until the final raffinate composition, $x_r = 0.01$, is achieved. This requires four theoretical stages plus a fraction. Additional details on the derivation of this procedure are provided by Foust, Wenzel, Clump, Maus, and Anderson (*Principles of Unit Operations*, 2d ed, Wiley, New York, 1980) and Treybal (*Mass-Transfer Operations*, 3d ed., McGraw-Hill, New York, 1980).

Shortcut Methods These methods are often preferred for repetitive calculations of pilot-plant data and numerous design conditions. In distillation calculations the assumption of constant molar vapor and liquid flow rates gave rise to the McCabe-Thiele stepwise calculation method with straight operating lines and a curved equilibrium line. A similar concept can be achieved in liquid-liquid extraction by assuming a constant flow rate of feed solvent F' and a constant flow rate of extraction solvent S' through the extractor. The solute concentrations are then given as the weight ratio of solute to feed solvent X and the weight ratio of solute to extraction solvent Y , i.e., Bancroft coordi-

nates. These concentrations and coordinates will essentially give a straight operating line on an XY diagram for stages 2 through $r - 1$ in Fig. 15-12. Equilibrium data using these weight ratios have already been shown to follow straight-line segments on a log-log plot (see Fig. 15-9). The main problem, then, is to evaluate the primary ratio of extraction solvent to feed solvent passing through the extractor in stages 2 through $r - 1$.

Robbins ("Liquid-Liquid Extraction," in Schweitzer, *Handbook of Separation Techniques for Chemical Engineers*, McGraw-Hill, New York, 1979, sec. 1.9) reported that most liquid-liquid extraction systems can be treated as having either (A) immiscible solvents, (B) partially miscible solvents with a low solute concentration in the extract, or (C) partially miscible solvents with a high solute concentration in the extract.

In case A the solvents are immiscible, so the rate of feed solvent alone in the feed stream F' is the same as the rate of feed solvent alone in the raffinate stream R' . In like manner, the rate of extraction solvent alone is the same in the stream entering S' as in the extract stream leaving E' (Fig. 15-12). The ratio of extraction-solvent to feed-solvent flow rates is therefore $S'/F' = E'/R'$. A material balance can be written around the feed end of the extractor down to any stage n (see Fig. 15-12) and then rearranged to a McCabe-Thiele type of operating line with a slope of F'/S' [Eq. (15-11)].

$$Y_{n+1} = \frac{F'}{S'} X_n + \frac{E'Y_e - F'X_f}{S'} \quad (15-11)$$

Similarly, the same operating line can be derived from a material balance around the raffinate end of the extractor up to stage n [Eq. (15-12)].

$$Y_n = \frac{F'}{S'} X_{n-1} + \frac{S'Y_s - R'X_r}{S'} \quad (15-12)$$

The overall extractor material balance is given by Eq. (15-13).

$$Y_e = \frac{F'X_f + S'Y_s - R'X_r}{E'} \quad (15-13)$$

The end points of the operating line on an XY plot (Fig. 15-13) are X_r , Y_s and X_f , Y_e , and the number of theoretical stages can be stepped off graphically. The equilibrium curve is taken from the Hand type of correlation shown earlier (Fig. 15-9). When the equilibrium line is straight, its intercept is zero, and the operating line is straight, the number of theoretical stages can be calculated with one of the Kremser equations [Eqs. (15-14) and (15-15)]. When the intercept of the equilibrium line is not zero, the value of Y_e/K_s should be used

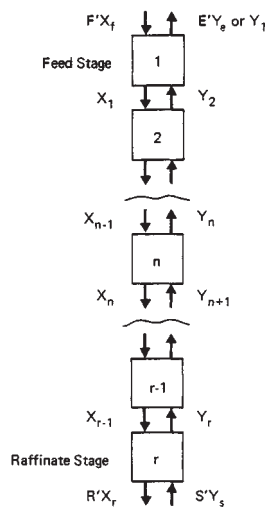


FIG. 15-12 Countercurrent extraction cascade.

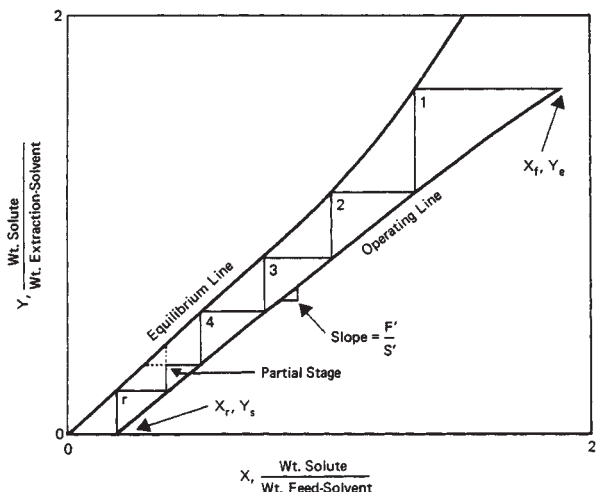


FIG. 15-13 Graphical calculation of countercurrent stages (Bancroft coordinates).

instead of Y_s/m , where K'_s is the partition ratio in Bancroft coordinates at Y_s .

When $\mathcal{E} \neq 1.0$,

$$N = \frac{\ln \left[\left(\frac{X_f - Y_s/m}{X_r - Y_s/m} \right) \left(1 - \frac{1}{\mathcal{E}} \right) + \frac{1}{\mathcal{E}} \right]}{\ln \mathcal{E}} \quad (15-14)$$

When $\mathcal{E} = 1.0$,

$$N = \frac{X_f - Y_s/m}{X_r - Y_s/m} - 1 \quad (15-15)$$

The value of m is the slope of the equilibrium line dY/dX [Eq. (15-4)]. This is equal to K' [Eq. (15-3)] at low concentrations where the equilibrium line is straight. The value of \mathcal{E} , the **extraction factor**, is calculated by dividing the slope of the equilibrium line m by the slope of the operating line F'/S' [Eq. (15-16)].

$$\mathcal{E} = mS'/F' \quad (15-16)$$

The solution to the Kremser equation is shown graphically in Fig. 15-14. When a system responds with a constant number of theoretical stages N , the solute concentration in the raffinate X_r can readily be evaluated as the result of changing the ratio of solvent to feed [Eqs. (15-17) and (15-18)].

When $\mathcal{E} \neq 1.0$,

$$\frac{X_r - Y_s/m}{X_f - Y_s/m} = \frac{\mathcal{E} - 1}{\mathcal{E}^{N+1} - 1} \quad (15-17)$$

When $\mathcal{E} = 1.0$,

$$\frac{X_r - Y_s/m}{X_f - Y_s/m} = \frac{1}{N + 1} \quad (15-18)$$

When the equilibrium line is not straight, Treybal (*Liquid Extraction*, 2d ed., McGraw-Hill, New York, 1963) recommends that the geometric mean value of m be used. The geometric mean of the slope of the equilibrium line at the concentration leaving the feed state m_1 and at the raffinate concentration leaving the raffinate stage m_r is $\sqrt{m_1 m_r}$.

Example 3: Shortcut Calculation, Case A Let us solve the problem in Example 2 by using the shortcut calculation method assuming immiscible solvents, case A.

From the problem,

$$F' = 100(1 - 0.2) = 80 \text{ kg water/h}$$

$$X_f = 0.2/0.8 = 0.25 \text{ kg acetic acid/kg water}$$

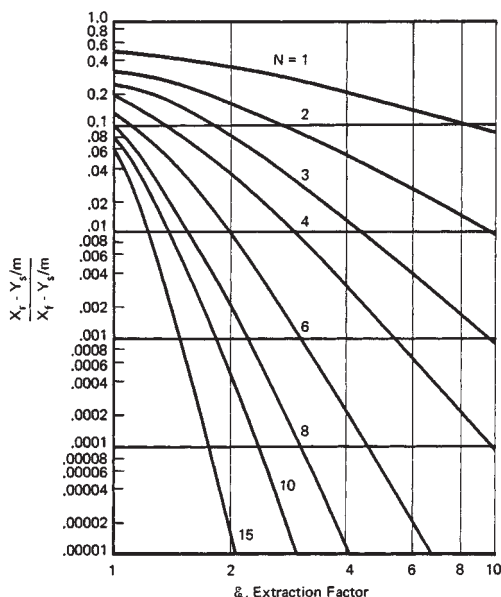


FIG. 15-14 Graphical solution to the Kremser equation.

$$X_r = 0.01/0.99 = 0.01 \text{ kg acetic acid/kg water}$$

$$S' = 200(1 - 0.001) = 199.8 \text{ kg MIBK/h}$$

$$Y_s = 0.2/199.8 = 0.001 \text{ kg acetic acid/kg MIBK}$$

If we assume $R' = F'$ and $E' = S'$, calculate Y_e from Eq. (15-13):

$$Y_e = \frac{80(0.25) + (199.8)(0.001) - 80(0.01)}{199.8} = 0.097 \frac{\text{kg acetic acid}}{\text{kg MIBK}}$$

From the correlation of equilibrium data (Table 15-3), $Y = 0.930(X)^{1.10}$, for X between 0.03 and 0.25.

Calculate $X_1 = (0.097/0.930)^{1/1.10} = 0.128$:

$$m = dY/dX = (0.930)(1.10)(X)^{0.1}, \text{ for } X \text{ between } 0.03 \text{ and } 0.25$$

$$m_1 = 0.833 \text{ at } X = 0.128$$

$$m_r = dY/dX = K' = 0.656, \text{ for } X \text{ below } 0.03$$

$$K'_s = 0.656 \text{ at } Y_s = 0.001$$

$$\mathcal{E} = \sqrt{m_1 m_r} S'/F' = (0.739)(199.8)/80 = 1.85$$

N is determined from Fig. 15-14, Eq. (15-14), or the McCabe-Thiele type of plot (Fig. 15-13):

$$N = \frac{\ln \left[\left(\frac{0.25 - 0.001/0.656}{0.01 - 0.001/0.656} \right) \left(1 - \frac{1}{1.85} \right) + \frac{1}{1.85} \right]}{\ln 1.85} = 4.3$$

From solubility data at $Y = 0.1039$ (Table 15-1) the extract layer contains $5.4/85.7 = 0.0630$ kg water/kg MIBK and $y_e = (0.097)/(1 + 0.097 + 0.063) = 0.084$ weight-fraction acetic acid in the extract.

For cases *B* and *C*, Robbins ("Liquid-Liquid Extraction," in Schweitzer, *Handbook of Separation Techniques for Chemical Engineers*, McGraw-Hill, New York, 1979, sec. 1.9) developed the concept of pseudo solute concentrations for the feed and solvent streams entering the extractor that will allow the Kremser equations to be used.

In case *B* the solvents are partially miscible, and the miscibility is nearly constant through the extractor. This frequently occurs when all solute concentrations are relatively low. The feed stream is assumed to dissolve extraction solvent only in the feed stage and to retain the same amount throughout the extractor. Likewise, the extraction solvent is assumed to dissolve feed solvent only in the raffinate stage. With these assumptions the primary extraction-solvent rate moving through the extractor is assumed to be S' , and the primary feed-

solvent rate is assumed to be F' . The extract rate E' is less than S' , and the raffinate rate R' is less than F' because of solvent solubilities.

The slope of the operating line is F'/S' , just as in Eqs. (15-11) and (15-12), but only stages 2 through $r - 1$ will fall directly on the operating line. And one knows that X_1 will be on the equilibrium line in equilibrium with Y_e by definition (see Fig. 15-12). One can calculate a pseudo feed concentration X_f that will fall on the operating line [Eq. (15-11)] at $Y_{n+1} = Y_e$ [Eq. (15-19)].

$$X_f^B = X_j + \frac{S' - E'}{F'} Y_e \quad (15-19)$$

Likewise, one knows that Y_r will be on the equilibrium line with X_r (see Fig. 15-12). One can therefore calculate a pseudo concentration of solute in the inlet extraction solvent Y_s^B that will fall on the operating line [Eq. (15-12)] where $X_{n-1} = X_r$ [Eq. (15-20)].

$$Y_s^B = Y_s + \frac{F' - R'}{S'} X_r \quad (15-20)$$

For case B, the two pseudo inlet concentrations X_f^B and Y_s^B can be used in the Kremser equation with the actual value of X_r and $\mathcal{E} = mS'/F'$ to calculate rapidly the number of theoretical stages required. The graphical stepwise solution shown in Fig. 15-13 can also be used. The operating line will go through points X_r , Y_s^B and X_f^B , Y_e with a slope of F'/S' . In one example studied by Robbins [*Chem. Eng. Prog.*, 76(10), 58 (1980)], the actual feed and extract compositions gave a point to the left of the equilibrium line on an XY graph like Fig. 15-13 because the solubility of the solvent was so high. But the use of the pseudo feed composition still gave an accurate calculation of the number of theoretical stages as confirmed by a right-triangular graphical calculation.

Example 4: Shortcut Calculation, Case B Let us solve the problem in Example 2 by assuming case B. The solute (acetic acid) concentration is low enough in the extract so that we may assume that the mutual solubilities of the solvents remain nearly constant. The material balance can be calculated by an iterative method.

From equilibrium data (Table 15-1) the extraction-solvent (MIBK) loss in the raffinate will be about $0.016/0.984 = 0.0163$ kg MIBK/kg water, and the feed-solvent (water) loss in the extract will be about $5.4/85.7 = 0.0630$ kg water/kg MIBK.

First iteration: assume $R' = F' = 80$ kg water/h. Then, extraction solvent in raffinate = $(0.0163)(80) = 1.30$ kg MIBK/h. Estimate $E' = 199.8 - 1.3 = 198.5$ kg MIBK/h. Then feed solvent in extract = $(0.063)(198.5) = 12.5$ kg water/h.

Second iteration: calculate $R' = 80 - 12.5 = 67.5$ kg water/h. $E' = 199.8 - (0.0163)(67.5) = 198.7$ kg MIBK/h.

Third iteration: converge $R' = 80 - (0.063)(198.7) = 67.5$ kg water/h. Y_e is calculated from the overall extractor material balance [Eq. (15-13)]:

$$Y_e = \frac{(80)(0.25) + (199.8)(0.001) - (67.5)(0.01)}{198.7} = 0.0983 \frac{\text{kg acetic acid}}{\text{kg MIBK}}$$

$$Y_e = \frac{0.0983}{1 + 0.0983 + 0.0630} = 0.0846$$

weight fraction acetic acid in extract.

From the correlation of equilibrium data (Table 15-3),

$$Y_e = 0.930(X)^{1.10}, \text{ for } X \text{ between } 0.03 \text{ and } 0.25$$

The raffinate composition leaving the feed (first stage) is calculated:

$$X_1 = (0.0983/0.930)^{1/1.10} = 0.130$$

$$m_1 = dY/dX = (0.930)(1.10)(X)^{0.1}$$

$$m_r = dY/dX = K' = 0.656$$

$$m_1 = 0.834 \text{ at } X_1 = 0.13$$

$$m_r = 0.656 \text{ at } X_r = 0.01$$

$$K' = 0.656 \text{ at } Y_s = 0.001$$

$$\mathcal{E} = \sqrt{m_1 m_r} S'/F' = (0.740)(199.8)/80 = 1.85$$

X_f^B is calculated from Eq. (15-19):

$$X_f^B = 0.25 + \frac{(199.8 - 198.7)(0.0983)(0.0983)}{80} = 0.251$$

Y_s^B is calculated from Eq. (15-20):

$$Y_s^B = 0.001 + \frac{(80 - 67.5)(0.01)}{199.8} = 0.0016$$

N is determined from Fig. 15-13, Eq. (15-14), or a McCabe-Thiele type of plot (Fig. 15-13) for case B.

$$N = \frac{\ln \left[\left(\frac{0.251 - 0.0016/0.656}{0.01 - 0.0016/0.656} \right) \left(1 - \frac{1}{1.85} \right) + \frac{1}{1.85} \right]}{\ln 1.85} = 4.5 \text{ theoretical stages}$$

A less frequent situation, case C, can occur when the solute concentration in the extract is so high that a large amount of feed solvent is dissolved in the extract stream in the "feed stage" but a relatively small amount of feed solvent (say one-tenth as much) is dissolved by the extract stream in the "raffinate stage." The feed stream is assumed to dissolve the extraction solvent only in the feed stage just as in case B. But the extract stream is assumed to dissolve a large amount of feed solvent leaving the feed stage and a negligible amount leaving the raffinate stage. With these assumptions the primary feed-solvent rate is assumed to be R' , so the slope of the operating line for case C is R'/S' . Again the extract rate E' is less than S' , and the raffinate rate R' is less than F' .

The pseudo feed concentration for case C, X_f^C , can be calculated from Eq. (15-21).

$$X_f^C = \frac{F'}{R'} X_j + \frac{S' - E'}{R'} Y_e \quad (15-21)$$

And the value of Y_s will fall on the operating line for case C. The extraction factor for case C is calculated from Eq. (15-22).

$$\mathcal{E}^C = mS'/R' \quad (15-22)$$

On an XY diagram for case C the operating line will go through points X_r , Y_s and X_f^C , Y_e with a slope of R'/S' similar to Fig. 15-13. When using the Kremser equation for case C, one uses the pseudo feed concentration X_f^C from Eq. (15-21) and the stripping factor \mathcal{E}^C from Eq. (15-22). One uses the raffinate concentration X_r and inlet solvent concentration Y_s without modification.

For the first time through a liquid-liquid extraction problem, the right-triangular graphical method may be preferred because it is completely rigorous for a ternary system and reasonably easy to understand. However, the shortcut methods with the Bancroft coordinates and the Kremser equations become valuable time-savers for repetitive calculations and for data reduction from experimental runs. The calculation of pseudo inlet compositions and the use of the McCabe-Thiele type of stage calculations lend themselves readily to programmable calculator or computer routines with a simple correlation of equilibrium data.

COUNTERCURRENT MASS-TRANSFER-UNIT CALCULATIONS

The concept of a mass-transfer unit was developed many years ago to represent more rigorously what happens in a differential contactor rather than a stagewise contactor. For a straight operating line and a straight equilibrium line with an intercept of zero, the equation for calculating the number of mass-transfer units based on the overall raffinate phase N_{or} is identical to the Kremser equation except for the denominator when the extraction factor is not equal to 1.0 [Eq. (15-23)].

When $\mathcal{E} \neq 1.0$,

$$N_{or} = \frac{\ln \left[\left(\frac{X_f - Y_s/m}{X_r - Y_s/m} \right) \left(1 - \frac{1}{\mathcal{E}} \right) + \frac{1}{\mathcal{E}} \right]}{1 - 1/\mathcal{E}} \quad (15-23)$$

The number of mass-transfer units N_{or} is identical to the number of theoretical stages when the extraction factor \mathcal{E} is 1.0 [Eq. (15-24)].

When $\mathcal{E} = 1.0$,

$$N_{or} = [(X_f - Y_s/m)/(X_r - Y_s/m)] - 1 \quad (15-24)$$

The differences become pronounced when values of the extraction factor are high [Eq. (15-25)].

$$N_{or} = N \ln \mathcal{E}/(1 - 1/\mathcal{E}) \quad (15-25)$$

Even staged equipment may be modeled best by the number of mass-transfer units when the extraction factor is much higher than 1.5, especially if the stage efficiencies are low.

The response of solute concentration in the raffinate X_r to the solvent-to-feed ratio S'/F' can be calculated by Eqs. (15-26) and (15-27) for a constant number of transfer units based on the overall raffinate phase N_{or} .

When $\mathcal{E} \neq 1.0$,

$$\frac{X_r - Y_s/m}{X_f - Y_s/m} = \frac{1 - 1/\mathcal{E}}{e^{N_{or}(1 - 1/\mathcal{E})} - 1/\mathcal{E}} \quad (15-26)$$

When $\mathcal{E} = 1.0$,

$$\frac{X_r - Y_s/m}{X_f - Y_s/m} = \frac{1}{N_{or} + 1} \quad (15-27)$$

The solution to these equations is shown graphically in Fig. 15-15. Note that the raffinate composition is not reduced appreciably when the extraction factor \mathcal{E} is increased from 5 to infinity. This is true because mass transfer from the raffinate phase limits the performance. This is typical of the performance of many devices including actual staged equipment. However, if there is sufficient residence time in each stage of a staged device so that high stage efficiencies can be achieved, then the raffinate can be reduced substantially by increasing the extraction factor above 5 (see Fig. 15-14). However, the solute concentration in the extract stream would be quite dilute.

Example 5: Number of Transfer Units Let us calculate the number of transfer units required to achieve the separation in Example 3. The solution to the problem is the same as in Example 3 except that the denominator is changed in the final equation [Eq. (15-25)]:

$$N_{or} = 4.5 \frac{\ln 1.85}{1 - 1/1.85} = 6.0 \text{ transfer units}$$

STAGE EFFICIENCY AND HEIGHT OF A THEORETICAL STAGE OR TRANSFER UNIT

The overall stage efficiency of a staged extraction system is simply the number of theoretical stages divided by the number of actual stages times 100 [Eq. (15-28)].

$$\text{Percent stage efficiency} = 100N/\text{number of actual stages} \quad (15-28)$$

A similar term of number of transfer units per actual stage could also be envisioned.

The height equivalent to a theoretical stage (HETS) in an extraction tower is simply the height of the tower Z_t divided by the number of theoretical stages achieved [Eq. (15-29)].

$$\text{HETS} = Z_t/N \quad (15-29)$$

Likewise, the height of a transfer unit based on raffinate-phase compositions H_{or} is the height of tower divided by the number of transfer units [Eq. (15-30)].

$$H_{or} = Z_t/N_{or} \quad (15-30)$$

The contribution to the height of a transfer unit overall based on the raffinate-phase compositions is the sum of the contribution from the resistance to mass transfer in the raffinate phase H_r plus the contribution from the resistance to mass transfer in the extract phase H_e , divided by the extraction factor \mathcal{E} [Eq. (15-31)].

$$H_{or} = H_r + H_e/\mathcal{E} \quad (15-31)$$

At high extraction factors the height of a transfer unit is mostly dependent on the resistance to the transfer of solute from the raffinate phase.

Prediction methods attempt to quantify the resistances to mass transfer in terms of the raffinate rate R and the extract rate E , per tower cross-sectional area A_t , and the mass-transfer coefficient in the raffinate phase k_r and the extract phase k_e , times the interfacial (droplet) mass-transfer area per volume of tower a [Eqs. (15-32) and (15-33)].

$$H_r = R/A_t k_r a \quad (15-32)$$

$$H_e = E/A_t k_e a \quad (15-33)$$

The mass-transfer coefficients depend on complex functions of diffusivity, viscosity, density, interfacial tension, and turbulence. Similarly, the mass-transfer area of the droplets depends on complex functions of viscosity, interfacial tension, density difference, extractor geometry, agitation intensity, agitator design, flow rates, and interfacial rag deposits. Only limited success has been achieved in correlating extractor performance with these basic principles. The lumped parameter H_{or} deals directly with the ultimate design criterion, which is the height of an extraction tower.

FRACTIONATION STAGES

One of the most sophisticated separations achievable by liquid-liquid extraction is fractionation. Two solutes can be separated almost completely by isolating one solute b into the extraction solvent S' and another solute c into a wash solvent W' (Fig. 15-16). The bottom section of a fractionation extraction is about the same as the countercurrent extractions described earlier, with the extraction solvent S' entering the bottom and extracting, i.e., stripping, one of the solutes b almost completely from the raffinate R' . As the extract stream moves above the feed stage, it is contacted countercurrently with a wash solvent W' that scrubs the unwanted solute c out of the extract stream. This in effect purifies the solute b that is being extracted. The stripping section and the washing (enriching) section will each have its own operating line on a McCabe-Thiele type of XY diagram (Fig. 15-17). The overall material balance must be met at the feed stage.

For the case in which the extraction solvent can be assumed to be totally immiscible with the wash solvent and there is no solvent in the feed, the extraction factor \mathcal{E} must be greater than 1.0 for component b and less than 1.0 for component c [Eq. (15-34)].

$$\mathcal{E} = mS'/W' \quad (15-34)$$

For a symmetrical separation of component b from c , Brian (*Staged Cascades in Chemical Processing*, Prentice-Hall, Englewood Cliffs, N.J., 1972) reported that the ratio of wash solvent to extraction solvent W'/S' should be set equal to the geometric mean of the two slopes of the equilibrium lines [Eq. (15-35)].

$$W'/S' = \sqrt{m_b/m_c} \quad (15-35)$$

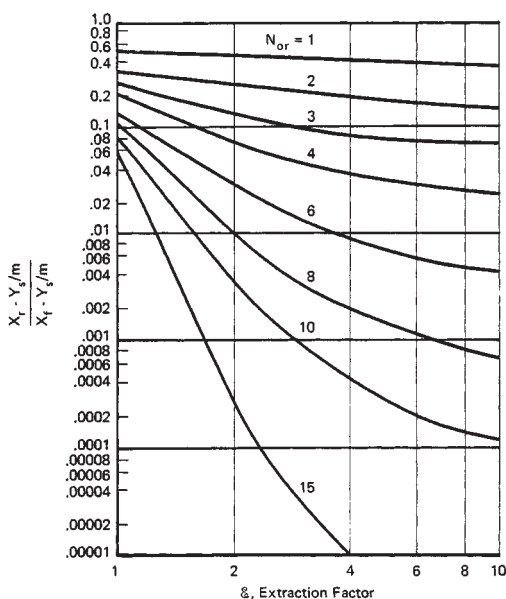


FIG. 15-15 Graphical solution to the mass-transfer-unit equations.

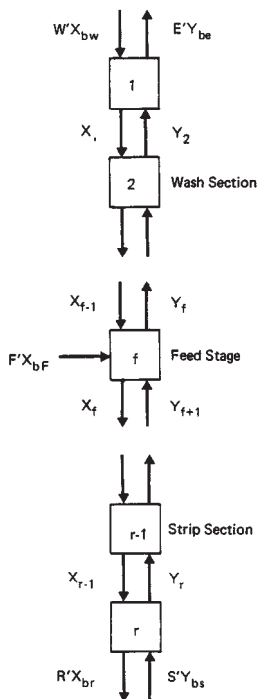
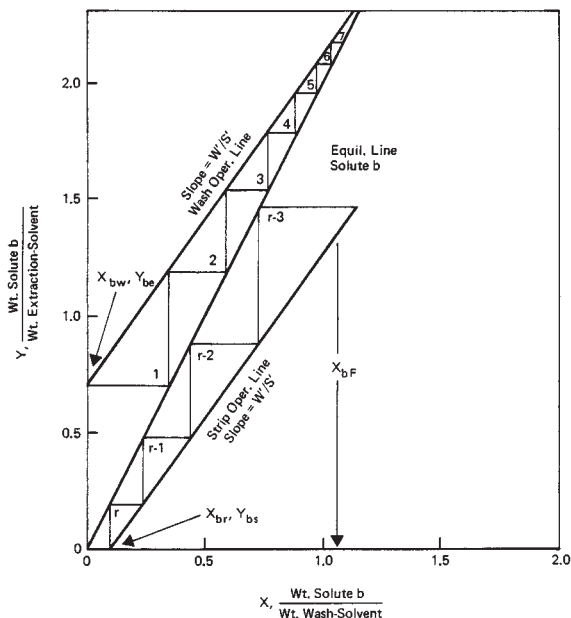


FIG. 15-16 Liquid-liquid fractionation cascade.

The ratio of wash solvent to extraction solvent is the same in the enriching section as in the stripping section if no solvent is added in the feed. The degree of separation to be achieved can be chosen for the process design, such as 99 percent of component b into the extract stream and 99 percent of component c into the raffinate stream. Then the feed rate can be chosen so that the solute loadings in the extract stream and

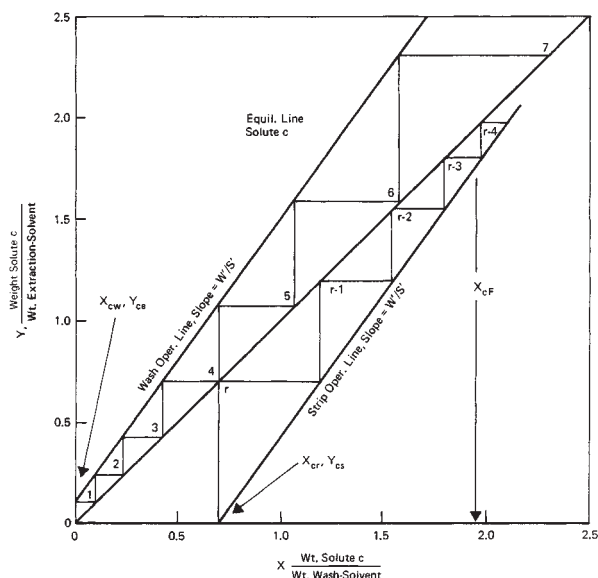

 FIG. 15-17 Graphical calculation of fractionation stages for solute b .

the raffinate stream are reasonable. This becomes especially critical near the feed stage, where the solute loadings are highest.

An overall material balance can be calculated around the extractor, and then an XY plot can be constructed for each solute (Figs. 15-17 and 15-18). The solute concentrations at the raffinate end of the extractor, X_{br} and Y_{bs} , can be plotted for component b , and the operating line can be drawn with a slope of W'/S' with no solvent in the feed. The solute concentrations at the extract end of the extractor, X_{bw} and Y_{be} , can also be plotted for component b with the enriching-section operating line also having the slope W'/S' if no solvents were added with the feed. The theoretical stages can be stepped off for each section of the extractor by starting at the extract end, stage 1, and stepping toward the feed stage f , then restarting at the raffinate end, stage r , and stepping toward the feed stage f (Fig. 15-17). A similar procedure is repeated for component c (Fig. 15-18).

The feed-stage number is found by matching the concentrations and stage number. This occurs at the point where the feed should be introduced (see Treybal, *Mass-Transfer Operations*, 3d ed., McGraw-Hill, New York, 1980). The procedure for matching concentrations is carried out by plotting the stage number on the vertical axis and the raffinate concentration X for each component (Fig. 15-19). The concentrations are matched when the rectangle $HJLK$ can be drawn as shown. The number of stages in the wash section including the feed stage is determined from the position of line HJ . The total number of stages r is determined from the position of LK , which is also at the feed stage.

The solute concentrations can be seen to be highest at the feed stage (Figs. 15-17 and 15-18). Also the solute concentrations increase as the number of theoretical stages is increased. For a given flow rate of feed, the flow rates of the solvents entering the extraction must be sufficiently high so that neither solubility limits nor a plait point is exceeded, nor a pinch point is reached between the operating lines and the equilibrium lines. The presence of solvents in the feed stream will change the slope of one or both of the operating lines, and several ratios of extraction solvent to wash solvent may have to be evaluated to find the optimum. The final optimization is usually carried out in pilot-plant equipment. Theoretically the use of solute reflux to the ends of the extraction cascade can reduce the number of theoretical stages required by a factor of 2 according to Brian (*Staged Cascades in Chemical Processing*, Englewood Cliffs, N.J., 1972), but again the amount of solvent flow rates may have to be increased to avoid a pinch point or plait point near the feed stage.


 FIG. 15-18 Graphical calculation of fractionation stages for solute c .

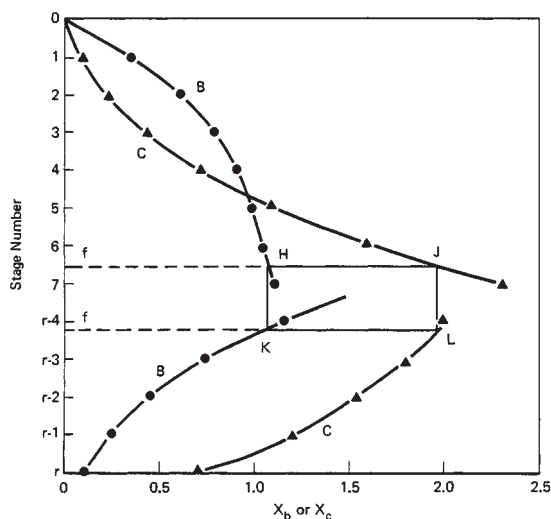


FIG. 15-19 Matching concentrations at the feed stage.

COUNTERCURRENT LIQUID-LIQUID HEAT TRANSFER

Heat may be transferred between two insoluble liquids in countercurrent flow through an extractor, and the performance can be evaluated in the same general manner as in mass transfer (Fig. 15-20). For a differential contactor the number of overall heat-transfer units based on the hot phase N_{oh} can be derived from the same equations used for the number of mass-transfer units based on the feed (raffinate) phase [Eq. (15-36)].

$$N_{oh} = \int_{T_r}^{T_f} \frac{dT}{T-t} = \frac{Z_t}{N_{oh}} = \frac{Z_t U_o a_r A_t}{F C_r} \quad (15-36)$$

where T = temperature of the hot (raffinate) phase, t = temperature of

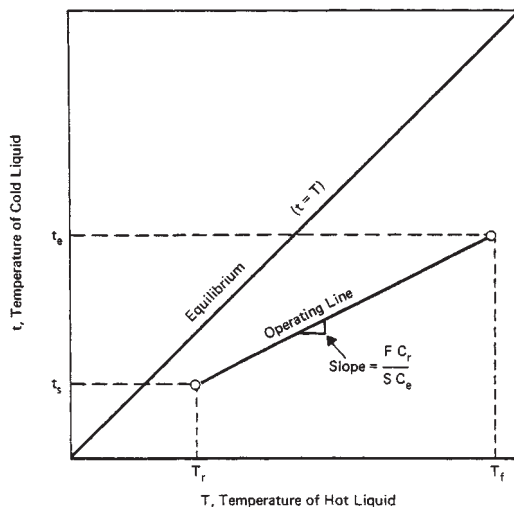


FIG. 15-20 Countercurrent heat transfer.

the cold (extract) phase, Z_t = height of tower, H_{oh} = height of an overall heat-transfer unit based on the hot (raffinate) phase, U_o = overall heat-transfer coefficient, a_r = heat-transfer surface of the droplets per volume, A_t = cross-sectional area of tower, F = hot feed rate, and C_r = heat capacity of raffinate and feed. The solution to the integral in Eq. (15-36) is identical with Eqs. (15-23) and (15-24), where $X_f = T_f$, $X_r = T_r$, $Y_s = T_s$, $E = SC_r/FC_r$, S = cold solvent rate, and C_e = heat capacity of solvent and extract. The slope of the equilibrium line $m = dT/dt = 1.0$ since $t = T$ at equilibrium. The height of a heat transfer unit H_{oh} is reported by Von Berg [in C. Hanson (ed.), *Recent Advances in Liquid-Liquid Extraction*, Pergamon, New York, 1971, chap. 11] to be shorter than the height of a mass-transfer unit H_{or} by a factor of 3 to 20. As an alternative, the Kremser equations [Eqs. (15-14) and (15-15)] could be used to calculate the number of theoretical heat-transfer stages.

LIQUID-LIQUID EXTRACTION EQUIPMENT

Liquid-liquid contacting equipment may be generally classified into two categories: **stagewise** and **continuous (differential) contact**.

STAGewise EQUIPMENT (MIXER-SETTLERS)

The function of a stage is to contact the liquids, allow equilibrium to be approached, and to make a mechanical separation of the liquids. The contacting and separating correspond to mixing the liquids, and settling the resulting dispersion; so these devices are usually called **mixer-settlers**. The operation may be carried out in batch fashion or with continuous flow. If batch, it is likely that the same vessel will serve for both mixing and settling, whereas if continuous, separate vessels are usually but not always used.

In principle, at least, any mixer may be coupled with any settler to provide the complete stage. There are several combinations which are especially popular. Continuously operated devices usually, but not always, place the mixing and settling functions in separate vessels. Batch-operated devices may use the same vessel alternately for the separate functions.

RATES OF MASS TRANSFER

Measurements simply of the extent of extraction in an agitated vessel lead to the overall "volumetric" mass-transfer coefficients, K_{caw} or

K_{Da_w} , or the equivalent stage efficiency. The coefficients K_C and K_D are made up of the coefficients for the individual liquids, k_c and k_D :

$$\frac{1}{K_D} = \frac{1}{k_D} + \frac{1}{m'_{CD} k_C}; \quad \frac{1}{K_C} = \frac{1}{k_C} + \frac{m'_{CD}}{k_D} \quad (15-37)$$

The evidence is that the coefficients k_C and k_D and the interfacial area a_w depend differently upon operating variables. For purposes of design, therefore, it is ultimately necessary to have separate information on the quantities k_C , k_D , and a_w . The role of an additional surface resistance is emphasized by the studies of Kishinevski and Moehalova [Zh. Prikl. Khim., **33**, 2049 (1960)].

Information on the coefficients is relatively undeveloped. They are evidently strongly influenced by rate of drop coalescence and breakup, presence of surface-active agents, "interfacial turbulence" (Marangoni effect), drop-size distribution, and the like, none of which can be effectively evaluated at this time.

Continuous-Phase Coefficients There have been a large number of measurements of k_C for solid particles and gas bubbles suspended in agitated liquids [for review, see Miller, *Ind. Eng. Chem.*, **56**(10), 18 (1964)]. A typical correlation of these data is that of Calderbank and Moo-Young [*Chem. Eng. Sci.*, **16**, 39 (1961)]:

$$k_{Csc}^{2/3} = 0.13(P\mu_{CG}/\nu\rho^2)^{1/4} \quad (15-38)$$

Schindler and Treybal [*Am. Inst. Chem. Eng. J.*, **14**, 790 (1968)], how-

ever, found that for liquid dispersions of ethyl acetate saturated with water, agitated in water by flat-blade turbine impellers, k_C was appreciably larger than that given by Eq. (15-38) for baffled vessels and even higher for unbaffled vessels (no air-liquid interface). The increase was attributed to the rate of coalescence of the droplets as the dispersion emerged from the impeller and recirculated through the tank and to their redispersion at the impeller. It was described by an expression of the form

$$k_C = k_S + C(D_C/\theta_C)^{0.5} \quad (15-39)$$

where k_S was calculated from Harriott's data for small-diameter solids [Harriott, *Am. Inst. Chem. Eng. J.*, **8**, 93 (1962)]. The continuous phase was found to be completely back-mixed and of uniform composition throughout for both baffled and unbaffled vessels.

Dispersed-Phase Coefficients There have been no direct measurements of k_D for liquid dispersions in agitated vessels. If the drops are small (as they usually are), internal circulation causes them to behave like rigid spheres with an enhanced diffusivity D_D . In stirred vessels, the ratio D_D/D_p has been estimated to lie in the range of about 1:2 [Olney, *Am. Inst. Chem. Eng. J.*, **7**, 348 (1961); Treybal *Liquid Extraction*, 2d ed., McGraw-Hill, New York, 1963]. For a pump-mix impeller (Fig. 15-28), Coughlin and von Berg [Chem. Eng. Sci., **21**, 3 (1966)], on the other hand, estimate k_D to be higher than that for circulating drops but not so large as that for oscillating drops (see below). These estimates do not take into account drop coalescence, interfacial turbulence, etc.; they are based on an assumed value for k_C and measured overall coefficients.

Overall Coefficients and Stage Efficiency If it is assumed that values of a_{ws} , k_C , k_D (and therefore K_D) can somehow be estimated, the stage efficiency can be calculated through

$$E_{MD} = 1 - \exp\left(-\frac{K_D a_{ws} Z}{V_D}\right) = 1 - \exp\left[-\frac{K_D a_{ws} \theta (V_C + V_D)}{V_D}\right] \quad (15-40)$$

See also Treybal [*Am. Inst. Chem. Eng. J.*, **4**, 202 (1958); **6**, 5M (1960)] and Ölander [Chem. Eng. Sci., **18**, 47 (1963); **19**, 275 (1964)]. The remaining discussion is confined to measured values of stage efficiency or volumetric overall coefficients. These are largely of value only for the particular systems studied. For this reason, one fairly complete study will be described, and the others will only be mentioned.

Figure 15-21 summarizes the results for the extraction of *n*-butylamine from kerosine into water in a continuously operated mixer [$T = 0.37$ m (1.23 ft); $Z = 0.48$ m (1.562 ft)] fed cocurrently upward, with and without four wall baffles and with a variety of impellers [Overcashier, Kingsley, and Olney, *Am. Inst. Chem. Eng. J.*, **2**, 529 (1956)]. When unbaffled, the vessel was full and without an air-liquid interface. E_O represents the overall countercurrent efficiency of a single stage. E_O at zero agitator speed was 0.18 at a liquid residence time of 1.08 min. The improved performance in the absence of baffles may be attributed to the reduction in back mixing and to the reduced power requirement for a given impeller speed. In the absence of baffles, vertical location of the impeller is immaterial. With baffles, the best performance is given with the impeller at 0.667 Z from the bottom, the worst at 0.25 Z from the bottom. For the spiral turbine, wall baffles and stator-ring baffles produced the same power-efficiency relationship. Off-center unbaffled operation at a propeller was intermediate between centered baffled and centered unbaffled operation. The data for propellers, spiral turbines, and flat-blade turbines, $d_i = 0.10$ to 0.25 m (0.333 to 0.833 ft), in both unbaffled and baffled tanks, with a flow rate to produce a residence time $\theta = 0.18$ h, kerosine-water ratio = 1.57 by volume, are empirically correlated by

$$E_O = 1 - \frac{0.318(10^{15})(d_i/d_p)^b}{N_{Re}^{3.2} N_{Fr}^{1.37}} \quad (15-41)$$

where $b = 0$ for baffled operation and 1.6 for unbaffled operation.

Other detailed studies are the following:

1. Hixson and Smith [*Ind. Eng. Chem.*, **41**, 973 (1949)]. Batch extraction of iodine from water into carbon tetrachloride; unbaffled vessels, propeller agitated. Log $(1 - E)$ is linear with time.

2. Karr and Scheibel [Chem. Eng. Prog., **50**, Symp. Ser. 10, 73 (1954)]. Continuous extraction of acetic acid between methyl isobutyl ketone and water, and

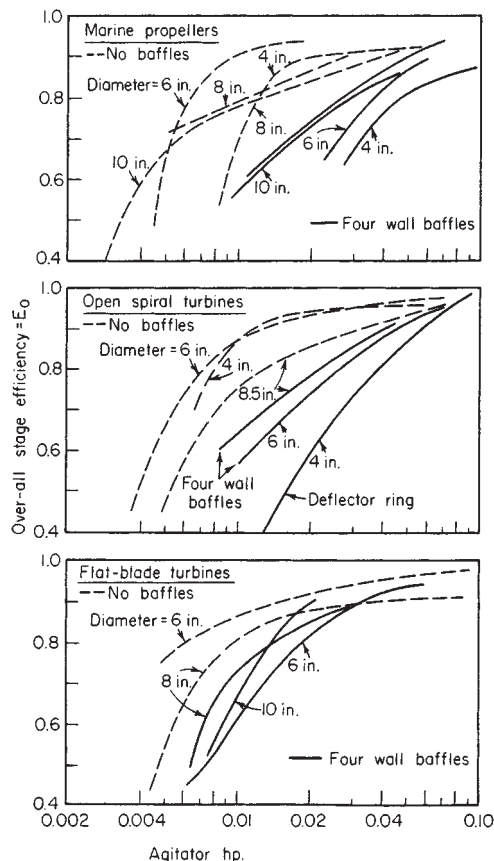


FIG. 15-21 Continuous extraction of *n*-butylamine from kerosine into water. $T = 1.23$ ft, $Z = 1.56$ ft, no air-liquid interface, impellers centered, $V_R/V_E \times 1.57$, residence time $\times 1.08$ min. To convert feet to meters, multiply by 0.3048; to convert inches to centimeters, multiply by 2.54; and to convert horsepower to kilowatts, multiply by 0.746. [Overcashier, Kingsley, and Olney, *Am. Inst. Chem. Eng. J.*, **2**, 529 (1956), with permission.]

xylene and water, and of acetone between xylene and water; unbaffled vessels consisting of the unpacked section of the extractor of Fig. 15-44. Rate of extraction is larger when organic liquid is dispersed in the extractant than with other arrangements.

3. Flynn and Treybal [*Am. Inst. Chem. Eng. J.*, **1**, 324 (1955)]. Continuous extraction of benzoic acid from toluene and kerosine into water; baffled vessels, turbine agitators. Stage efficiency is correlated with agitator energy per unit of liquid treated.

4. Mottel and Colvin (U.S. AEC DP-254, 1957). Continuous heat transfer between kerosine and water; vessel of Pump-Mix design (Fig. 15-28).

5. Ryon, Daley, and Lowrie [Chem. Eng. Prog., **55**(10), 70, (1959), U.S. AFC ORNL-2951, 1960]. Continuous extraction of uranium from sulfate-ore-leach liquors and kerosine + tributyl phosphate and di(2-ethylhexyl)-phosphoric acid; baffled vessels, turbine agitated. There is strong evidence of the influence of a slow chemical reaction.

6. Ryon and Lowrie (U.S. AEC ORNL-3381, 1960). Batch and continuous extraction of uranium from aqueous sulfate solutions into kerosine + amines, stripping of extract with aqueous sodium carbonate; baffled vessels, turbine agitated. A detailed process study.

7. David and Colvin [Am. Inst. Chem. Eng. J., **7**, 72 (1961)]. Continuous heat transfer between kerosine and water; unbaffled vessel. Open impellers (paddles and propellers) are better than closed (centrifugal and disk impellers) at the same tip speed.

8. Simard et al. [Can. J. Chem. Eng., **39**, 229 (1961)]. Continuous extraction of uranium from aqueous nitrate solutions into kerosine + tributyl phosphate and from sulfate solutions containing triacrylamine; unbaffled vessel, propeller agitated. Process details for high recovery and low reagent costs.

9. Rushton, Nagata, and Rooney [Am. Inst. Chem. Eng. J., **10**, 298 (1964)].

Batch extraction of octanoic acid from water and corn syrup into xylene, paraffin oil, and their mixtures; baffled vessel, turbine impeller. K_{ca_w} proportional to $N^{2.1} \mu_c^{0.6} \mu_D^{-0.55}$.

10. Coughlin and von Berg [Chem. Eng. Sci., **21**, 3 (1966)]. Continuous heat transfer and extraction of ethylbutyric acid between kerosine and water; unbaffled vessel, Pump-Mix design (Fig. 15-28). Interfacial area measured.

Scale-Up of Mixers For the details associated with the design and scale-up of agitated vessels, the reader is referred to Section 18 which covers this topic in great detail. The intention here is to provide only some of the general principles involved which have particular application to liquid-liquid extraction.

For extraction, the mixing usually takes place either in a vessel which also serves as the settler (these can be baffled or unbaffled), or a separate mixing compartment (usually baffled if there is a gas-liquid interface, and usually unbaffled if it is liquid filled).

The most common impellers are the marine impeller or disc flat-blade turbine; the flow patterns which typically result are illustrated in Fig. 15-22.

The power for agitation of two-phase mixtures in vessels such as these is given by the curves in Fig. 15-23. At low levels of power input, the dispersed phase holdup in the vessel (ϕ_D) can be less than the value in the feed (ϕ_{DF}); it will approach the value in the feed as the agitation is increased. Treybal (*Mass Transfer Operations*, 3d ed., McGraw-Hill, New York, 1980) gives the following correlations for estimation of the dispersed phase holdup based on power and physical properties for disc flat-blade turbines:

Baffled vessels, impeller power/vessel volume $> 105 \text{ W/m}^3 = 2.2 \text{ ft lb}_f/\text{ft}^3\cdot\text{s}$:

$$\frac{\phi_D}{\phi_{DF}} = 0.764 \left(\frac{P q_D \mu_c^2}{v_L \sigma^3 g_c} \right)^{0.300} \left(\frac{\mu_c^3}{q_D \rho_c^2 \sigma g_c} \right)^{0.178} \left(\frac{\rho_c}{\Delta \rho} \right)^{0.0741} \times \left(\frac{\sigma^3 \rho_c g_c^3}{\mu_c^4 g} \right)^{0.276} \left(\frac{\mu_D}{\mu_c} \right)^{0.136} \quad (15-42)$$

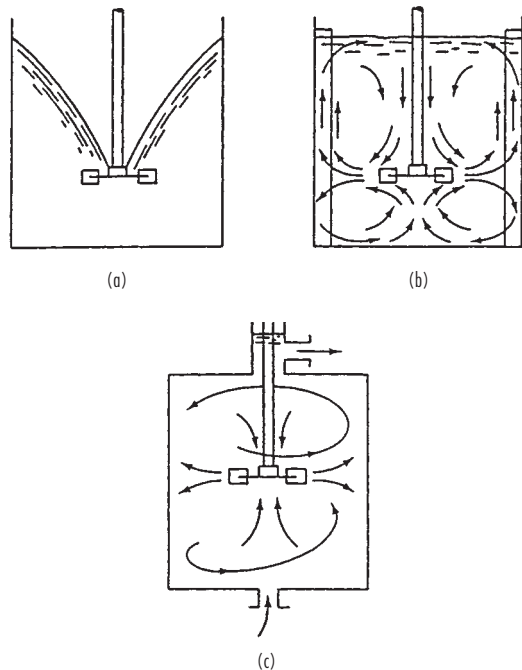


FIG. 15-22 Liquid agitation by a disc flat blade turbine in the presence of a gas-liquid interface (a) without wall baffles, (b) with wall baffles, and (c) in full vessels without a gas-liquid interface (continuous flow) and without baffles. [Courtesy Treybal, *Mass Transfer Operations*, 3rd ed., p. 148, McGraw-Hill, NY, (1980).]

Unbaffled vessels, full, no gas-liquid surface, no vortex:

$$\frac{\phi_D}{\phi_{DF}} = 3.39 \left(\frac{P q_D \mu_c^2}{v_L \sigma^3 g_c} \right)^{0.247} \left(\frac{\mu_c^3}{q_D \rho_c^2 \sigma g_c} \right)^{0.427} \left(\frac{\rho_c}{\Delta \rho} \right)^{0.430} \times \left(\frac{\sigma^3 \rho_c g_c^3}{\mu_c^4 g} \right)^{0.401} \left(\frac{\mu_D}{\mu_c} \right)^{0.0987} \quad (15-43)$$

He then recommends that the following relationships be used to estimate the mixture average density and viscosity for the power calculations:

Baffled vessels:

$$\rho_M = \rho_c \phi_c + \rho_D \phi_D \quad (15-44)$$

$$\mu_M = \frac{\mu_c}{\phi_c} \left(1 + \frac{1.5 \mu_D \phi_D}{\mu_c + \mu_D} \right) \quad (15-45)$$

Unbaffled vessels, no gas-liquid interface, no vortex:

$$\mu_M = \begin{cases} \frac{\mu_c}{\phi_c} \left(1 + \frac{6 \mu_o \phi_o}{\mu_o + \mu_c} \right); & \phi_w > 0.4 \\ \frac{\mu_o}{\phi_o} \left(1 - \frac{1.5 \mu_c \phi_w}{\mu_o + \mu_c} \right); & \phi_w < 0.4 \end{cases} \quad (15-46a)$$

$$(15-46b)$$

In scale-up, there are three types of similarity to be considered:

1. *Geometric similarity.* Two vessels are geometrically similar if the ratio of all corresponding dimensions is the same

2. *Kinematic similarity.* Two vessels are kinematically similar if they are first geometrically similar and have the same ratio of velocities in corresponding positions of the vessel

3. *Dynamic similarity.* Two vessels are dynamically similar if they are first kinematically similar and all force ratios are equal in corresponding positions of the vessel

For most liquid-liquid extraction applications, the mixing section is usually scaled up on the principle of geometric similarity, and the power is based on maintaining the same power per unit volume. Treybal [*Chem. Eng. Prog.*, **62**(9), 67 (1966)] demonstrates that, for geometrically similar vessels with equal holding time and power per unit volume, the stage efficiency for liquid extraction is likely to increase on scale-up, so this is generally a conservative approach.

Because of the difficulty in obtaining good data on mass-transfer coefficients and interfacial area as outlined earlier, it is necessary that bench or pilot scale experiments be performed to obtain the data needed for scale-up. The usual procedure is to determine a suitable range of residence times at various power inputs for a given mixer geometry. Most extractions are mass-transfer limited, so relatively short residence times are adequate (in the range of 1–3 minutes). However in some cases (such as metal extractions), there is actually a reactive-extraction taking place, and residence time becomes more critical; times in the range of 10–15 minutes are not unusual.

Besides looking at just the mixing, it is important at this time to also consider the settling time of the phases after mixing since this will impact on the settler design. Higher intensity of mixing may decrease the residence time for mass transfer, but at the same time create fine dispersions which are difficult to settle.

With the batch data, Slater and Godfrey in Lo, Baird, and Hanson, *Handbook of Solvent Extraction*, Wiley, New York, 1983, recommend that an approach to equilibrium be used to provide the fundamental basis for scale-up; they define the approach to equilibrium (E_f) as:

$$E = \frac{C_i - C_t}{C_i - C_e} \quad (15-47)$$

It has been found that this data can be correlated for batch extraction using the following correlation:

$$1 - E_b = e^{(-kt_b)} \quad (15-48)$$

Once the value of k is obtained from the batch data, it can be related to a continuous extraction via the correlation:

$$E_f = \frac{kt_c}{1 + kt_c} \quad (15-49)$$

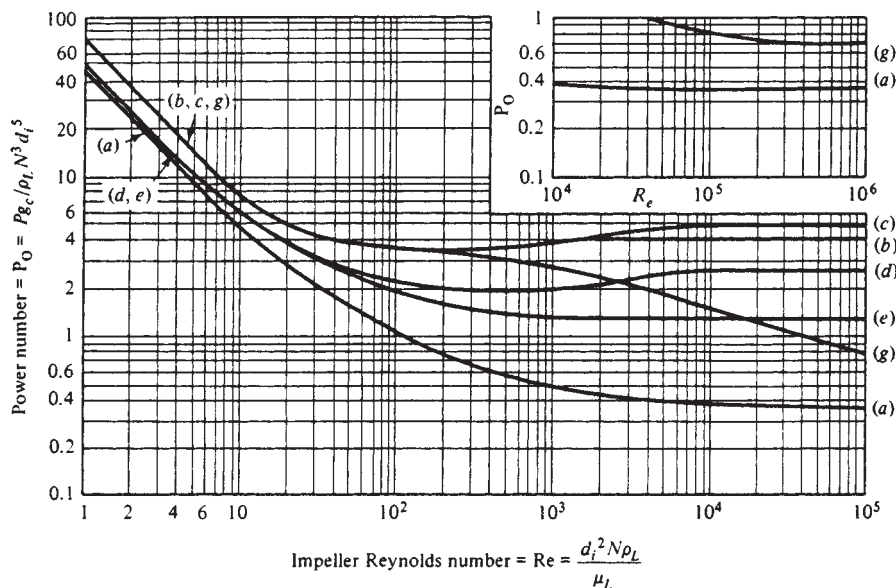


FIG. 15-23 Power for agitation impellers immersed in single-phase liquids, baffled vessels with a gas-liquid surface [except curves (c) and (g)]. Curves correspond to: (a) marine impellers, (b) flat-blade turbines, $w = d_i/5$, (c) disk flat-blade turbines with and without a gas-liquid surface, (d) curved-blade turbines, (e) pitched-blade turbines, (g) flat-blade turbines, no baffles, no gas-liquid interface, no vortex.

Notes on Fig. 15-23

1. The power P is only that imparted to the liquid by the impeller. It is not that delivered to the motor drive, which additionally includes losses in the motor and speed-reducing gear. These may total 30 to 40 percent of P . A stuffing box where the shaft enters a covered vessel causes additional losses.
2. All the curves are for axial impeller shafts, with liquid depth Z equal to the tank diameter d_t .
3. Curves a to e are for open vessels, with a gas-liquid surface, fitted with four baffles, $b = d_i/10$ to $d_i/12$.
4. Curve a is for marine propellers, $d_i/d_t = 1/5$, set a distance $C = d_i$, or greater from the bottom of the vessel. The effect of changing d_i/d_t is apparently felt only at very high Reynolds numbers and is not well established.
5. Curves b to e are for turbines located at a distance $C = d_i$, or greater from the bottom of the vessel. For disk flat-blade turbines, curve c , there is essentially no effect of d_i/d_t in the range 0.15 to 0.50. For open types, curve b , the effect of d_i/d_t may be strong, depending upon the group nb/d_i .
6. Curve g is for disk flat-blade turbines operated in unbaffled vessels filled with liquid, covered, so that no vortex forms. If baffles are present, the power characteristics at high Reynolds numbers are essentially the same as curve b for baffled open vessels, with only a slight increase in power.
7. For very deep tanks, two impellers are sometimes mounted on the same shaft, one above the other. For the flat-blade disk turbines, at a spacing equal to $1.5d_i$, or greater, the combined power for both will approximate twice that for a single turbine.
8. SOURCE: Treybal, *Mass Transfer Operations*, 3d ed., p. 152, McGraw-Hill, NY, 1963.

where E = approach to equilibrium of a single-stage contact
 C_i = initial concentration
 C_t = concentration of time t
 C_e = concentration of equilibrium
 E_b = approach to equilibrium for a batch process
 E_r = approach to equilibrium for a continuous process
 t_b = mixing time for a batch process
 t_c = residence time for a continuous process

Having established the residence time and power input, the scale-up can be now done using the principle of geometric similarity together with equal power per unit volume discussed earlier.

The above covers most conventional mixers; there is another class of mixers, called pump-mix impellers, where the impeller serves not only to mix the fluids, but also to move the fluids through the extraction stages. These are specialized designs, often used in the metals extraction industries. For these types of impellers, a knowledge of the power characteristics for pumping is required in addition to that for mixing. For a more detailed treatment of these special cases, the reader is referred to Lo et al.

Recycling some of one of the settled liquids back to the agitated

vessel sometimes improves settling of the dispersion. In addition, the stage efficiency of a stirred vessel can be considerably enhanced by recycling the liquid favored by solute distribution, whereas recycling the other liquid reduces the stage efficiency. When solute distribution favors the dispersed phase and mass-transfer rates are poor, recycling the settled dispersed phase can result in minimizing the volume of a cascade of extraction vessels [Treybal, *Ind. Eng. Chem. Fundam.*, **3**, 185 (1964)]. See also Gel'perin et al. (*Khim. Neft. Mashinostr.*, 1966, 23).

Extractive reaction, in which a solvent extracts one of the products to enhance the yield, is considered by Piret, Trambouze, et al. [*Am. Inst. Chem. Eng. J.*, **6**, 394, 574 (1960); **7**, 138 (1961)]. See also Schmitz and Amundsen [*Chem. Eng. Sci.*, **18**, 265, 415, 447 (1963)].

SETTLERS

Emulsions and Dispersions The mixture of liquids leaving a mixer is a cloudy dispersion which must be settled, coalesced, and separated into its liquid phases in order to be withdrawn as separate liquids from a stage. For a dispersion to "break" into separate phases, both sedimentation and coalescence of the drops of the dispersed

phase must occur. Unstable dispersions usually have droplet diameters of about 1 mm or larger and settle rapidly. Stable dispersions, or emulsions, are generally characterized by droplet diameters of about 1 μm or less. The unstable dispersions are preferred in liquid-liquid-extraction operations and chemical-reaction systems involving two liquid phases that ultimately need to be separated. Dispersions and emulsions are usually characterized by the terms **water-in-oil** (meaning aqueous liquid droplets dispersed in organic liquid continuous phase) and **oil-in-water** (organic droplets in aqueous liquid). **Dual emulsions** and **liquid-membrane systems** are those in which the continuous phase is also present as very small droplets within larger drops of the other liquid. See Becher, *Emulsions: Theory and Practice*, ACS Monogr. 175, Reinhold, New York, 1957; and Li and Shrier, in Li (ed.), *Recent Developments in Separation Science*, vol. I, CRC Press, Cleveland, 1972, p. 163.

The "breaking" of a dispersion in a batch settler may be divided into two periods: (1) primary break, or rapid settling and coalescence of most of the dispersed phase, which often leaves a fog of very small droplets suspended as parts per million in the majority phase; and (2) secondary break, which represents the slow settling of the fog. Most industrial settlers are designed for the primary break since the slow secondary break would require much longer residence times. The small amount of entrainment to a subsequent stage seldom influences stage efficiency in a multistage cascade. However, for conserving solvent and desolventizing the effluent streams from the final stages of a cascade, it may be necessary to clarify as completely as possible, including the use of coalescers to eliminate secondary fog.

Sedimentation Isolated droplets, settling or rising in a stagnant liquid under the force of gravity, generally move more rapidly than solid spheres. The rate of settling or rising is more rapid for large droplet size, large density difference between phases, and low viscosity of the continuous phase. Felix and Holder [*Am. Inst. Chem. Eng. J.*, **1**, 296 (1955)] show considerably shorter settling time of petroleum-oil dispersions in water and phenol by reducing the continuous-phase viscosity simply by raising the temperature.

Coalescence The coalescence of droplets can occur whenever two or more droplets collide and remain in contact long enough for the continuous-phase film to become so thin that a hole develops and allows the liquid to become one body. A clean system with a high interfacial tension will generally coalesce quite rapidly. Particulates and polymeric films tend to accumulate at droplet surfaces and reduce the rate of coalescence. This can lead to the buildup of a "rag" layer at the liquid-liquid interface in an extractor. Rapid drop breakup and rapid coalescence can significantly enhance the rate of mass transfer between phases.

Gravity Settlers; Decanters These are tanks in which a liquid-liquid dispersion is continuously settled and coalesced and from which the settled liquids are continuously withdrawn. They can be either horizontal or vertical. Figure 15-24 shows some typical horizontal decanters. For an uninstrumented decanter the height of the heavy-phase-liquid leg above the interface is balanced against the height of the light-liquid phase above the interface, Eq. 15-50.

$$(Z_h - Z_i)\rho_h = (Z_L - Z_i)\rho_L \quad (15-50)$$

The velocity of the liquid entering the decanter should be kept low to minimize disturbance of the interface. Sometimes an impingement baffle, or "picket fence," has been used. In other cases, opposing inlets as in Fig. 15-24c and d have been used. For an external jackleg shown in Fig. 15-24a the heavy-liquid takeoff requires a siphon break to prevent emptying the vessel by siphoning. Some problems can occur because of pressure drop through the outlet piping and variable levels under flow conditions. The horizontal weirs in Fig. 15-24b and the circular weirs in Fig. 15-24c can be designed for a very low crest height at maximum design flow rates. When rag builds up at the interface, sometimes it can be purged by withdrawing a small stream, filtering out the solids, and returning the liquids to the decanter. The decanter can also be instrumented with an interface detector and automatic control valve on the heavy-phase flow. The light phase can still overflow from the vessel.

For general reviews, see Ingersoll [*Pet. Refiner*, **30**(6), (1951)] and Hart [*Pet. Process.*, **2**, 282, 471, 513, 632 (1947)]. In the petroleum industry, settler volumes have frequently been sufficiently large so as to provide a holding time from 0.5 to 1.0 h, which in most cases is probably excessive and costly. For most thin liquids, in which unusual emulsification problems do not occur, 5 to 10 min is ample. The size of the settler seems to be set by the rate of flow per unit of horizontal cross-sectional area as well as holding time [Williams et al., *Trans. Inst. Chem. Eng. (London)*, **36**, 464 (1958)]; Ryon, Daley, and Lowrie [*Chem. Eng. Prog.*, **55**(10), 70 (1959)], for the settling of aqueous uranium solutions and kerosene-alkyl phosphate solvents, used decanters of the type shown in Fig. 15-24b. The depth of the decanter having been chosen, these authors recommend that the horizontal cross section for the prevailing flow rate be set at twice the value which would give a dispersion-band thickness equal to the depth of the tank. In this manner dispersions of 9.08 m³/h aqueous + 15.90 m³/h solvent (40 gal/min aqueous + 70 gal/min solvent) were successfully settled in a decanter of 1.4-min holding time.

Gravity settlers, basically of the type shown in Fig. 15-24a, were used by Wilke et al. (UCRL-10625, 1963; UCRL-11182, 1964) to settle water and Aroclor (specific gravity, 1.36). The dispersion may

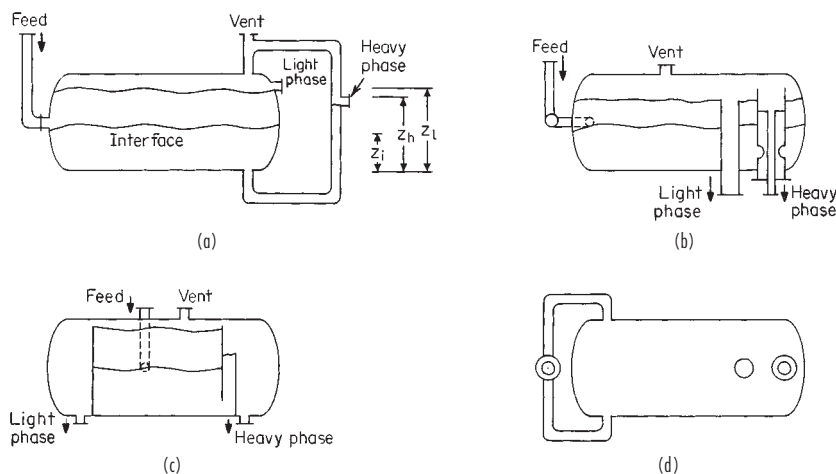


FIG. 15-24 Gravity decanters. (a) External jackleg, side view. (b) Straight weirs, side view. (c) Circular weirs, side view. (d) Circular weirs, top view.

occupy a wedge-shaped volume in the region of the interface at low flow rates instead of covering the entire interface as for higher flow rates. Important variables influencing the performance are (1) the value of ϕ_D in the entering liquid mixture, (2) whether the dispersion is introduced above or below the interface, and (3) the distance of an impact baffle from the inlet pipe. The length of the dispersion wedge for kerosine-water (dispersed) is proportional to V_D/d_p^3 (Jeffreys and Pitt, paper at AIChE meeting, Salt Lake City, May 1967). Higher temperatures (to decrease viscosity) and longer residence times within each phase improve the settling of water (dispersed)-coconut fatty acids [Manchanda and Woods, *Ind. Eng. Chem. Process Des. Dev.*, **7**, 182 (1968)].

In the extraction of uranium from ore leach liquors with kerosine-reagent solvents, there is a saving in the cost of thickeners and filters if the aqueous liquors are not clarified before extraction. If such slurries are extracted, however, it is necessary to increase the solvent-aqueous ratio in the extractor in order to make the organic phase continuous; otherwise, unseparable emulsions are produced. Table 15-6 gives the data of Shaw and Long [Chem. Eng., **64**(11), 251 (1957)] for settling areas required for such extractions. The high organic-aqueous ratios are obtained by recycling settled organic phase from the settler to the mixer. Entrainment of organic solvent with the settled solids represents a serious problem in such operations.

TABLE 15-6 Settling of Aqueous Uranium Leach Liquors with Kerosine-Alkyl Phosphate Solvent*

Nature of aqueous feed	Organic-aqueous ratio required	Permissible settler flow rate, U.S. gal/(min-ft ²) horizontal area
Clear liquor	4	1.4-1.6
Slimes (5% solids)	8	0.6
Dense pulps (50-60% solids)	10	0.3

*Shaw and Long, *Chem. Eng.*, **64**(11), 251 (1957).

To convert gallons per minute-square foot to cubic meters per hour-square meter, multiply by 2.44.

CYCLONES

Cyclones have been suggested as simple means of enhancing by centrifugal force the rate of settling of liquid dispersions. Tepe and Woods (U.S. AEC AEC-D-2864, 1943) report a few data for the separation of isobutanol-water dispersions in such devices, but the results were poor. The most thorough studies are those of Simkin and Olney [*Am. Inst. Chem. Eng. J.*, **2**, 545 (1956)] and of Hitchon [At. Energy Res. Etab. (Gt. Brit.) CE/R-2777, 1959], who conclude that high extraction efficiencies (requiring high degrees of dispersion) and good clarification of both effluents cannot be obtained in one stage. Tepe and Woods (loc. cit.) also tried *helical coils of pipe* for separating isobutanol-water mixtures, with poor results.

CENTRIFUGES

Mechanical centrifuges, high-speed machines, have been used for many years for separating liquid-liquid dispersions, for example, in the separation of caustic solutions and oils in the soap-making process, more recently in uranium extractions, and in many others. By enhancing the settling rate (without, however, influencing coalescence), they reduce the settling time considerably. See, for example, Landis [*Chem. Eng. Prog.*, **61**(10), 58 (1965)]. For details see Section 19.

SETTLER AUXILIARIES

These include the use of coalescers, separating membranes, and electrical devices and the addition of emulsion-breaking reagents. These last are used for treating permanent emulsions and will not be discussed here.

Coalescers The small drops of a fine dispersion may be caused to coalesce and thus become larger by passing the dispersion through a coalescer. The enlarged drops then settle more rapidly. Coalescers are mats, beds, or layers of porous or fibrous solids whose properties are

especially suited for the purpose at hand. In an extensive study, Sareen et al. [*Am. Inst. Chem. Eng. J.*, **12**, 1045 (1966)] found, in part, that (1) coalescence is promoted by decreased fiber diameter, (2) a minimum bed density is required to achieve complete coalescence, dependent upon the system characteristics, (3) wetting of the fibers by droplets of dispersed phase is not necessary for good coalescence, (4) a fibrous bed of medical cotton can be made to coalesce almost any kind of liquid dispersed in another except if $\sigma < 3$ mN/m (dyn/cm), (5) cotton fibers are best supported from collapse by mixing with fibers of glass or Dynel [see also Langdon et al., *Petro/Chem Eng.*, **1963**(11), 35], (6) the optimum bed thickness of a mixed bed depends on the ratio of cotton to support (0.75 in for 50 percent cotton), (7) the maximum velocity through the bed with effective coalescing increases with bed depth, but increased pressure drop causes redispersion, presumably at values depending upon the liquid system, and (8) some surfactants interfere with coalescence, but others do not. For tests on petroleum-brine emulsions and Fiberglass, see Burtis and Kirkbride [*Trans. Am. Inst. Chem. Eng.*, **42**, 413 (1946)] and Hayes et al. [*Chem. Eng. Prog.*, **45**, 235 (1949)]. Beds of granular solids such as sand, etc., and bats of excelsior, steel wool, and the like have also been used.

Separating Membranes If the capillary size of a porous substance is very small, the liquid which preferentially wets the solid may flow through the capillaries readily but strong interfacial films block the capillaries for flow of nonwetting liquid. Sufficient pressure will cause disruption of the films and permit passage of the nonwetting liquid, but regulation of the pressure commensurate with the pore size permits perfect phase separation. Separating membranes of this type are made of a variety of materials such as porcelain, paper which has been coated with special resins, and the like and may be either hydrophilic or hydrophobic in character. They are made thin so as to permit maximum passage of the wetting liquid [see Jordan, *Trans. Am. Soc. Mech. Eng.*, **77**, 393 (1955); and Belk, *Chem. Eng. Prog.*, **61**(10), 72 (1965)]. In practice, the dispersion is usually first passed through a coalescer so as to permit settling of the bulk of the dispersed phase before the mixture is presented to the separating membrane, thus relieving the load on the membrane.

Figure 15-25 shows a combination device containing coalescers and both hydrophobic and hydrophilic separating membranes. Coalescers

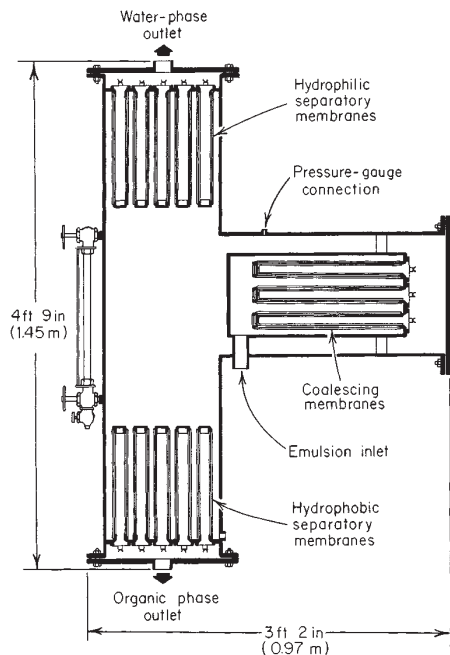


FIG. 15-25 Combination coalescer, settler, and membrane separator. (Courtesy of Sela Corporation of America.)

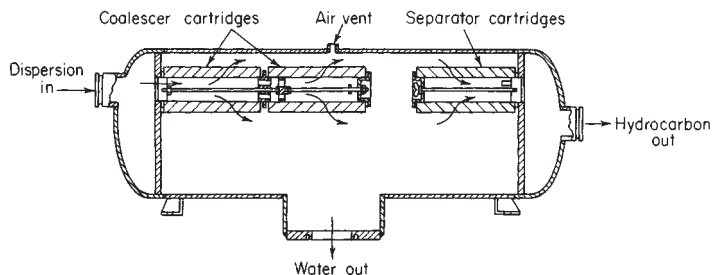


FIG. 15-26 Fuel-water separator. (Courtesy of Warner-Lewis Co. Division, Fram Corp.)

and separating membranes are fashioned in the form of hollow cylinders, and flow is radially through the wall. After passing through the coalescers, the bulk of the liquids settles in the vertical member of the device, and then the settled phases are passed through their respective separating membranes. Devices of this type are designed to handle 0.57 to 6.81 m³/h (150 to 1800 gal/h), delivering completely separated phases; and further settling is unnecessary. Figure 15-26 shows another design for removing dispersed water from jet fuel or gasoline, available in sizes to handle from 68 to 250 m³/h (300 to 1100 gal/min) and delivering clear effluents. In this case only a hydrophobic membrane is required [Redmon, *Chem. Eng. Prog.*, **59**(9), 87 (1963)].

Electrical Devices Subjecting electrically conducting emulsions or dispersions to high-voltage electric fields may cause rupture of the protective film about a droplet and thus induce coalescence. Dispersions of low conductivity are subject, in an electric field, to forces between particles resulting from acquired induced dipoles, which induce coalescence. These phenomena have been used particularly for the desalting of petroleum emulsified with brine, and for similar applications. Devices have been built to handle 828 m³/h (125,000 bbl/day) of crude oil, at costs of approximately 0.1 to 0.5 cent/bbl [Waterman, *Chem. Eng. Prog.*, **61**(10), 51 (1965)]. For a detailed study see Sjoblom and Goren [*Ind. Eng. Chem. Fundam.*, **5**, 519 (1966)] and Brown and Hanson [*Trans. Faraday Soc.*, **61**, 1754 (1965)]. Figure 15-27 shows schematically the flow through a typical device.

MIXER-SETTLER COMBINATIONS

Any mixer and settler can be combined to produce a stage, and the stages in turn arranged in a multistage cascade.

A great many commonly used arrangements have been developed in an effort to reduce or eliminate interstage pumping and to reduce costs generally. Only a few of the more commonly used types are mentioned here.

A compact alternating arrangement of mixers and settlers has been adopted in many of the "box-type" extractors developed originally for processing radioactive solutions, but now used in principle for many processes, with literally dozens of modifications. An example is the Pump-Mix mixer-settler (Fig. 15-28), in which adjacent stages have common walls [Coplan, Davidson, and Zebroski, *Chem. Eng. Prog.*, **50**, 403 (1954)]. The impellers in this case pump as well as mix by drawing the heavy liquid upward through the hollow impeller shaft and discharging it at a higher level through the hollow impeller. These extractors or variants of them have been built not only in relatively large sizes but also in miniature for bench-scale work.

Figure 15-29 represents still further modification for low cost [Hazen and Henrickson, *Min. Eng.*, 994 (1957); Quinn, Trefoil (Denver Equipment Company) Bull. M4-B90, 1957]. At *a* and *b* in the figure, the settler is a circular tank $d_t = 4.9$ m (16 ft), $Z = 2.1$ m (7 ft), with the mixing vessel, 1.2 by 1.2 m (4 by 4 ft), contained inside. Agitators are turbines, $d_i = 0.46$ m (1.5 ft), operated at 150 r/min (1.12 kW) and 200 r/min (2.02 kW). The aqueous feed is 22.7-m³/h (100-gal/min) uranium-bearing ore leach liquor, the organic solvent 4.5-m³/h (20-gal/min) alkyl phosphate solutions in kerosene. Adjacent stages are at 0.3-m (1-ft) elevation difference, allowing gravity flow of the aqueous liquor, while the organic phase is pumped in countercurrent by air

lifts. Provision is made for recycle of settled organic phase by overflow to the mixer, the amount of which can be adjusted by changing the height of the organic-overflow pipe. The vanadium extractor at *c* in the figure is a box type, built into a circular tank, $d_t = 9.8$ m (32 ft), $Z = 2.1$ m (7 ft). The 0.46-m- (18-in-) diameter turbines draw 5.6 kW (7.5 hp). Other modifications of the box-type mixer-settler (Denver Equipment Company, Denver, Bull. A1-B6), with capacities of from 0.23- to 5700-m³/h (1- to 25,000-gal/min) liquid flow, have been extensively used in a great variety of metal separations in process metallurgy. These provide for intrastage recycle of liquids, particularly advantageous when very low solvent-feed ratios typical of good solvents must be used and when it is desired to make the minority liquid continuous in order to improve settling characteristics. See also Williams et al. [*Trans. Inst. Chem. Eng. (London)*, **36**, 464 (1958)] and Hanson and Kaye [*Chem. Process Eng.*, **44**, 27, 654 (1963); **45**, 413 (1964)].

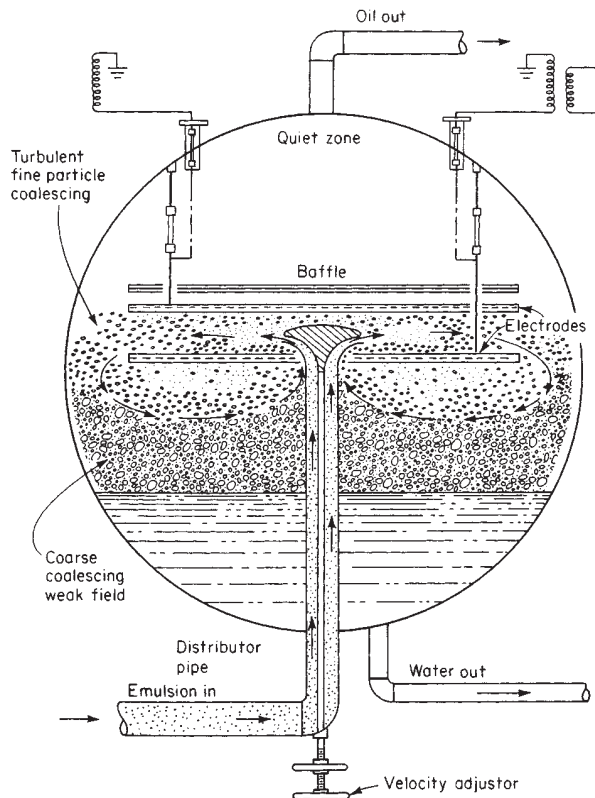


FIG. 15-27 Internal circulation and electric field, Petreco Cylelectric coalescer (schematic). [Waterman, *Chem. Eng.*, **61**(10), 51 (1965), with permission.]

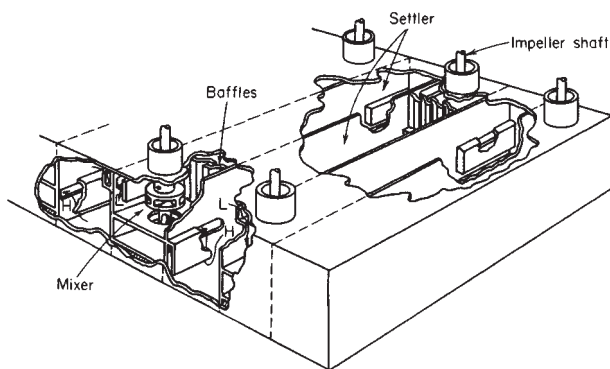


FIG. 15-28 Pump-Mix mixer-settler. [Coplan, Davidson, and Zebroski, *Chem. Eng. Prog.*, **50**, 403 (1954), with permission.]

Vertical arrangement of the stages is desirable, since then a single drive may be used for agitators and the floor-space requirement of a cascade is reduced to that of a single stage. See, for example, Hanson and Kaye, loc. cit. In the Lurgi extractor, the mixer and settlers are in separate vertical shells interconnected with piping [Guccione, *Chem. Eng.*, 78 (July 4, 1966)].

A great many other devices are known. The Fenske extractor [Fenske and Long, *Chem. Eng. Prog.*, **51**, 194 (1955); *Ind. Eng. Chem.*, **53**, 791 (1961); *Ind. Eng. Chem. Fundam.*, **1**, 152 (1962)] is a vertical stack of mixer-settler stages, with mixing done by a vertically moving reciprocating plate in each mixer. One very successful device, particularly in the extraction of radioactive solutions, uses a centrifuge instead of a settler to separate the mixed liquids, and the pump-mixer

and centrifuge of each stage operate on a common shaft [Clark, U.S. AEC DP-752 (1962); Kisbaugh, *ibid.*, DP-841 (1963)]. See also Goncharenko et al. (*Tr. Vses. Khemosorbtzii Nauchn-Tekhn. Sovesh. Protessy Zhidkostnoi Ekstraktsii Khemosorbtzii*, 2d, Leningrad, **1964**, 75) and Berestovoi et al. (*ibid.*, 171). Still another uses a cyclone (hydroclone) for separating [Whatley and Woods, U.S. AEC ORNL-3533 (1964); Finsterwalder, *ibid.*, ORNL-4088 (1967)]. The Graesser extractor (Coleby, U.S. Patent 3,017,253, 1962) is a horizontal shell filled with stratified settled liquids, with a series of buckets revolving around the inner periphery which rain droplets of one liquid through the other. It has been used primarily in Europe for easily emulsified liquids.

Overall Stage Efficiencies The mixer-settler extractors described have generally produced overall stage efficiencies in excess of 80 percent, usually nearly 90 to 95 percent.

CONTINUOUS (DIFFERENTIAL) CONTACT EQUIPMENT

Equipment in this category is usually arranged for multistage countercurrent contact of the insoluble liquids, without repeated complete separation of the liquids from each other between stages or their equivalent. Instead, the liquids remain in continuous contact throughout their passage through the equipment.

General Characteristics Countercurrent flow is maintained by virtue of the difference in densities of the liquids and either the force of gravity (vertical towers) or centrifugal force (centrifugal extractors). Only one of the liquids may be pumped through the equipment at any desired velocity. The maximum velocity for the second is then fixed; if it is attempted to exceed this limit, the second liquid will be rejected and the extractor will be **flooded**.

It cannot be overemphasized that knowledge of the characteristics of such equipment is surprisingly underdeveloped. The number of quantities that influence the rate of extraction is very large, and many of them are not well understood. Most of the available data were taken

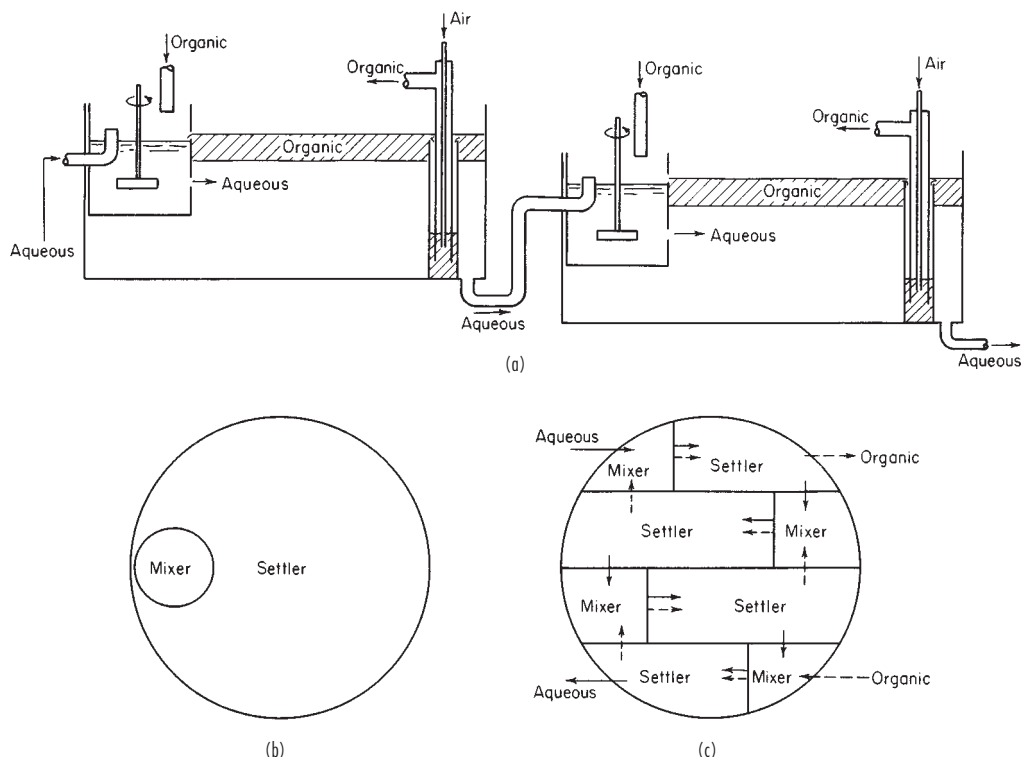


FIG. 15-29 Kerr-McGee multistage mixer-settler. (a) and (b) For uranium. (c) For vanadium extraction.

from small laboratory devices, frequently only a few inches in diameter and a few feet high. For these reasons the generalizations given here should be used only for very rough estimates, with allowance for generous factors of safety.

Axial Dispersion The devices in this category are subject to axial (longitudinal) dispersion within both liquids or departure from strictly "plug," countercurrent flow. The result of this axial mixing is to decrease the effective concentration driving force in the contactor as illustrated in Fig. 15-30. As a result, the towers must be taller than simple application of the plug-flow numbers of transfer units would indicate. The problem has been extensively studied by Sleicher [Am. Inst. Chem. Eng. J., **5**, 145 (1959)] and Vermeulen et al. [U.S. AEC UCRL-3911, 1958; suppl., 1958; 10928, 1963; Ind. Eng. Chem. Fundam., **2**, 113, 304 (1963); Chem. Eng. Prog., **62**(9), 95 (1966)]. The two studies lead to essentially the same results although they are expressed somewhat differently. For a review, see Li and Zeigler [Ind. Eng. Chem., **59**(3), 30 (1967)]. The subject of axial mixing has also been treated extensively by Pratt and Baird (*Handbook of Solvent Extraction*, Wiley, NY, 1983, pp. 197-247). It will not be possible to outline in detail here all the considerations taken into account; for these the original papers should be consulted. For present purposes the procedure to be used in design, as developed by Vermeulen et al., will be outlined. It is limited to cases in which flow rates, distribution coefficients, and mass-transfer coefficients are constant throughout the extractor. For the final design it is important to conduct pilot tests in equipment which closely resembles that being considered for the full-size plant, and at conditions which simulate the conditions expected in the full-size plant.

1. Obtain $N_{IOR,plug}$ from Colburn's equation [Trans. Am. Inst. Chem. Eng., **35**, 211 (1938)]:

$$N_{IOR,plug} = \frac{1}{1 - V_R/m'V_E} \ln \left[\left(\frac{c_{R1} - c_{E2}/m'}{c_{R2} - c_{E2}/m'} \right) \left(1 - \frac{V_R}{m'V_E} \right) + \frac{V_R}{m'V_E} \right] \quad (15-51)$$

2. Obtain H_{IOR} (from data correlations, etc.) and Z_{plug} :

$$Z_{plug} = N_{IOR,plug} H_{IOR} \quad (15-52)$$

3. Solve Eqs. (15-53) to (15-55) together with Fig. 15-31 simultaneously by trial and error to obtain N_{IOR} :

$$1/N_{IOR} = 1/N_{IOR,plug} - 1/N'_{IOR} \quad (15-53)$$

$$N'_{IOR} = (N_{Pe,B})_E + \frac{\ln(V_R/m'V_E)}{V_R/m'V_E - 1} \quad (15-54)$$

Equation (15-54) is applicable only for cases in which $N_{IOR}V_R/m'V_E$ and $(N_{Pe,B})_E \geq 1.0$.

$$(N_{Pe,B})_E = \left(\frac{V_R/m'V_E}{f_R N_{Pe,R} B} + \frac{1}{f_E N_{Pe,E} B} \right)^{-1} \quad (15-55)$$

4. The final height of the effective portion of the tower, Z , is then

$$Z = Z_{plug}(N_{IOR}/N_{IOR,plug}) \quad (15-56)$$

In these expressions, $B = Z/d$, $N_{Pe,E} = dV_E/E_E$, $N_{Pe,R} = dV_R/E_R$, where d = some characteristic length such as d_f for packed towers or T for spray towers. E_E and E_R are the longitudinal dispersion coefficients, which must ultimately be deter-

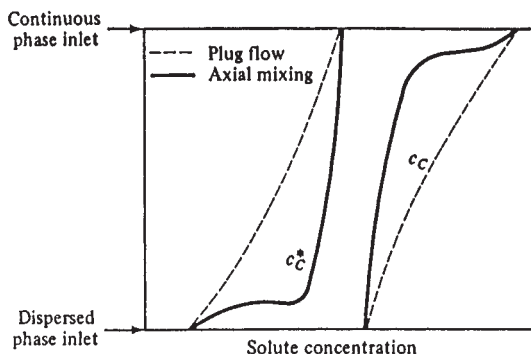


FIG. 15-30 Effect of axial mixing on concentration profiles in towers subject to axial mixing.

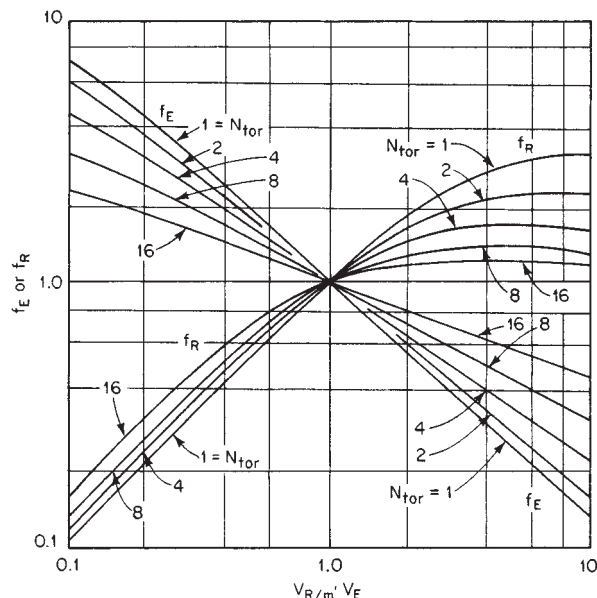


FIG. 15-31 Factors for Eq. 15-67. [Vermeulen et al., Chem. Eng. Prog., **62**(9), 95 (1966), with permission.]

mined experimentally. They are usually reported as E_C , E_D , $N_{Pe,C}$, and $N_{Pe,D}$, since they are more characteristic of the continuous or dispersed nature of the liquid than whether the liquid is extract or raffinate. For plug flow, $E = 0$; for complete mixing, $E = \infty$. In using these expressions, H_{IOR} should represent data that have been corrected for axial dispersion; unfortunately, very few data have been so corrected. Rod [Br. Chem. Eng., **9**, 300 (1964)] presents a graphical calculation suitable even for curvilinear equilibrium curves.

Devices that are stagelike in character (sieve trays, compartmented extractors, etc.) are perhaps better treated by a somewhat different procedure which space does not permit outlining here. See Sleicher [Am. Inst. Chem. Eng. J., **6**, 529 (1960)], Miyauchi and Vermeulen [Ind. Eng. Chem. Fundam., **2**, 304 (1963)], and Van der Laan [Chem. Eng. Sci., **7**, 187 (1958)].

Equipment Classification Equipment can be broadly classified into the following categories, generally in order of increasing complexity of internal construction. Those most generally used are:

- I. Gravity-operated extractors
 - A. No mechanical agitation
 1. Spray towers
 2. Packed towers
 3. Perforated-plate (sieve-plate) towers
 - B. Mechanically agitated extractors
 1. Towers with rotating stirrers
 2. Pulsed towers
 - a. Liquid contents pulsed
 - b. Reciprocating plates

II. Centrifugal extractors

Spray Towers These are simple gravity extractors, consisting of empty towers with provisions for introducing and removing liquids at the ends (see Fig. 15-32). The interface can be run above the top distributor, below the bottom distributor, or in the middle, depending on where the best performance is achieved. Because of severe axial back mixing, it is difficult to achieve the equivalent of more than one or two theoretical stages or transfer units on one side of the interface. For this reason they have only rarely been applied in extraction applications.

Distributors Most spray columns operate with the drops being formed at the ends of jets from the dispersed phase inlet distributor. The orifices or nozzles for introducing the dispersed phase are usually not smaller than 0.13 cm (0.05 in) in diameter in order to avoid clogging, nor larger than 0.64 cm (0.25 in) in order to avoid formation of

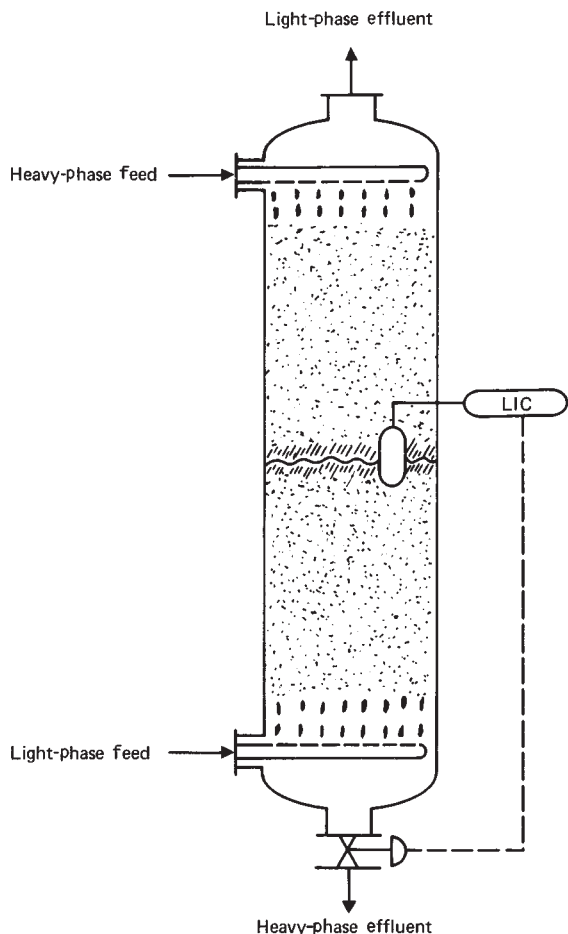


FIG. 15-32 Spray tower with both phases dispersed.

excessively large drops. They should be designed to eliminate wetting by the dispersed liquid. The following equation is recommended for calculating the velocity at which a jet appears:

$$V_{oj} = \left[\frac{3\sigma(1 - d_o/d_{oj})}{\rho_d d_o} \right]^{0.3} \quad (15-57)$$

The value of d_{oj} can be found from the relationship:

$$d_{oj} = \frac{d_o}{\rho + q(\phi)^m} \quad \text{where} \quad \phi = \frac{d_o}{(\sigma/\Delta\rho g)^{0.5}} \quad (15-58)$$

where

V_{oj} = hole velocity where a jet appears

σ = interfacial tension

d_o = hole diameter

d_{oj} = drop diameter in jetting

ρ_d = dispersed phase density

$\Delta\rho$ = density difference

g = gravitational constant

ϕ, q, m = constants

For $\phi < 0.785$: $\rho = 1.0$, $q = 0.485$, $m = 2$

$\phi > 0.785$: $\rho = 0.12$, $q = 1.51$, $m = 1$

The distributor should be sized so that the hole velocity is greater than the jet formation velocity. As the velocity is increased, the jet reaches a maximum length at which it breaks into drops of approximately uniform size. It has been found that at this velocity the drop surface area

produced is also approximately at its maximum. Typical nozzle velocities are in the range of 0.1–0.25 m/s.

Holdup and Flooding At this point it is useful to introduce the concepts of holdup and flooding in column contactors. It is normal practice to select the phase which preferentially wets the internals of the column as the **continuous phase**. This then allows the **dispersed phase** to exist as discrete droplets within the column. If the dispersed phase were to preferentially wet the internals, this could cause the dispersion to prematurely coalesce and pass through the column as rivulets or streams which would decrease interfacial area and therefore column efficiency.

The volume of droplets within the contactor at any time is referred to as the operational holdup of the dispersed phase, generally expressed as a fraction of the contactor volume.

In a countercurrent-type column contactor, stable operation is possible as long as the rate of arrival of droplets in any section does not exceed the coalescence rate at the main interface; once this value is exceeded, droplet backup will occur at the interface and slowly build back into the column active area, a condition known as flooding. This is an inoperable condition.

Besides starting at the interface and building back into the column, flooding can also start in other sections of the column depending on local hydrodynamic conditions. If for any reason the velocity of the continuous phase is increased, this will increase the drag force on the droplets and cause the smaller droplets to rise (or fall) more slowly. As the continuous phase velocity is increased further, there is reached a point where a significant number of droplets stop rising (or falling), forming a dense region which eventually coalesces and forms a second interface in the column; this also is an inoperable condition. This same phenomenon can be caused at constant continuous phase velocity by inducing the formation of smaller droplets, such as by increased agitation. These smaller droplets can no longer overcome the continuous phase velocity drag force and holdup, thus inducing flooding.

The concepts of slip velocity and characteristic velocity are useful in defining the flooding point and operational regions of different types of column contactors. The slip (or relative) velocity is given by the equation:

$$V_s = \frac{V_c}{1 - \phi_d} + \frac{V_d}{\phi_d} \quad (15-59)$$

From this has been derived the concept of characteristic velocity which is defined by the general equation:

$$V_k = \frac{V_s}{(1 - \phi_d)} \quad (15-60)$$

The value of V_k may be identified with the average terminal velocity of the droplets within the contactor. Each different type of contactor will have a different and unique characteristic velocity.

As flooding is approached, the slip velocity continues to decrease until at the flood point is zero and the following relationship applies;

$$\left(\frac{\delta V_c}{\delta \phi_d} \right)_f = \left(\frac{\delta V_d}{\delta \phi_d} \right)_f = 0 \quad (15-61)$$

Applying the above to the relationship for slip velocity yields the following relationships at flooding:

$$V_{df} = 2V_k\phi_{df}(1 - \phi_{df}) \quad (15-62)$$

$$V_{cf} = V_k(1 - \phi_{df})^2(1 - 2\phi_{df}) \quad (15-63)$$

$$\phi_{df} = \frac{[1 + 8(V_c/V_d)^{10.5} - 3]}{4(V_c/V_d)^2 - 4} \quad (15-64)$$

where V_s = slip velocity

V_c = continuous phase velocity

V_d = dispersed phase velocity

ϕ_d = dispersed phase holdup

V_k = characteristic velocity

V_{cf} = continuous phase velocity of flooding

V_{df} = dispersed phase velocity of flooding

These relationships are not restricted to any type of contactor; they can be used to predict either the flooding velocity at a given holdup,

or the holdup at flooding. However, it requires the knowledge of the characteristic velocity under actual mass-transfer conditions, and this has not been easy to obtain. As a result, column contactors still require pilot tests for reliable scale-up to full size.

There are also other factors to be aware of which can have a significant impact of the holdup and flooding characteristics. One of the most important of these is the direction of mass transfer. When transfer is from the dispersed to continuous phases, there occurs what is known as the Marangoni effect which causes rapid interdroplet coalescence with resulting decrease in holdup, sometimes by as much as 50 percent. Also, changes in phase densities, particularly in the continuous phase, can have significant impact on axial mixing with resulting effects on extraction efficiency. Finally, the presence of contaminants can affect interfacial properties (in particular interfacial tension) as well as inhibit mass transfer.

Flooding can be estimated theoretically by setting $\partial V_c / \partial \phi_d = \partial V_d / \partial \phi_d = 0$ [Thornton, *Chem. Eng. Sci.*, **5**, 201 (1956)], using Eq. (15-61). On the basis of purely statistical comparison of observed and calculated data, the empirical correlation of Minard and Johnson [*Chem. Eng. Prog.*, **48**, 62 (1952)], slightly modified, is recommended:

$$V_{cf} = \frac{10,000 \Delta \rho^{0.28}}{[0.453 \mu_c^{0.075} \rho_c^{0.5} + d_p^{0.56} \rho_d^{0.5} (Q_d / Q_c)^{0.5}]^2} \quad (15-65)$$

Use U.S. customary units only in this equation. In sizing the column diameter, it is usually assumed that the continuous phase velocity will set at 40 percent of this value, and therefore the column diameter is calculated by:

$$d_t = \sqrt{\frac{4Q_c}{0.4\pi V_{cf}}} \quad (15-66)$$

where d_t = column diameter

Q_c = volumetric flow rate of the continuous phase

V_{cf} = velocity of the continuous phase of flooding

Mass Transfer As mentioned earlier, spray columns rarely develop more than 1 theoretical stage due to the axial mixing in the column. Nevertheless, it is necessary to determine what column height will give this theoretical stage. It is recommended by Cavers in Lo et al. *Handbook of Solvent Extraction* p. 323 and p. 327, John Wiley & Sons, New York, 1983 that the following equation be used to estimate the overall efficiency coefficient:

$$K_a = \frac{\phi_d(1 - \phi_d) \left(\frac{g^3 \Delta \rho^3}{\sigma \rho_c^2} \right)^{0.25}}{(N_{Sc,c})^{0.5} + \frac{1}{m} (N_{Sc,d})^{0.5}} \quad (15-67)$$

where K_a = overall mass transfer capacity coefficient based on the continuous phase

ϕ_d = dispersed phase holdup

$\Delta \rho$ = density difference of phases

σ = interfacial tension

ρ_c = density of the continuous phase

$N_{Sc,c}$ = Schmidt number—continuous phase

$N_{Sc,d}$ = Schmidt number—dispersed phase

m = distribution coefficient

With this value, the height of a transfer unit, $(HTU)_{oc}$ can be estimated from:

$$(HTU)_{oc} = \frac{V_c}{K_a} \quad (15-68)$$

where $(HTU)_{oc}$ = overall height of a transfer unit based on the continuous phase

V_c = continuous phase superficial velocity

On top of this should be put a safety factor of 30 percent due to the unreliability of the correlations.

There are not many data on the scale-up of spray columns from pilot to industrial scale, so these types of calculations must be used for

the column design. As mentioned earlier, because of its limitations, the spray column is only rarely used in industrial applications.

Heat Transfer Heat-transfer rates are generally large despite severe axial dispersion, with Ua_{av} frequently observed in the range 18.6 to 74.5 and even to 130 kW/(m³·K) [1000 to 4000 and even to 7000 Btu/(h·ft³·°F)] [see Bauerle and Ahlert, *Ind. Eng. Chem. Process Des. Dev.*, **4**, 225 (1965); and Greskovich et al., *Am. Inst. Chem. Eng. J.*, **13**, 1160 (1967); Sideman, in Drew et al. (eds.), *Advances in Chemical Engineering*, vol. 6, Academic, New York, 1966, p. 207, reviewed earlier work]. In the absence of specific heat-transfer correlations, it is suggested that rates be estimated from mass-transfer correlations via the heat-mass-transfer analogy.

Axial Dispersion For low values of ϕ_d and in the absence of interdrop coalescence, axial dispersion for the dispersed phase is evidently very small ($E_d \sim 0$). For the continuous phase, low μ_c and ϕ_d , Vermeulen et al. [*Chem. Eng. Prog.*, **62**(9), 95 (1966)] reviewed the available data and concluded that, for $d_t = 3.6$ to 15.2 cm (0.117 to 0.5 ft), E_c is given empirically by

$$E_c = c(V_d d_t)^{1/2} \quad (15-69)$$

where $c = 23.6$ for U.S. customary units and 7.2 for SI units. For treatment of heat transfer, particularly for high values of ϕ_d when axial dispersion evidently is the controlling factor, see Letan and Kehat [*Am. Inst. Chem. Eng. J.*, **11**, 804 (1965); **14**, 398 (1968)] and Mixon et al. [*ibid.*, **13**, 21 (1967)].

Packed Towers For a packed-tower liquid-liquid extractor the empty shell of a spray tower is filled with packing to reduce the vertical circulation of the continuous phase. The standard commercial packings used in vapor-liquid systems are also used in liquid-liquid systems. This includes Raschig and pall rings, Berl and Intalox saddles, and other random-dumped packings as well as the newer structured packings. The packing reduces the available free space for flow but also significantly reduces the height required for mass transfer. However, Nemunaitis, Eckert, Foote, and Rollinson [*Chem. Eng. Prog.*, **67**(11), 60 (1971)] reported little benefit from a packed height greater than 3.05 m (10 ft) and recommended redistributing the dispersed phase about every 1.52 to 3.05 m (5 to 10 ft) to generate new droplets and mass-transfer surfaces. From this perspective the packing allows a wider spacing between sieve plates than described for a conventional sieve-plate tower.

The pieces of random-dumped packing should be no larger than one-eighth of the tower diameter to minimize the wall effect which gives larger voids at the wall. The packing support can be an open grid or multiarch support if the dispersed phase is distributed to the top of the bed. But the packing support may also be a sieve plate with multiple light-liquid risers if the heavy phase is to be redispersed onto a lower bed. Or the packing support may be a sieve plate with multiple heavy-phase downcomers if the light phase is to be dispersed up into the bed. The streams of dispersed phase should be far enough apart to avoid coalescence at the dispersion plate, and the dispersed phase should not preferentially wet the packing. If the droplets wet the packing, they will coalesce and stream along the packing as rivulets. Eckert [*Hydrocarbon Process.*, 117 (March 1976)] recommends the use of packed towers when the interfacial tension is below 10 mN/m (dyn/cm).

Holdup It is recognized that the dispersed-phase holdup may be placed in two categories: a smaller portion which is permanent and a larger portion, free, which moves through the packing and enters into mass-transfer operations when a solute is transferred between phases. Vignes [*Chem. Ind. Genie Chim.*, **95**, 307 (1966)] further classifies the moving holdup into "free" and "semifree." The total is ϕ_d , which here refers to the volume of dispersed phase expressed as a fraction of the void space in the packed section. See Beckmann et al. [*Am. Inst. Chem. Eng. J.*, **1**, 426 (1955); **3**, 223 (1957)].

What follows is a very brief summary of the extensive work of Pratt and his coworkers, De'll, Gayler, Lewis, Jones, Roberts, and White [*Trans. Inst. Chem. Eng. (London)*, **29**, 89, 110, 126 (1951); **31**, 57, 69 (1953); *Chem. Ind. (London)*, 1952, p. 358]. For the standard commercial packings of 1.27-cm (1/2-in) size and larger, at low values of V_d , ϕ_d varies linearly with V_d up to values of $\phi_d = 0.10$. With further increase of V_d , ϕ_d increases sharply up to a "lower transition point,"

resembling "loading" in gas-liquid contact. At still higher values of V_d an upper transition point occurs, the drops of dispersed phase tend to coalesce, and V_d can increase without a corresponding increase in ϕ_d . This regime ends in flooding. Drops of the dispersed phase reach a characteristic size after leaving the distributor nozzles regardless of their initial size. For each system there is a critical packing size above which the mean drop size is a minimum. For smaller packing, the drop size is larger (and the interfacial area smaller). The critical size of packing, usually 1.27 cm ($\frac{1}{2}$ in) or more, is given by

$$d_{FC} = 2.42(\sigma g_c / \Delta \rho g)^{0.5} \quad (15-70)$$

For packing larger than d_{FC} , the characteristic drop diameter, for liquids that are in concentration equilibrium, is given by

$$d_p = 0.92(\sigma g_c / \Delta \rho g)^{0.5} (V_k \epsilon \phi_d / V_d) \quad (15-71)$$

For liquids that are not in concentration equilibrium and when an unequilibrated solute is present, the characteristic drop size will generally be larger. If the drops formed at the distributor nozzle are smaller than this, there may be a tendency to flood until they grow to size. Thornton [Ind. Chem., **39**, 632 (1963)] finds that large drops decay in exponential fashion to their final size. It is therefore best to design the nozzles to give drop sizes which are larger than that given by Eq. (21-67). V_k is a characteristic drop velocity (at $V_c = 0$, V_d approaching 0), and is given by Fig. 15-33. Below the upper transition point, the holdup is given by

$$\frac{V_d}{\phi_d} + \frac{V_c}{1 - \phi_d} = \epsilon V_k (1 - \phi_d) \quad (15-72)$$

Additional holdup correlations are offered by Sitarmayya and Laddha [Chem. Eng. Sci., **13**, 263 (1961)] and Ghosal et al. [Trans. Indian Inst. Chem. Eng., **11**, 23 (1958-1959)]. The interfacial area is given by

$$a = 6\epsilon \phi_d / d_p$$

It is generally desirable to design for ϕ_d in the range 0.15 to 0.25 (the lower value for $V_d/V_c < 0.5$).

Flooding Many correlations are available. By a comparison of the observed and calculated velocities at flooding for all available data, those of Crawford and Wilke [Chem. Eng. Prog., **47**, 423 (1951)] and Hoffing and Lockhart [Chem. Eng. Prog., **50**, 94 (1954)] are best and about equally effective. The Crawford-Wilke correlation is the simpler and is given in Fig. 15-34. Nemunaitis, Eckert, Foote, and Rollinson [Chem. Eng. Prog., **67**(11), 60 (1971)] updated the correlation using packing factors. See also Dell and Pratt [Trans. Inst. Chem. Eng. (London), **29**, 89, 270 (1951)], Fujita et al. [Chem. Eng. (Japan), **17**, 230 (1957)], Sakiadis and Johnson [Ind. Eng. Chem., **46**, 1229 (1954)], and Kafarov and Dytnerskii [Zh. Prikl. Khim., **30**, 1698 (1957)]. For very small packings, see Rao and Rao [Chem. Eng. Sci., **9**, 170 (1958)] and Venkatoramen and Laddha [Am. Inst. Chem. Eng. J., **6**, 355 (1960)]. It is recommended that flow rates be set at no more than 50 percent of the flooding values, less if the interfacial tension of the liquids is high.

Mass Transfer Extraction rates for packed towers are usually excellently correlated for a given situation on the coordinate system of Fig. 15-35. Treybal [Chem. Eng. Prog., **62**(9), 67 (1966)] has suggested means whereby overall H_{OC} 's may be resolved into constituent

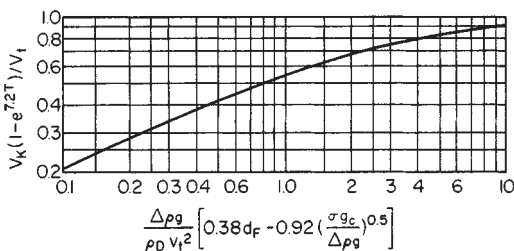


FIG. 15-33 Characteristic drop velocity for packed towers, for equilibrium liquids $d_F > d_{FC}$ and $T > 0.25$ ft. [Pratt, Ind. Chem., **31**, 552 (1955), with permission.]

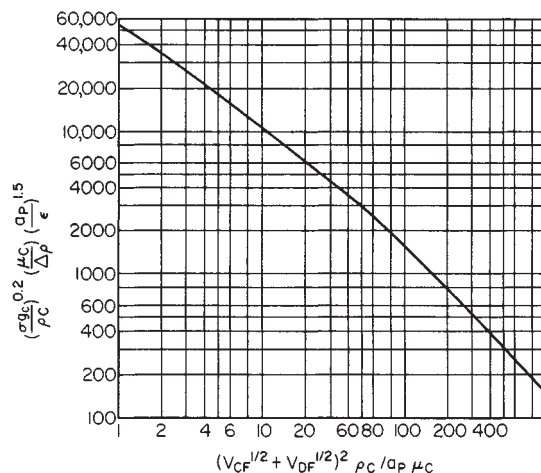


FIG. 15-34 Flooding in packed towers. Use only customary units in the variables. [Crawford and Wilke, Chem. Eng. Prog., **47**, 423 (1951), with permission.]

H_i 's. In connection with the data on this figure, it should be noted that economical values of $m'V_E/V_R$ will usually lie in the range between 1 and 2, so that overall heights of transfer units are not too unreasonable even for this high-interfacial-tension system. For lower interfacial tensions, H_{IOC} will ordinarily be appreciably less.

The number of variables that are known to influence the rate of extraction is exceedingly large, and includes at least the following:

- Size, shape, and material of packing
- Tower diameter
- Packing depth
- Dispersed-phase distributor design
- Which liquid is dispersed
- Direction of extraction, whether from dispersed to continuous, organic liquid to water, or the reverse
- Dispersed-phase holdup
- Flow rates and flow ratio of the liquids

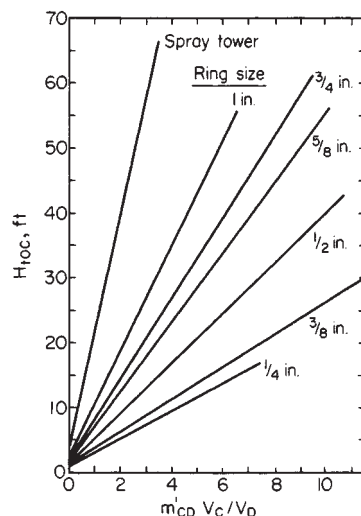


FIG. 15-35 Extraction of diethylamine from water into toluene (dispersed) in towers packed with unglazed porcelain Raschig rings. To convert feet to meters, multiply by 0.3048; to convert inches to centimeters, multiply by 2.54. [Leibson and Beckman, Chem. Eng. Prog., **49**, 405 (1953), with permission.]

Physical properties of the liquids
Presence or absence of surface-active agents

Although many attempts have been made to establish a method for estimating the extraction rates [see, for example, Ellis, *Ind. Chem.*, **28**, 483 (1952); Jeffreys and Ellis, *Congr. Chem. Eng. Des.*, **1962**, 65; and Treybal, *Liquid Extraction*, 2d ed., McGraw-Hill, New York, 1963], it is still most important to pilot-plant any new process. About the most that can be said is that, for a given system, packing, and method of operation, H_{ld} should be practically constant for all flow rates up to transition and that H_{lc} should vary roughly as $C(V_c/V_d)^n$, where C and n are constants, and to both H_i 's correction must be applied on scale-up for axial dispersion [Treybal, *Chem. Eng. Prog.*, **62**(9), 67 (1966)]. Table 15-7 lists additional selected data sources.

Axial Dispersion Vermeulen et al. [*Chem. Eng. Prog.*, **62**(9), 95 (1966)] summarized many of the data for packings. Their correlation for the continuous phase is shown in Fig. 15-36. For the dispersed phase, their correlation is given by

TABLE 15-7 Selected Sources of Packed-Tower Mass-Transfer Data

System	Tower diameter, in.	Packing	Ref.
Water-acetic acid-ethyl acetate, cyclohexane, methylcyclohexane, ethyl acetate + benzene	1	0.25-in. saddles	<i>b</i>
Water-acetic acid-methyl isobutyl ketone	1.95 3	0.23-in. rings 0.375-in. plastic spheres	<i>g</i> <i>j</i>
		0.375-in. plastic, ceramic rings	<i>k</i>
		0.5-in. plastic, ceramic saddles	<i>k</i>
Water-acetone-hydrocarbon	1.88	0.25-, 0.375-in. rings, 6-mm. beads	<i>o</i>
	2-4	0.5-, 0.75-in. rings	<i>a</i>
Water-adipic acid-ethyl ether	6	0.5-, 0.75-in. rings, 0.375-in. spheres	<i>e</i>
Water-benzoic acid-carbon tetrachloride	1.95	0.25-in. rings	<i>f</i>
Water-diethylamine-toluene	3, 4, 6	0.25-1-in. rings	<i>i</i>
	3	0.375-in. rings	<i>m</i>
Water-ethyl acetate	4	0.5-in. rings	<i>c</i>
Water-methylisobutyl-carbinol	4	0.5-in. rings	<i>n</i>
Water-methyl ethyl ketone	4	0.5-in. rings	<i>n</i>
Water-propionic acid-methyl isobutyl ketone	1.88	0.25-, 0.375-in. rings, 6-mm. beads	<i>o</i>
Acetone (aq.)-soybean oil, linseed oil	2	0.25-in. saddles, 0.5-in. rings	<i>p</i>
Petroleum-furfural	2	0.25-in. rings	<i>d</i>
	1.2	0.16-in. rings	<i>l</i>
Toluene-heptane-diethylene glycol	1.4, 2.25	Glass and brass rings	<i>h</i>

a Degaleesan and Laddha, *Chem. Eng. Sci.*, **21**, 199 (1966); *Indian Chem. Eng.*, **8**(1), 6 (1966).
b Eaglesfield, Kelly, and Short, *Ind. Chem.*, **29**, 147, 243 (1953).
c Gaylor and Pratt, *Trans. Inst. Chem. Eng. (London)*, **31**, 78 (1953).
d Garvin and Barber, *Pet. Refiner*, **32**(1), 144 (1953).
e Gier and Hougen, *Ind. Eng. Chem.*, **45**, 1362 (1953).
f Guyer, Guyer, and Mauli, *Helv. Chim. Acta*, **38**, 790 (1955).
g Guyer, Guyer, and Mauli, *Helv. Chim. Acta*, **38**, 955 (1955).
h Kishinevskii and Mochalova, *Zh. Prikl. Khim.*, **33**, 2344 (1960).
i Liebson and Beckmann, *Chem. Eng. Prog.*, **49**, 405 (1953).
j Moorhead and Himmelblau, *Ind. Eng. Chem. Fundam.*, **1**, 68 (1962).
k Osmon and Himmelblau, *J. Chem. Eng. Data*, **6**, 551 (1961).
l Sef and Moretu, *Nafta (Zagreb)*, **5**, 125 (1954).
m Shih and Kraybill, *Ind. Eng. Chem. Process. Des. Dev.*, **5**, 260 (1966).
n Smith and Beckmann, *Am. Inst. Chem. Eng. J.*, **4**, 180 (1958).
o Rao and Rao, *J. Chem. Eng. Data*, **6**, 200 (1961).
p Young and Sullans, *J. Am. Oil Chem. Soc.*, **32**, 397 (1955).
NOTE: To convert inches to centimeters, multiply by 2.54.

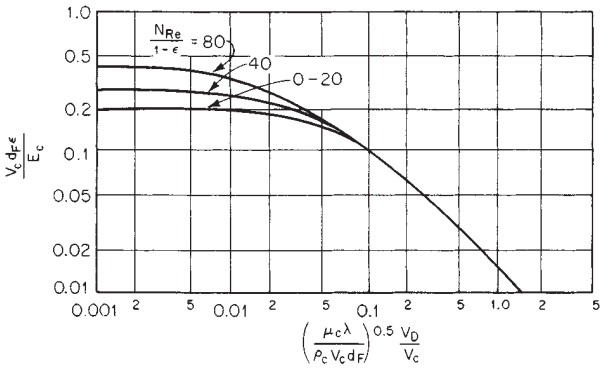


FIG. 15-36 Axial dispersion for the continuous phase in packed towers. Spheres (0.75-in., $\epsilon = 0.32$ to 0.41; 0.50-in., $\epsilon = 0.62$), Raschig rings (0.50-in., $\epsilon = 0.62$; 0.75-in., $\epsilon = 0.65$), Berl saddles (1.0-in., $\epsilon = 0.67$). Use customary units in the variables. [Vermeulen et al., *Chem. Eng. Prog.*, **62**(9), 95 (1966), with permission.]

1. Nonwetted carbon rings and wetted Berl saddles:

$$\log \frac{E_d}{V_d d_f} = 0.046 \frac{V_c}{V_d} + 0.301 \tag{15-73}$$

2. Wetted ceramic rings:

$$\log \frac{E_d}{V_d d_f} = 0.161 \frac{V_c}{V_d} + 0.347 \tag{15-74}$$

The measurements were made with kerosine or diisobutyl ketone dispersed in water. Additional work is reported by Komasaawa et al. [*Kagaku Kogaku*, **30**, 237, 450, 928, 1103 (1966); English version, **4**, 288, 363 (1966); **5**, 125, 182 (1967)], and Olbrich et al. [*Trans. Inst. Chem. Eng. (London)*, **44**, T207 (1966)].

GENERAL REFERENCES: Bussolari, Schiff, and Treybal, *Ind. Eng. Chem.*, **45**, 2413 (1953). Fujita and Tanizawa, *Chem. Eng. (Japan)*, **17**, 111 (1953). Garner, Ellis, and Hill, *Am. Inst. Chem. Eng. J.*, **1**, 185 (1955); *Trans. Inst. Chem. Eng. (London)*, **34**, 223 (1956). Major and Hertzog, *Chem. Eng. Prog.*, **51**, 17 (1955). Mayfield and Church, *Ind. Eng. Chem.*, **44**, 2253 (1952). Planovskii and Bulatov, *Khim. Mashinost.*, **1960**(2), 10; (3), 9. Pyle, Duffey, and Colburn, *Ind. Eng. Chem.*, **42**, 1042 (1950).

Perforated-Plate (Sieve-Plate) Towers A schematic diagram for the most common design of perforated-plate, or sieve-plate, tower, arranged for light liquid dispersed, is shown in Fig. 15-37. The light liquid flows through the perforations of each plate and is thereby dispersed into drops which rise through the continuous phase. The continuous liquid flows horizontally across each plate and passes to the plate beneath through the down spout. For heavy liquid dispersed,

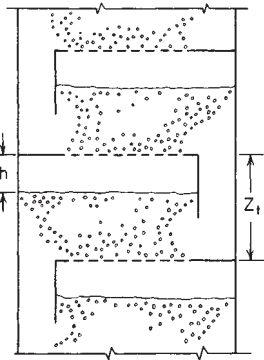


FIG. 15-37 Portion of a perforated-tray tower, arranged for light liquid dispersed.

the same design may be used, but turned upside down. The plates serve to eliminate essentially completely the vertical recirculation of continuous phase characteristic of the spray tower. Furthermore, extraction rates are enhanced by the repeated coalescence and redispersion into droplets of the dispersed phase. Towers of the simple design suggested by Fig. 15-38 have been used successfully in a great variety of services and for petroleum-refining processes have commonly been built to diameters of 3.66 m (12 ft). With careful design, these towers may have excellent flow capacities, and with systems of low interfacial tension equally excellent mass-transfer characteristics.

Many variations in design have been suggested and tried, for example, the use of tower packing in the down spouts to prevent entrainment of dispersed phase, arrangements in which both liquids must pass through perforations at each plate, arrangements with vertical perforated plates, etc. As examples of these, see Bradley (U.S. Patent 2,642,341, 1953), Williams (U.S. Patent 2,652,316, 1953), Maycock and Hartwig (U.S. Patent 2,729,550, 1956), and Pohlentz (U.S. Patent

2,872,295, 1959). Data are available only for arrangements of the sort shown in Fig. 15-39. In general, caplike sieve plates, bubble caps, and vertical perforated plates have not been as satisfactory as horizontal plates.

Sieve-Plate Design For best tray efficiency, it is well established that the dispersed phase must issue cleanly from the perforations. This requires that the material of the plates be preferentially wet by the continuous phase (requiring the use of plastics or plastic-coated plates in some instances) or that the dispersed phase issue from nozzles projecting beyond the plate surface. These may be formed by punching the holes and leaving the burr in place or otherwise forming the jets (see Mayfield and Church, loc. cit.). The liquid flowing at the larger volume rate should be dispersed.

Perforations are usually 0.32 to 0.64 cm ($\frac{1}{8}$ to $\frac{1}{4}$ in) in diameter, set 1.27 to 1.81 cm ($\frac{1}{2}$ to $\frac{3}{4}$ in) apart, on square or triangular pitch. There appears to be relatively little effect of hole size on extraction rate, except that with systems of high interfacial tension smaller holes will

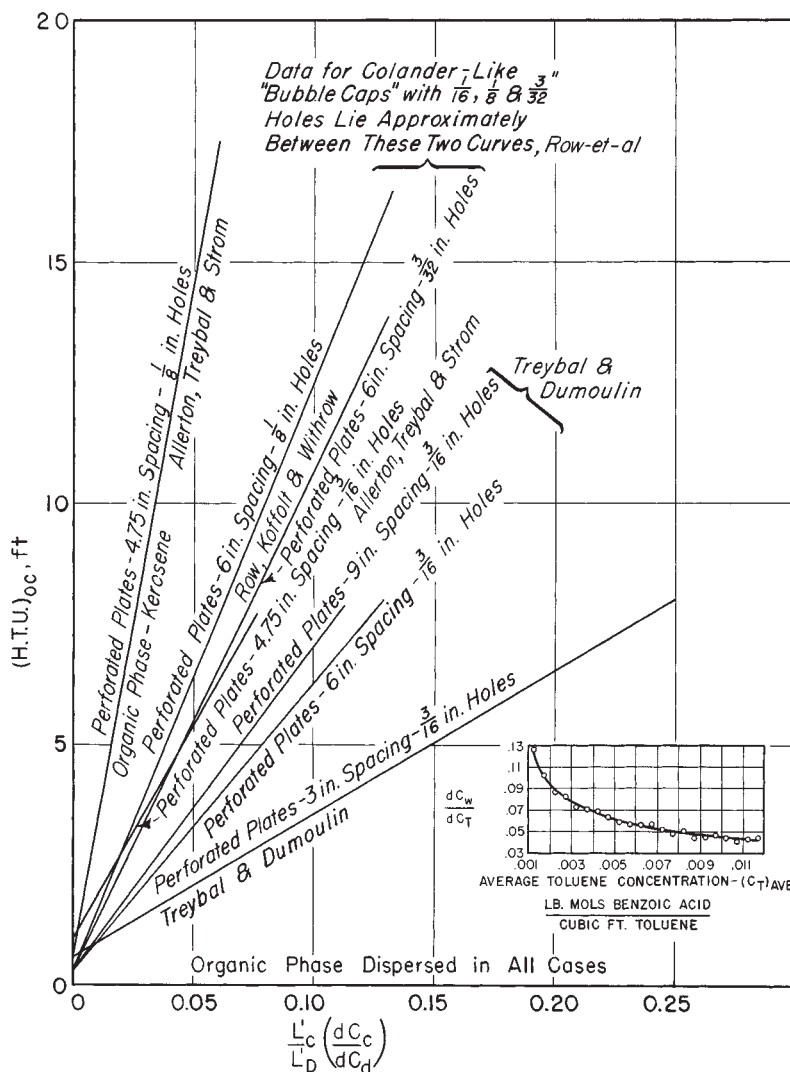


FIG. 15-38 Extraction rates for sieve-plate and modified bubble-plate columns. System: benzoic acid-water-toluene, except where noted. To convert feet to meters, multiply by 0.3048; to convert inches to centimeters, multiply by 2.54. [Allerton, Strom, and Treybal, *Trans. Am. Inst. Chem. Eng.*, **39**, 361 (1943); Row, Koffolt, and Withrow, *ibid.*, **37**, 559 (1941); Treybal and Dumoulin, *Ind. Eng. Chem.*, **34**, 709 (1942).]

produce somewhat better rates. The entire hole area is suitably set at 15 to 25 percent of the column cross section, subject, however, to check through calculations as outlined below. The velocity through the holes should be such that drops do not form slowly at the holes, but rather that the dispersed phase streams through the openings to be broken up into droplets at a slight distance from the plate. This generally requires average linear velocities through the holes of from 15.2 to 30.5 cm/s (0.5 to 1.0 ft/s). The plate area directly opposite down spouts is kept free of perforations. A scum or "interface-rag" bypass can be incorporated in the trays (see Mayfield and Church, op. cit.) at the expense of tray efficiency, or provision may be made for periodic withdrawal of accumulations through the side of the tower between plates.

Down spouts (or up spouts) are best set flush with the plate from which they lead, with no weir as in gas-liquid contact. The velocity of the continuous phase in the down spout V_d , which sets the down-spout cross section, should be set at a value lower than the terminal velocity of some arbitrarily small droplet of dispersed phase, say, 0.08 or 0.16 cm ($1/32$ or $1/16$ in) in diameter; otherwise, recirculation of entrained dispersed phase around a plate will result in flooding. The down spouts should extend beyond the accumulated layer of dispersed phase on the plate.

The depth of dispersed liquid h accumulating on each plate is determined by the pressure drop required for flow of the liquids,

$$h = h_c + h_D \quad (15-75)$$

For the dispersed phase,

$$h_D = h_\sigma + h_O \quad (15-76)$$

The available data indicate that, for the orifice effect,

$$h_O = \frac{(V_O^2 - V_D^2)\rho_D}{2g(0.67)^2 \Delta p} = \frac{V_O'^2 \rho_D}{28.9 \Delta p} \quad (15-77)$$

and that h_σ to overcome interfacial-tension effects may be estimated for drop formation at a low velocity through the holes,

$$h_\sigma = 6\sigma g/d_{p0.1} \Delta p g \quad (15-78)$$

where $d_{p0.1}$ = drop diameter produced by flow of dispersed phase at $V_O = 109$ m/h ($V_O' = 0.03$ m/s) [360 ft/h ($V_O' = 0.1$ ft/s)] through the perforations. At hole velocities of 0.3 m/s (1100 m/h) [1 ft/s (3600 ft/h)] or more, h_σ should be omitted, and $h_D = h_O$.

The head required for flow of continuous phase h_c includes losses due to (1) friction in the down spout, which should be negligible, (2) contraction and expansion upon entering and leaving the down spout, and (3) two abrupt changes in direction. These total 4.5 velocity heads:

$$h_c = 4.5V_d^2 \rho_c / 2g \Delta p \quad (15-79)$$

The distance between trays Z_t should be larger than h , sufficient so that (1) the "streamers" of dispersed liquid from the holes break up into drops before coalescing into the layer of liquid on the next plate, (2) the linear velocity of continuous liquid is not greater than that in the down spout to avoid excessive entrainment, and (3) the tower may be entered through handholes or manholes in the sides for cleaning.

Mass Transfer Mass-transfer rates may be expressed in terms of overall heights of transfer units and successfully correlated for any tower and system as in Fig. 15-38. No significance in terms of individual heights of transfer units for the separate phases should be given to the slope and intercept of such lines. The advantage gained by dispersing the liquid flowing at the larger rate, which results in low values for the abscissa of Fig. 15-38 and consequently low transfer-unit heights, is clear. Alternatively, since the plates resemble and basically behave in the manner of stages, the performance is frequently expressed in terms of stage efficiency, either overall E_O for the entire tower or, more satisfactorily, as Murphree efficiencies for each tray.

The system of Fig. 15-38 is one of high interfacial tension, so that the heights of transfer units are relatively high and stage efficiency low. For systems of low interfacial tension, on the other hand, stage efficiencies may be very much improved. Table 15-8 lists sources of mass-transfer data.

Treybal (*Liquid Extraction*, 2d ed., McGraw-Hill, New York, 1963)

TABLE 15-8 Mass-Transfer Data for Perforated-Tray Towers

System	Tower diameter, in.	Tray spacing, in.	Ref.
Benzene-acetic acid-water	1.97	3.9-6.3	<i>t</i>
	1.97	3.2-6.3	<i>s</i>
	2.2	2.8-6.3	<i>r</i>
	1.6×3.2	5.9	<i>p</i>
Benzene-acetone-water	3	4, 8	<i>m</i>
Benzene-benzoic acid-water	3	4	<i>m</i>
Benzene-monochloroacetic acid-water	1.97	3.9-6.3	<i>t</i>
Benzene-propionic acid-water	1.97	3.2-6.3	<i>s</i>
Carbon tetrachloride-propionic acid-water	1.97	3.9-6.3	<i>t</i>
Ethyl acetate-acetic acid-water	2	8-24	<i>j</i>
Ethyl ether-acetic acid-water	8.63	4-7.2	<i>n</i>
Gasoline-methyl ethyl ketone-water	3.75	4.5, 6	<i>k</i>
Kerosene-acetone-water	3	4, 8	<i>m</i>
Kerosene-benzoic acid-water	3.63	4.75	<i>a</i>
Isopar-H-benzyl alcohol, methyl benzyl alcohol, acetophenone-water	2×12	24	<i>b</i>
Methylisobutylcarbinol-acetic acid-water	3	6	<i>l</i>
Methyl isobutyl ketone-adipic acid-water	4.18	6	<i>e</i>
Methyl isobutyl ketone-butyric acid-water	4.8	6-23	<i>g</i>
Pegadol-propionic acid-water	4.8	6-11	<i>g</i>
Toluene-benzoic acid-water	8.75	6	<i>o</i>
	3.63	4.75	<i>a</i>
	3.56	3-9	<i>q</i>
	3	6	<i>l</i>
Toluene-diethylamine-water	2.72	9	<i>f</i>
	2	24	<i>j</i>
	4.18	6	<i>c, d</i>
	3.75	4.5, 6	<i>k</i>

a Allerton, Strom, and Treybal, *Trans. Am. Inst. Chem. Eng.*, **39**, 361 (1943).

b Angelo and Lightfoot, *Am. Inst. Chem. Eng. J.*, **14**, 53 (1968).

c Garner, Ellis, and Fosbury, *Trans. Inst. Chem. Eng. (London)*, **31**, 348 (1953).

d Garner, Ellis, and Hill, *Am. Inst. Chem. Eng. J.*, **1**, 185 (1955).

e Garner, Ellis, and Hill, *Trans. Inst. Chem. Eng. (London)*, **34**, 223 (1956).

f Goldberger and Benenati, *Ind. Eng. Chem.*, **51**, 641 (1959).

g Krishnamurthy and Rao, *Indian J. Technol.*, **5**, 205 (1967).

h Krishnamurthy and Rao, *Ind. Eng. Chem. Process Des. Dev.*, **7**, 166 (1968).

i Lodh and Rao, *Indian J. Technol.*, **4**, 163 (1966).

j Mayfield and Church, *Ind. Eng. Chem.*, **44**, 2253 (1952).

k Moulton and Walkey, *Trans. Am. Inst. Chem. Eng.*, **40**, 695 (1944).

l Murali and Rao, *J. Chem. Eng. Data*, **7**, 468 (1962).

m Nandi and Ghosh, *J. Indian Chem. Soc., Ind. News Ed.*, **13**, 93, 103, 108 (1950).

n Pyle, Duffey, and Colburn, *Ind. Eng. Chem.*, **42**, 1042 (1950).

o Row, Koffolt, and Withrow, *Trans. Am. Inst. Chem. Eng.*, **37**, 559 (1941).

p Shiotsuka and Murakami, *Kagaku Kogaku*, **30**, 727 (1966).

q Treybal and Dumoulin, *Ind. Eng. Chem.*, **34**, 709 (1942).

r Ueyama and Koboyashi, *Bull. Univ. Osaka Prefect.*, **A7**, 113 (1959).

s Zheliznyak, *Zh. Prikl. Khim.*, **40**, 689 (1967).

t Zheliznyak and Brounshtein, *Zh. Prikl. Khim.*, **40**, 584 (1967).

NOTE: To convert inches to centimeters, multiply by 2.54.

has shown that good estimates of the rate of extraction, or stage efficiency, may be made by computing the rates of extraction for drop formation, drop rise (by computing dispersed-phase holdup and drop velocity and by considering the continuous phase to be of uniform concentration vertically), and drop coalescence (see the subsections "Single Drops Immersed in Immiscible Liquids" and "Spray Towers." See also Skelland and Cornish [*Can. J. Chem. Eng.*, **43**, 302 (1965)]. Specifically, Angelo and Lightfoot [*Am. Inst. Chem. Eng. J.*, **14**, 531 (1968)] have had good success in applying the surface-stretch theory to drop formation and drop rise for oscillating drops on a perforated-tray extractor. Zheleznyak and Brounshtein [*Zh. Prikl. Khim.*, **40**, 584, 689 (1967)] have shown that if the mass-transfer resistance lies within the drop phase, the approach to equilibrium of that phase produced by an extractor is simply related to the approach reached in one section.

The following empirical expression (Treybal, *Liquid Extraction*, 2d ed., McGraw-Hill, New York, 1963) has been found to represent all the available data reasonably well, considering the great variety of circumstances and the considerable scatter in many of the original data:

$$E_o = \frac{89,500 Z_t^{0.5}}{\sigma g_c} \left(\frac{V_D}{V_C} \right)^{0.42} = \frac{0.9 Z_t^{0.5}}{\sigma'} \left(\frac{V_D}{V_C} \right)^{0.42} \quad (15-80)$$

Use only U.S. customary units in this equation. Krishnamurthy and Rao [*Ind. Eng. Chem. Process Des. Dev.*, **7**, 166 (1968)] suggest that Eq. (21-77) is improved if the right-hand side is multiplied by $0.1123/d_o^{0.35}$.

Mechanically Agitated Gravity Devices Owing to the usual small density differences between the contacted liquids, the energy available from simple counterflow under the force of gravity is insufficient to disperse one liquid in the other and to establish turbulence levels to the extent necessary for rapid mass transfer, particularly for systems of high interfacial tension. Application of energy, mechanically applied through stirring devices, pulsations, etc., assists. The devices of major importance are considered below in order of increasing complexity of design.

Rotary-Disk Contactors (RDC)

GENERAL REFERENCES: Logsdail, Thornton, and Pratt, *Trans. Inst. Chem. Eng. (London)*, **35**, 301 (1957). Misek, *Collect. Czech. Commun.*, **28**, 426, 570, 1631 (1963); **32**, 4018 (1967) (in English); *Ratacní Diskové Extraktory a Jejich Vypocty*, SNTL, Prague, 1964. Olney et al., *Am. Inst. Chem. Eng. J.*, **8**, 252 (1962); **10**, 827 (1964). Reman et al., U.S. Patent 2,601,674 (1952); *Chem. Eng. Prog.*, **51**, 141 (1955); **62**(9), 56 (1966); *Joint Symposium: Scaling-Up Chemical Plant and Processes*, London, 1957, p. 26.

Refer to Fig. 15-39. The tower is formed into compartments by horizontal doughnut-shaped or annular baffles, and within each compartment agitation is provided by a rotating, centrally located, horizontal disk. Somewhat similar devices have been known for some time. The features here are that the rotating disk is smooth and flat and of a diameter less than that of the opening in the stationary baffles, which facilitates fabrication and apparently improves extraction rates. The typical proportions of the internals of the RDC are as follows:

$$d_s/d_t = 0.7$$

$$d_r/d_t = 0.6$$

Z_t/d_t —the following table applies

For	$0 < d_t < 0.1 \text{ m}$	$Z_t = (d_t)^{0.5}$
	$0.1 < d_t < 1.0 \text{ m}$	$Z_t/d_t = 0.15$

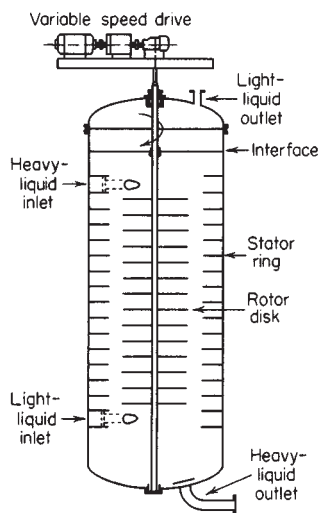


FIG. 15-39 Rotating-disk (RDC) extractor. (Courtesy of Glitsch Process Systems Inc.)

$$1.0 < d_t < 1.5 \text{ m} \quad Z_t/d_t = 0.12$$

$$1.5 < d_t < 2.5 \text{ m} \quad Z_t/d_t = 0.10$$

$$2.5 < d_t < 2.5 \text{ m} \quad Z_t/d_t = 0.08$$

where d_s = stator diameter
 d_t = tower diameter
 d_r = rotor diameter
 Z_t = stage height

The general proportions may be varied from one end of the tower to the other to accommodate changing liquid volumes and physical properties. These towers have been used in diameters ranging from a few inches for laboratory work up to 2.4 m (8 ft) in diameter by 12.2 m (40 ft) tall for purposes of deasphalting petroleum. Other commercial services include furfural extraction of lubricating oils, desulfurization of gasoline, phenol recovery from wastewaters, and many others. Columns up to 4.5 m in diameter and up to 50 m in height have been constructed.

A reliable design procedure for new systems, without the necessity for laboratory work, is not yet established. The data available show that the flow capacity increases with (1) decreased rotor speed, (2) decreased diameter of rotating disks, (3) increased diameter of opening in the stationary baffles, and (4) increased compartment height. Logsdail et al. (loc. cit.) have proposed that the slip velocity of Eq. 15-83, in the absence of mass transfer, can be set equal to $V_K(1 - \phi_D)$, where V_K is a "characteristic" velocity which can be related to the liquid properties, speed of agitation, and tower geometry. Kung and Beckmann [*Am. Inst. Chem. Eng. J.*, **7**, 319 (1961)] and Olney et al. (loc. cit.) have also used this. Misek (loc. cit.), however, has had considerable success by setting the slip velocity equal to $V_K(1 - \phi_D) \exp[\phi_D(z - 4.1)]$, where z is a "coalescence coefficient" which depends on the liquid properties. Evidently mass transfer has a profound effect, as a result of drop coalescence; variation in the flooding rate from -15 to +200 percent has been noted in the extraction of acetone to and from water, respectively, with organic solvents. See also Kagan et al., *Izv. Vyssh. Uchebn. Khim. Khim. Tekhnol.*, **9**, 836 (1966). Drop-size distribution which has an important influence on axial dispersion in the dispersed phase has been studied extensively by Misek and Olney (loc. cit.).

The value of HETS becomes smaller with (1) increased rotor speed but passes through a minimum, (2) increased diameter of rotating disks, (3) decreased diameter of stationary baffle opening, and (4) decreased compartment height. Reman and Olney [*Chem. Eng. Prog.*, **51**, 141 (1955)] show a correlation of stage height for two sizes of RDCs with the system water-kerosine-butylamine, as in Fig. 15-40. That such correlations cannot be general is indicated by these authors' data on caustic extraction of gasoline, which show quite different

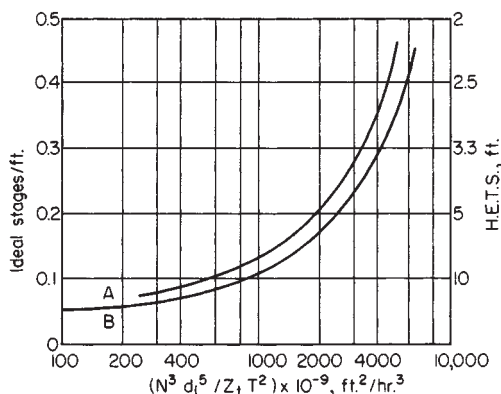


FIG. 15-40 Extraction in RDC columns, water-butylamine-kerosine (continuous). $d_t = 0.33$ and 1.33 ft . Curve A: $V_D = 50.7$, $V_C = 78.9 \text{ ft/h}$. Curve B: $V_D = 25.4$, $V_C = 78.9 \text{ ft/h}$. Use customary units in the variables. [Data of Reman and Olney, *Chem. Eng. Prog.*, **51**, 141 (1955).]

curves. Logsdaile, Thornton, and Pratt (loc. cit.) tentatively suggest that data can be correlated through

$$\frac{H_{IOC}}{V_c} \left(\frac{g^2 \rho_c}{\mu_c} \right)^{1/3} \phi_D = C \left[\frac{\mu_{cg}}{V_K^3 (1 - \phi_D)^3 \rho_c} \right]^{2\beta/3} \left(\frac{\Delta \rho}{\rho_c} \right)^{2(\beta-1)/3} \quad (15-81)$$

the constants C and β to be determined for each system. For toluene-water-acetone, $\beta = 0.13$; for butyl acetate-water-acetone, $\beta = 0.4$; in both cases, transfer was from water to organic solvent. For transfer in the reverse direction, V_K could not be computed (see above).

A large number of studies of axial mixing have been made [Gel'perin et al., *Teor. Osn. Khim. Tekhnol.*, **1**, 666 (1967); Kagan et al., *Zh. Prikl. Khim.*, **39**, 88 (1966); Miyauchi et al., *Am. Inst. Chem. Eng. J.*, **12**, 508 (1966); Stainthorpe and Sudall, *Trans. Inst. Chem. Eng. (London)*, **42**, 198 (1964); Stemerding and Zuideweg, *Chem. Ing. Tech.*, **35**, 844 (1963); and Strand et al., *Am. Inst. Chem. Eng. J.*, **8**, 252 (1962)]. Reman [*Chem. Eng. Prog.*, **62**(9), 56 (1966)] recommends, for the continuous phase in columns 0.08 to 2.13 m (3 in to 7 ft) in diameter,

$$E_c = 0.5Z_i V_c + 0.012d_i N Z_i (d_s/d_i)^2 \quad (15-82)$$

For the dispersed phase firm relationships have not been established, but at high rotor speeds, E_D may be 1 to 3 times E_c . In any event, axial mixing for the liquid flowing at the lower rate becomes very severe for extreme flow ratios (>10).

Costs are given by Clerk (*Chem. Eng.*, 232 (Oct. 12, 1964)).

Several modifications of the design have appeared. Modifications of the rotors include perforation of the disk [Krishnara et al., *Br. Chem. Eng.*, **12**, 719 (1967)] and radially supported arc plates [Nakamura and Hiratsuka, *Kagaku Kogaku*, **30**, 1003 (1966)]. An "asymmetric" modification, with off-center rotors and arrangement of settling spaces for the liquids between dispersions (Misek, loc. cit.) is available in Europe.

As stated above, the design of an RDC contactor usually involves the performance of pilot tests due to the large number of factors which can influence performance. These pilot plant data must then be scaled-up to full commercial size. The following procedure is recommended.

1. Pilot plant tests are conducted using the actual plant materials since small amounts of contaminants can have significant effects on throughput and efficiency. These tests are usually conducted in columns ranging from 0.075–0.15 m diameter; the column height (and therefore number of compartments) should be sufficient to accomplish the separation desired; this may require several iterations on column height.

2. The column is run over a range of total throughputs ($V_o + V_c$) and agitation speeds; at each condition the concentrations of the streams are measured after equilibrium is reached; the holdup is also measured by stopping the agitation, isolating the column, and measuring the change in the interface level. The flooding point is determined at each specific throughput by increasing the agitation speed until the column floods.

3. From the above data, the combination of specific throughput and agitation speed which gives the optimum performance in terms of separation can be determined. At this condition the following relationships can be calculated:

$$\text{Slip Velocity:} \quad V_s = \frac{V_d}{\phi_d} + \frac{V_c}{1 - \phi_d} \quad (15-83)$$

$$\text{Specific Power Input} = \frac{(N_s)^3 (d_r)^5}{(Z_i)(d_i)^2} \quad (15-84)$$

where N_s = rotational speed
 d_r = rotor diameter
 Z_i = stage height
 d_i = tower diameter

Max Continuous Phase Velocity at Flooding

$$V_{cf} = \frac{V_c e^{(-\phi_{df})}}{[V_d/V_c]/\phi_{df}} \quad (15-85)$$

where V_{cf} = velocity of the continuous phase at flooding
 ϕ_{df} = holdup of the dispersed phase at flooding
 V_d = dispersed phase velocity
 V_s = slip velocity

4. For design, the slip velocity is derated to 70–80 percent of the calculated value to give some margin of safety; this sets the design value of the continuous phase velocity (V_c). The column cross-sectional area (and therefore diameter) is set by Q_c/V_c . With the diameter set, the other dimensions can be set using the ratios given above.

5. The rotor speed of the scaled up tower is based on maintaining the same specific power input number as used on the pilot column; it can be determined by substituting the specific values into the relationship:

$$\frac{N_s^3 R_i^5}{Z_i d_i^2}$$

6. For the column height, the pilot plant data must be corrected for the effect of axial mixing. The height of a transfer unit (HTU) can be determined from the pilot plant data; to this must be added the height of a diffusion unit (HDU). This is done by determining the axial mixing coefficients of the continuous and dispersed phases according to the following relationships:

$$E_c = 0.5V_c Z_i + 0.012d_i N Z_i (d_s/d_i)^2 \quad (15-86)$$

$$E_d = E_c \left[\frac{4.2 \times 10^5}{d_i^2} \left(\frac{V_d}{\phi_d} \right)^{3.3} \right] \quad (15-87)$$

where E_c = diffusion coefficient, continuous phase; E_d = diffusion coefficient, dispersed phase; V_c , Z_i , d_r , N_s , Z_i , d_i , ϕ_d = same as defined previously; see Nomenclature list.

From these the continuous and dispersed phase Péclet numbers can be determined from the relationships:

$$\frac{1}{(\text{Pe})_c} = \frac{E_c(1 - \phi_d)}{Z_i V_c} \quad (15-88)$$

$$\frac{1}{(\text{Pe})_d} = \left[\frac{1}{(\text{Pe})_c} \right] \left[\frac{\phi_d V_c}{(1 - \phi_d) V_d} \right] \left[\frac{4.2 \times 10^5}{d_i^2} \left(\frac{V_d}{\phi_d} \right)^{3.3} \right] \quad (15-89)$$

where $(\text{Pe})_c$ = Péclet number, continuous phase
 $(\text{Pe})_d$ = Péclet number, dispersed phase

The HDU is then calculated from the relationship:

$$\text{HDU} = \frac{Z_i}{(\text{Pe})_c} + \frac{Z_i}{(\text{Pe})_d} \quad (15-90)$$

And finally, the effective height of a transfer unit is calculated from:

$$(\text{HTU})_{\text{eff}} = \text{HTU} + \text{HDU} \quad (15-91)$$

where HDU = height of a diffusion unit
 HTU = height of a transfer unit
 $(\text{HTU})_{\text{eff}}$ = effective height of a transfer unit

Lightnin Mixer (Oldshue-Rushton) Tower

GENERAL REFERENCES: Bibaud and Treybal, *Am. Inst. Chem. Eng. J.*, **12**, 472 (1966). Dykstra, Thompson, and Clouse, *Ind. Eng. Chem.*, **50**, 161 (1958). Gustison, Treybal, and Capps, *Chem. Eng. Prog.*, **58**, Symp. Ser. **39**, 8 (1962). Gutoff, *Am. Inst. Chem. Eng. J.*, **11**, 712 (1965). Oldshue and Rushton, *Chem. Eng. Prog.*, **48**, 297 (1952). Miyauchi et al., *Am. Inst. Chem. Eng. J.*, **12**, 508 (1966).

The Oldshue-Rushton (Mixco) extractor is similar in construction to the RDC in the fact that it is a relatively open design, consisting of a series of compartments separated by horizontal stator baffles. The major difference from the RDC is that the height/diameter ratio of the compartments is greater, each compartment is fitted with vertical baffles, and the mixing is accomplished by means of a turbine impeller rather than a disc.

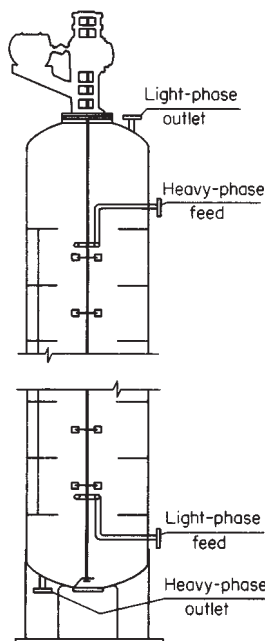


FIG. 15-41 Mixco (Oldshue-Rushton) extractor.

Refer to Fig. 15-41. The extractor is an extension of the simple baffled mixing vessel into a multistage column. Although commercial application has been made, data are scarce and are limited to towers of small diameter. The preferred proportions are $Z_t = 0.5d_t$, $d_s > d_i$.

For water (continuous) and toluene or kerosine (dispersed), in a tower with $d_t = 0.152$ m (0.5 ft), $Z_t = 0.082$ m (0.27 ft), $d_i = 0.051$ m (0.1667 ft), dispersed-phase holdup is given by Eq. (15-70) with $V_s = V_k(1 - \phi_d)$ and the following relationship by Wong (M.Ch.E. thesis, New York University, 1963):

$$V_k \mu_c / \sigma g_c = 1.77(10^{-4})(g/d_i N^2)(\Delta \rho / \rho_c)^{0.9} \quad (15-92)$$

For the same liquids axial mixing is described by (Bibaud and Treybal, loc. cit.)

$$E_c \phi_c / V_c Z_t = -0.1400 + 0.0268(d_i N \phi_c / V_c) \quad (15-93)$$

$$\frac{d_i^2 N}{E_d} = 0.393(10^{-8}) \left(\frac{d_i^3 N^2 \rho_c}{\sigma g_c} \right)^{1.54} \left(\frac{\rho_c}{\Delta \rho} \right)^{4.18} \left(\frac{d_i^2 N \rho_c}{\mu_c} \right)^{0.61} \quad (15-94)$$

See also Miyauchi et al. (loc. cit.), who express the axial mixing in terms of interstage flow. For the continuous phase with no dispersed-phase flow, see Bibaud and Treybal, and Gutoff (loc. cit.).

Figure 15-42 presents some of the data of Oldshue and Rushton (loc. cit.) which show an optimum agitator speed for each configuration studied. The optimum would be expected to vary with physical properties of the liquids contacted. HETS is improved, although capacity is decreased, by smaller openings in the stationary baffles. The effect of stage openings of efficiency and throughput for the system MIBK-acetic acid-water in a 6-inch (150 mm) diameter column is shown in Table 15-9. In the more difficult (because of high interfacial tension) extraction of uranium between kerosine-diluted solvents and aqueous solutions, Dykstra et al. (loc. cit.) have also shown the development of an optimum impeller speed. Gustison et al. (loc. cit.) have found it possible to correlate the stage efficiency with the ratio of flow rates (V_d/V_c) and the distribution coefficient, which varies considerably with concentration in the extraction of uranium. They also found it possible to scale up performance from 0.152- to 0.305-m (6- to 12-in) diameter geometrically, on the assumption that the continuous phase was thoroughly mixed in each compartment, by applying equal power per unit volume of liquids treated on the large and the small

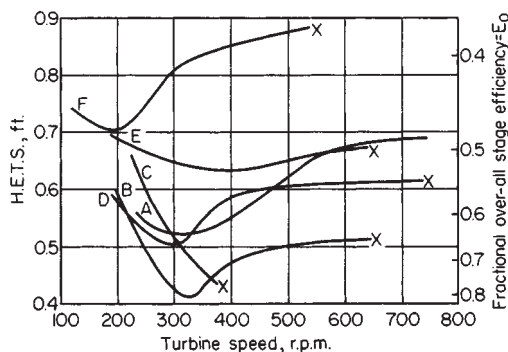


FIG. 15-42 Extraction in Mixco columns, methyl isobutyl ketone-acetic acid-water (continuous). $d_t = 0.5$ ft, $Z_t = 0.333$ ft, $X =$ flooded condition. To convert feet to meters, multiply by 0.3048; to convert feet per hour to meters per hour, multiply by 0.3048.

scale and using the same mass velocities of flow. Bibaud (loc. cit.) found that, for butylamine extracted from kerosine (dispersed) into water, the extraction rates corrected for axial mixing in either phase were described by assuming the drops to be rigid spheres, with Thornton's correlation [*Ind. Chem.*, **39**, 298 (1963)] for drop size.

A somewhat related design has been studied by Nagata, Eguchi, and coworkers [*Chem. Eng. (Japan)*, **17**, 20 (1953); **20**, 2 (1956); *Mem. Fac. Eng., Kyoto Univ.*, **19**, 102 (1957); *Kagaku Kogaku*, **22**, 483 (1958)]. This column is characterized by the relatively small, separate openings between compartments for passage of liquids and the eccentric location of the impeller shaft. In a pilot-plant column, $d_t = 0.3$ m (0.983 ft), phenol was extracted from water [$V_c = 11.6$ m/h (38.1 ft/h)] into benzene [$V_d = 6.4$ m/h (21 ft/h)] at a stage efficiency of 0.618.

Because of the above limitations in prediction of column performance based on correlations, the design of an Oldshue-Rushton must also be based on pilot-plant tests. The minimum column diameter which can be used to give reliable scale-up data is 6 inches (150 mm); it is usually fitted with stages 3 inches (75 mm) high, and the stage opening is 2.4 inches (60 mm). The column should be high enough to accomplish the complete extraction; if it is not it will be necessary to "rerun" the extract and raffinate phases to examine effects in the dilute regions of the column.

The following procedure is followed:

1. The column is run over a range of total throughputs ($V_o + V_c$)

TABLE 15-9 Effect of Size of Opening between Compartments*

Compartment opening, mm	Maximum stage efficiency	Minimum HETS, mm	Flow rate, $\text{kg s}^{-1} \text{m}^{-2}$
Constant flow rate			
0	100	2560	0†
54	83	3098	2.9†
82	52	4953	2.9
152	38	6731	2.9
At maximum efficiency			
0	100	2560	0†
54	83	3098	2.9†
82	67	3860	5.4†
152	38	6731	6.0 ^b

*Typical data for operation with methyl isobutyl ketone, water, acetic acid; four stages; 101.6-mm stage height, 152-mm-diameter column; extraction, water \rightarrow ketone.

†Optimum flow rate.

Oldshue in Lo, Baird, Hanson, *Handbook of Solvent Extraction*, p. 436, John Wiley & Sons, NY, 1983. Used with permission.

and agitation speeds; at each condition the concentrations of the streams are measured after equilibrium has been reached. The flooding point is determined at each throughput by increasing the agitation speed until the column floods.

2. From the above data, the condition of throughput and agitation speed which gives the optimum performance can be determined.

3. Based on this design-specific throughput and the required production column rates, the diameter of the commercial column can be calculated. The stage geometry is next set by maintaining geometric similarity to the pilot column.

4. Finally, the production column agitator speed is determined by maintaining the same power per unit volume as was used on the pilot column.

The above approach will usually result in a conservative design, since the stage efficiency is usually much higher in the production column than in the pilot column. A comparison of the controlling parameters which exist in the pilot and production scales are depicted in Fig. 15-43.

Scheibel Extraction Towers The original Scheibel tower design [Chem. Eng. Prog., 44, 681, 771 (1948); U.S. Patent 2,493,265, 1950] used knitted-mesh packed sections in a tower for coalescence with a centrally located impeller between the packed sections for drop breakup. Scheibel and Karr [Ind. Eng. Chem., 42, 1048 (1950)] presented data on a 0.305-m- (12-in-) diameter column of this design (Fig. 15-44) for systems which are difficult to extract because of high interfacial tension or easy because of low interfacial tension. Excellent values of HETS were obtained with a wide variety of conditions. Low throughput and ratios of flow rates greatly different from unity required high agitator speeds for best results. Both direction of extraction and which phase was dispersed influenced the rates. The liquids of Fig. 15-44 were also used in tests involving the mixing sections alone (see operating characteristics of mechanically agitated vessels). Honekamp and Burkhart [Ind. Eng. Chem. Process Des. Dev., 1, 176 (1962)] found very little change in drop size to occur within the knitted-wire mesh and measured extraction rates in the mesh zone for one system.

A second Scheibel tower design [Am. Inst. Chem. Eng. J., 2, 74 (1956); U.S. Patent 2,850,362, 1958] reduced HETS and permitted more direct scale-up. The impellers are surrounded by stationary

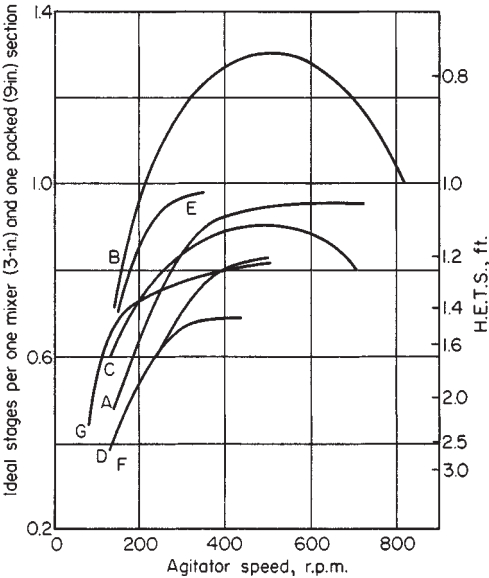
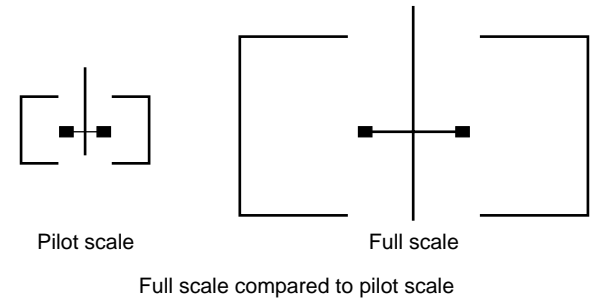


FIG. 15-44 Extraction in first Scheibel column. $T = 0.94$ ft, $d_i = 0.333$ ft, height of mixer section = 3 in, height of packed section = 9 in. To convert inches to centimeters, multiply by 2.54; to convert feet to meters, multiply by 0.3048; and to convert feet per hour to meters per hour, multiply by 0.3048. [Data of Scheibel and Karr; Ind. Eng. Chem., 42, 1048 (1950).]

Curve	System	V_D , ft/h	V_C , ft/h
A	MIBK(C)–water(D,E)–acetic acid	41.7	41.7
B	MIBK(D)–water(C,E)–acetic acid	41.7	41.7
C	MIBK(C)–water(D,E)–acetic acid	23.2	23.2
	MIBK(C,E)–water(D)–acetic acid		
	MIBK(D)–water(C,E)–acetic acid		
D	<i>o</i> -Xylene(D)–water(C,E)–acetone	25.9	17.3
E	<i>o</i> -Xylene(D,E)–water(C)–acetone	22.1	21.2
F	<i>o</i> -Xylene(C)–water(D,E)–acetone	25.9	17.3
G	<i>o</i> -Xylene(C,E)–water(D)–acetone	21.1	22.1

MIBK = methyl isobutyl ketone; C = continuous; D = dispersed; E = extractant.



Residence time	Higher
Blend time, undispersed	Longer
Interstage mixing, undispersed	Different
Interstage mixing, disp.	Different
Concentration gradient, disp.	Higher
Max. impeller zone shear rate	Higher
Ave. impeller zone shear rate	Lower
Ave. tank zone shear rate	Lower
Turbulent shear rates	Different

FIG. 15-43 Mixing factors compared for pilot and full scale. [Oldshue in Lo, Baird, and Hanson, Handbook of Solvent Extraction, John Wiley & Sons, NY, 1983. Used with permission.]

shroud baffles to direct the flow of droplets as they are discharged from the tips of the impellers. Data taken from a 0.305-m- (12-in-) diameter tower are shown in Fig. 15-46 and correlated in terms of the power applied per unit volume of liquids handled per compartment. For the impeller used, the power number at turbulent Reynolds numbers is $N_{Po} = 1.85$. The data show that while packing in alternate sections may increase mass-transfer rates, it decreases flow capacity. For many industrial systems, the knitted mesh was not used because of fouling (Fig. 15-45). Towers up to 3 m (9.8 ft) in diameter are in service. A third design by Scheibel (U.S. Patent 3,389,970, 1968) uses closed impellers plus horizontal baffles in the tower.

Scheibel (Ref. 2) has shown that the efficiency of a mixing stage can be correlated to the power per unit of throughput, and is related to the ratio of dispersed/continuous phase flow rates; this is shown in Fig. 15-47.

This figure shows an optimum power input; below this value efficiency drops off due to reduced interfacial area; above this value efficiency decreases due to increased axial mixing of the continuous and dispersed phases.

Scheibel has found that the power input can be correlated by the following equation:

$$P = 1.85 \left[\frac{(d_i)^5 \rho (N_s)^3}{g_c} \right] \tag{15-95}$$

where P = Power input per mixing stage

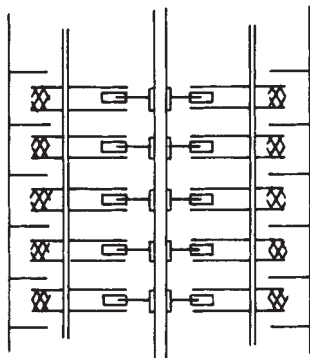


FIG. 15-45 Second Scheibel extractor with horizontal baffles and no wire-mesh packing between stages. [Reprinted with permission of Am. Inst. Chem. Eng. J., 2, 74 (1956).]

d_i = impeller diameter
 ρ = average stage density
 N_i = impeller rotational speed
 g_c = gravitational constant

As with the design of the other columns described above, the design of a Scheibel column must be based on pilot plant tests and scale-up. The following procedure is recommended:

1. Pilot tests are usually conducted in 0.075-m diameter columns; the column should contain a sufficient number of stages to complete the extraction; this may require several iterations on column height.
2. The column is run over a range of throughputs ($V_d + V_c$) and agitation speeds; at each condition the concentrations of the streams

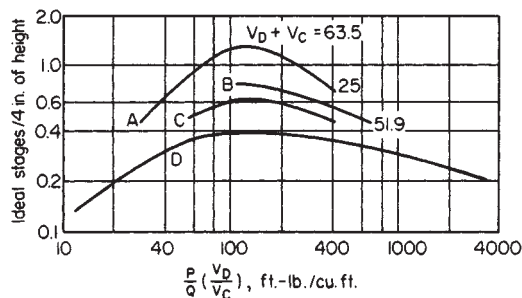


FIG. 15-46 Extraction in second Scheibel column. $T = 0.94$ ft, $d_i = 0.333$ ft, height of packed section = height of mixer section = 2 in. Use customary units in the variables. [Data of Scheibel, Am. Inst. Chem. Eng. J., 2, 74 (1956).]

Curve	System
A, B*	Methyl isobutyl ketone-water-acetic acid
C*	<i>o</i> -Xylene-water-acetic acid
D†	<i>o</i> -Xylene-water-phenol
	Methyl isobutyl ketone-water-acetic acid
	<i>o</i> -Xylene-water-acetic acid

*Alternate mixing and packed sections.

†Packing omitted. Agitators in alternate and also every section.

are measured after equilibrium is reached (usually 3–5 turnovers of column volume). At each throughput the flood point is determined by increasing the agitation until flooding is induced. A minimum of three throughput ranges are examined in this manner.

3. From the above data, the combination of specific throughput and agitation speed which gives the optimum performance in terms of separation can be determined. This determines the design specific

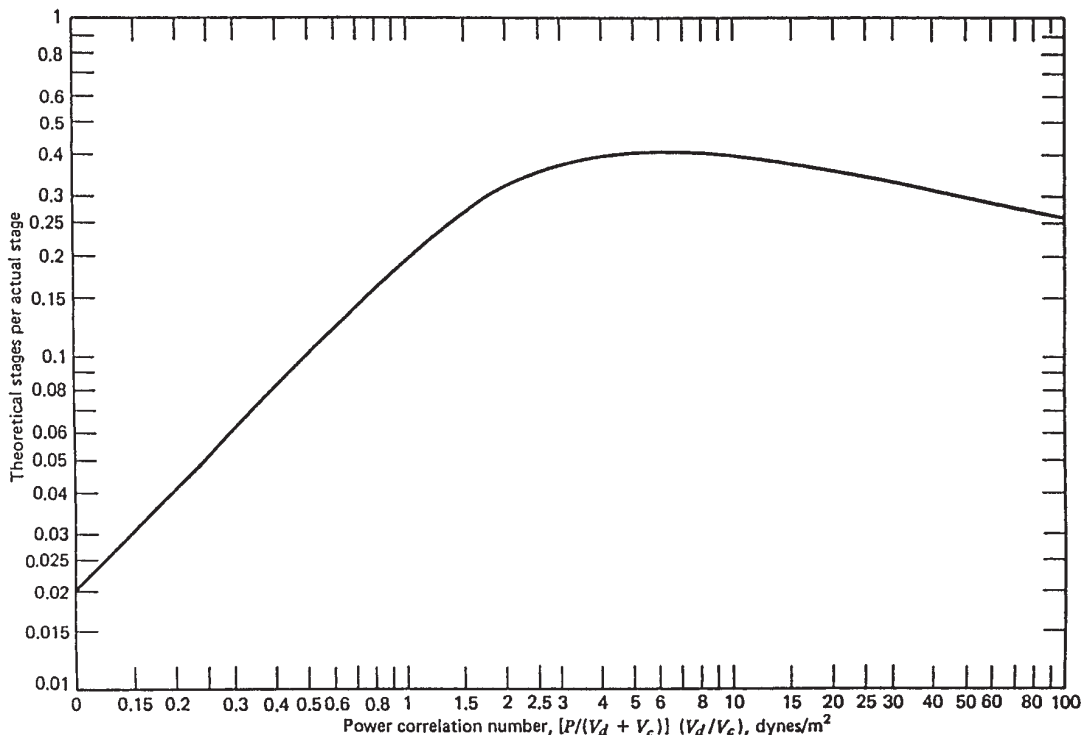


FIG. 15-47 Correlation of mixing-stage efficiency with power input and liquid flow rates. [Scheibel in Lo, Baird, Hanson, Handbook of Solvent Extraction, p. 428 John Wiley & Sons, NY, 1963. Used with permission.]

throughput value ($\text{m}^3/\text{m}^2\text{-h}$) and agitation speed (RPM).

4. Unlike the RDC and Oldshue-Rushton columns where the specific throughput of the scaled-up version is the same as the pilot column, it is the characteristic of the Scheibel column that the throughput of the scaled-up column is on the order of 3–5 times greater than that achieved on the pilot column. The reason for this is that the restricted geometry of the 0.075 m diameter column limits throughput; these restrictions are removed in the scaled-up columns.

5. Once the column diameter is determined, the stage geometry can be fixed. The geometry of a stage is a complex function of the column diameter; in the pilot (0.075 m) column the stage height to diameter ratio is on the order of 1.3; on a 3-m diameter column it is on the order of 1.8.

6. The principle of the Scheibel Column scale-up is to maintain the efficiency of the stage. Therefore, the scaled-up column will have the same number of actual stages as the pilot column. The only difference is that the stages will be taller to take into account the effect of axial mixing. With the agitator dimensions determined, the speed is then calculated to give the same power input per unit of throughput.

The scale-up of the Scheibel column is still considered proprietary, and therefore the vendor (Glitsch Process Systems Inc.) should be consulted for the final design. From pilot tests in 0.075-m diameter column, industrial columns up to 3 m in diameter and containing 90 actual stages have been provided.

Because of its internal baffling which controls the mixing patterns on the stages, the Scheibel column has proven to be one of the more efficient extractors in terms of height of a theoretical stage; this makes it ideally suited for applications which require a large number of stages, or are located indoors with headroom restrictions. Holmes, Karr, and Cusack (*Solvent Extraction and Ion Exchange*, vol. 8, no. 3, pp. 515–528, 1990) have published results comparing the efficiency of the Scheibel column to other extractors on the system toluene-acetone-water.

Kühni Tower The extraction towers designed at Kühni [see Mögli and Bühlmann, in Lo, Baird, and Hanson (eds.), *Handbook of Solvent Extraction*, Wiley-Interscience, New York, 1983, sec. 13.5]

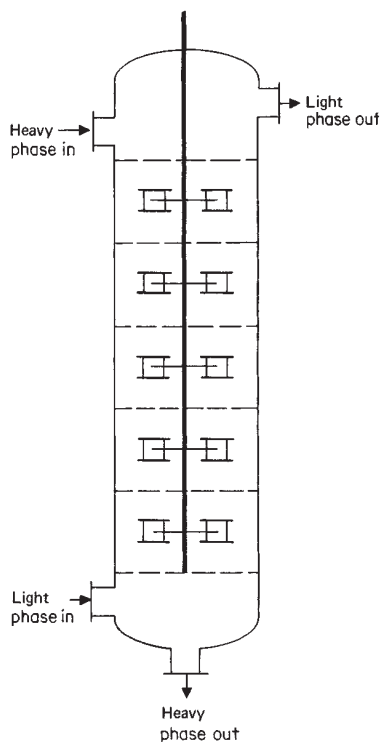


FIG. 15-48 Kühni tower.

use shrouded (closed) impellers on a central shaft in the tower (Fig. 15-48). The droplet size can be controlled by the speed and diameter of the impeller, while the circulation rate can be controlled by the design of the width of the impeller. A perforated plate between each stage can control the droplet holdup by the percentage of open area in the plate.

Treybal Tower Treybal [U.S. Patent 3,325,255, 1967]; *Chem. Eng. Prog.*, 60(5), 77 (1964)] adapted a mixer-settler cascade in tower form in which the liquids are settled between stages.

Karr Reciprocating Plate Tower Up to this point, the agitated columns presented have all imparted their energy to the fluids by means of rotating elements (discs or impellers). However, there is another class of agitated columns which impart their energy by means of reciprocating plates or pulsing of the liquids. This results in a more uniform drop-size distribution due to the fact that the shear forces are more uniform over the entire cross section of the column.

The reciprocating plate extractor developed by Karr [*Am. Inst. Chem. Eng. J.*, 5, 446 (1959)] is a mechanically agitated tower using dual-flow plates with 50 to 60 percent open area, mounted on a central shaft and reciprocated vertically (Fig. 15-49). Typical perforated plates and baffle plates for a 35 $\frac{3}{4}$ -in (0.9-m) diameter column are shown in Fig. 15-50. A typical stroke length is 2.54 cm (1 in) with a speed of 10 to 400 strokes per minute and a plate spacing of 5 to 15 cm (2 to 6 in). Scale-up relationships by Karr (*Sep. Sci. Technol.*, 15(4), 877 (1980)) show that HETS increases with tower diameter to the 0.38 power in the most difficult case. Laboratory columns of 2.54- and 5.08-cm- (1- and 2-in-) diameter are used to scale up to towers as large as 1.5 to 2.0-m (5 to 6.5-ft) in diameter. A high volumetric efficiency is

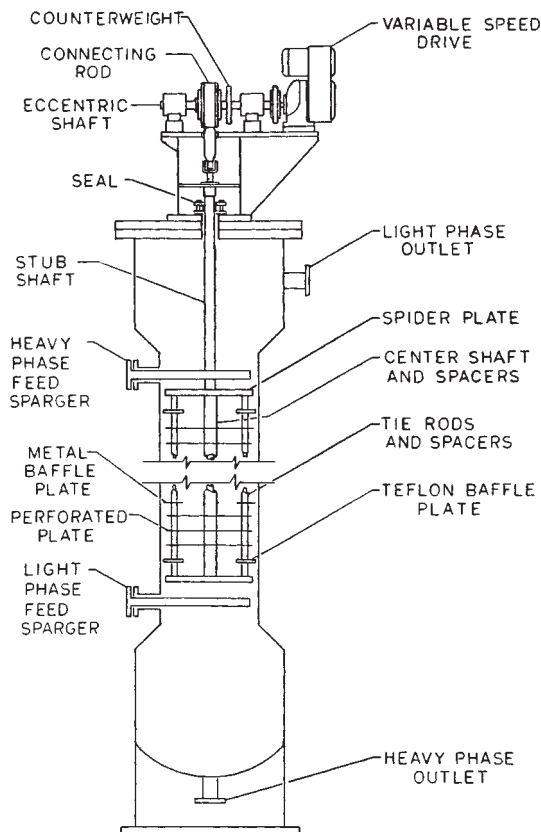


FIG. 15-49 Schematic arrangement of the 900-mm (36-in) reciprocating-plate column. (Courtesy of Glitsch Process Systems Inc.)

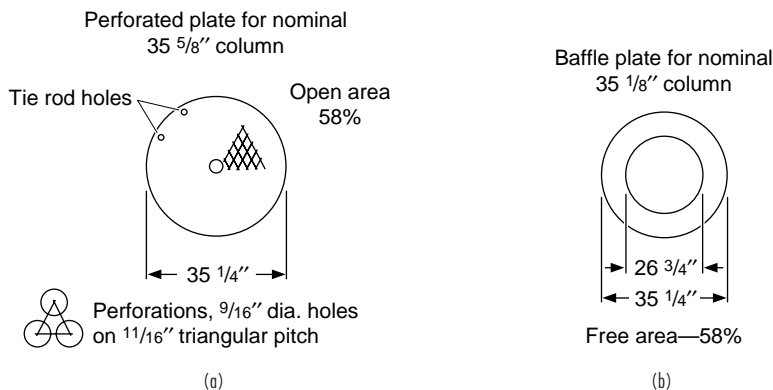


FIG. 15-50 (a) Typical perforated plate. (b) Typical baffle plate.

achieved as measured by total volumetric throughput per cross-sectional area divided by HETS.

One of the chief characteristics of the Karr column is its high-volumetric efficiency when compared to other extractors. Volumetric efficiency is defined as:

$$\text{Volumetric efficiency} = \frac{V_d + V_c}{\text{HETS}} \quad (15-96)$$

Karr, Holmes, and Cusack have given comparisons of the Karr column volumetric efficiency with other types of extractors. In Table 15-10 are data showing the values of HETS and volumetric efficiency over a range of column diameters from 1–36 in (0.025–0.9 m); Fig. 15-51

shows how the HETS varies with agitation, again over a range of diameters but at relatively constant total throughput. It was from these data that Karr and Lo developed the scale-up procedure for this type of column.

As with the other extractors, the final design of a Karr column depends on the scale-up from a pilot test. The following procedure is recommended.

1. For scale-up up to 2 m in diameter, testing in a pilot column of 0.025 m is sufficient; if the anticipated scaled-up diameter is greater than 2 m, then the pilot tests should be conducted in a 0.050-m diameter. The column should be tall enough to accomplish the complete extraction; this may require several iterations on column height.

TABLE 15-10 Summary of Minimum HETS Values and Volumetric Efficiencies for a Reciprocating-Plate Column*

Column diameter in.	Amplitude, in.	Plate spacing, in.	Agitator speed, strokes/min	Extractant	Dispersed phase	Minimum HETS	Throughput, gal hr ⁻¹ ft ⁻²	Volumetric efficiencies V _d /HETS, h ⁻¹
<i>MIBK-acetic acid-water system</i>								
1	1/2	1	360	MIBK	Water	3.1	572	296
			401			2.8	913	523
1	1/2	1	278	Water	MIBK	4.2	459	175
			152			8.1	1030	204
3	1/2	1	330	MIBK	Water	4.9	600	196
	1/2	1	245			6.3	1193	304
	1/2	2	355			7.5	1837	393
	1/2	1	320	Water	Water	4.3	548	205
	1/2	1	230			6.7	1168	280
	1/2	2	367	Water	Water	5.0	1172	376
			240			7.75	1707	353
12 (with baffle)	1/2	1	430	Water	MIBK	5.8	547	151
			285			5.7	1167	328
	1/2	1	244	MIBK	MIBK	4.4	599	218
			170			5.6	1193	342
	1/2	1	250	MIBK	Water	7.2	602	134
			225			7.2	1200	268
			150			14.0	1821	208
	1/2	1	225	Water	Water	7.0	555	127
			200			9.5	1170	197
			150			11.05	1694	246
	1/2	1	275	Water	MIBK	9.5	1179	199
	1/2	1	200	MIBK	MIBK	7.8	595	123
			150			6.2	1202	311
<i>Xylene-acetic acid-water system</i>								
3	1	1	267	Water	Water	9.1	424	75
3	1/2	1	537	Water	Water	8.2	424	83
3	1/4	1	995	Water	Water	7.7	424	88
3	1	2	340	Water	Water	9.1	804	142
36	1	1	168	Water	Water	23.3	425	29†
36	1	1	168	Xylene	Water	20.0	442	36†

*Lo, Baird, Hanson, *Handbook of Solvent Extraction*, John Wiley & Sons, NY, p. 37, 1983.

†Because of instrumentation limits, the maximum volumetric efficiencies have not been explored. Used with permission.

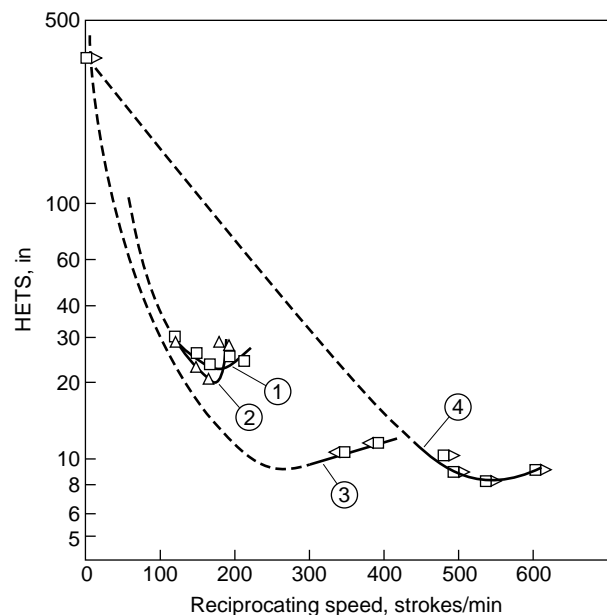


FIG. 15-51 Effect of reciprocating speed on HETS, *o*-xylene-acetic acid-water system. (Lo and Prochaska in Lo et al., p. 377.)

Curve No.	Column diam, in	Phase dispersed	Phase extractant	Double amplitude, in	Plate spacing, in	Total throughput gal/(h)(ft ²)
1	36	Water	Water	1	1	425
2	36	Water	Xylene	1	1	442
3	3	Water	Water	1	1	424
4	3	Water	Water	1/2	1	424

Predicted minimum based on exponents of 0.36 in Eq. (15-98) and 0.14 in Eq. (15-99).

2. The column is first optimized with regard to plate spacing; what is desired is for the tendency to flood to be equal over the entire column length. If one particular section appears to be limiting the throughput, then the plate spacing should be increased in this area; this will decrease the power input into that section. Likewise, in sections which appear to be undermixed, plate spacing should be decreased. It has been found that the following correlation can be used to estimate the relative plate spacing in the column:

$$l \propto \frac{1}{(\Delta\rho)^{5/3}(\sigma)^{3/2}} \quad (15-97)$$

where l = relative plate spacing
 $\Delta\rho$ = density difference of the two phases
 σ = interfacial tension

3. Once the plate spacing is optimized, the column is run over a range of total throughputs ($V_d + V_c$) and agitation speeds. There should be a minimum of three throughput levels, and at each throughput three agitation speeds. After equilibrium is attained at each condition (usually 3–5 turnovers of column volume), samples are taken and separation measured. At each condition the flood point is also determined. It is a characteristic of the Karr column that on the small diameters, the optimum efficiency usually occurs just before the flood point.

4. From these data, plots are made of volumetric efficiency and agitation speed at each throughput level; from these plots the condition which gives the maximum volumetric efficiency is selected for scale-up.

5. The following parameters are kept constant on the scale-up: total throughput per unit area, plate spacing, and stroke length. The

height and agitation speed of the scaled-up column is then calculated from the following relationships:

$$Z_2/Z_1 = (d_{i2}/d_{i1})^{0.38} \quad (15-98)$$

$$(SPM_2/SPM_1) = (d_{i1}/d_{i2})^{0.14} \quad (15-99)$$

where Z_1 = plate stack height in pilot column
 Z_2 = plate stack height in scaled-up column
 d_{i1} = diameter of pilot column
 d_{i2} = diameter of scaled up column
 SPM_1 = reciprocating speed of pilot column
 SPM_2 = reciprocating speed of scaled-up column

6. For the scaled-up column, suitable baffle plates are required to control axial mixing. For the final column layout the equipment vendor (Glitsch Process Systems Inc.) should be consulted.

The Karr process is particularly well suited for systems which tend to emulsify since its uniform shear characteristics tend to minimize emulsion formation. It is also particularly well suited for corrosive systems (since the plates can be constructed of non-metals) or for systems containing significant solids (due to its large open area and hole size on the plates). Slurries containing up to 30 percent solids have been successfully processed in Karr columns.

Pulsed Columns These are extractors in which a rapid reciprocating motion of relatively short amplitude is applied to the liquid contents. The agitation so produced has been found to give improved rates of extraction. The principle originated with van Dijk (U.S. Patent 2,011,186, 1935). Because agitation was necessary to reduce tower heights and consequently the expense of massive shielding, and because pulsing provided a means of agitation not requiring moving parts, bearings, and the like in contact with highly corrosive, dangerously radioactive liquids, pulsed columns have been freely applied in the extraction and separation of metals from solutions of atomic energy operations. With very few exceptions, applications appear thus far to be limited to this area. There are two major types of columns: (1) ordinary (spray, packed, etc.) extractors on which pulsations are imposed and (2) a special sieve-plate design. Their characteristics are quite different.

Pulsing Devices Refer to Fig. 15-52. At *a*, a reciprocating plunger or piston pump from which the check valves have been removed is connected to the space containing continuous phase, as shown. This arrangement suffers the disadvantages that (1) the corrosive liquid may be in direct contact with the piston and (2) too rapid pulsing, especially with volatile organic liquids, may cause cavitation. The pipe connecting column and pulser may be of any length to pass through shielding, barriers, and the like, but high pressure drop in the transfer pipe contributes to cavitation difficulties. An alternative arrangement using an air pulse is shown at *b* in the figure [Thornton, *Chem. Eng. Prog.*, **50**, *Symp. Ser.* 13, 39 (1954); U.S. Patent 2,818,324, 1957]. This keeps corrosive liquids out of contact with the pulsing device and obviates the cavitation problem but because of the compressibility of the gas requires greater application of pulsing power for the same results. For design, see Week and Knight [*Ind. Eng. Chem. Process Des. Dev.*, **6**, 480 (1967); **7**, 156 (1968)]. For pulsing at the natural frequency of the column, Baird [*Proc. Am. Inst. Chem. Eng.-Inst. Chem. Eng. Joint Meeting*, London, **1956**(6), 53] connected the liquid space to a volume of gas which acts as a spring. Flexible bellows or diaphragms of reinforced rubber, plastic, or metal in contact with the liquids may be flexed mechanically or by an electromagnetic transducer (Thornton, loc. cit.). If hydraulically activated, these may have a life of up to 30,000,000 cycles or more [Jealous and Johnson, *Ind. Eng. Chem.*, **47**, 1159 (1955)]. With suitable cam mechanisms, pulsations whose amplitude-time characteristics appear as sine, square, or sawtooth wave shapes are possible.

Pressure at the pulsing device and the conditions for cavitation and "water hammer" may be estimated by the methods of Williams and Little [*Trans. Inst. Chem. Eng. (London)*, **32**, 174 (1954)] provided the pressure-drop characteristics of the tower internals are known. Jealous and Johnson (loc. cit) have had good success in computing the power required for pulsing. Since power requirement alternates, the use of a flywheel on the pulse mechanism to act as an energy reservoir is suggested as a means of reducing power requirements. Alterna-

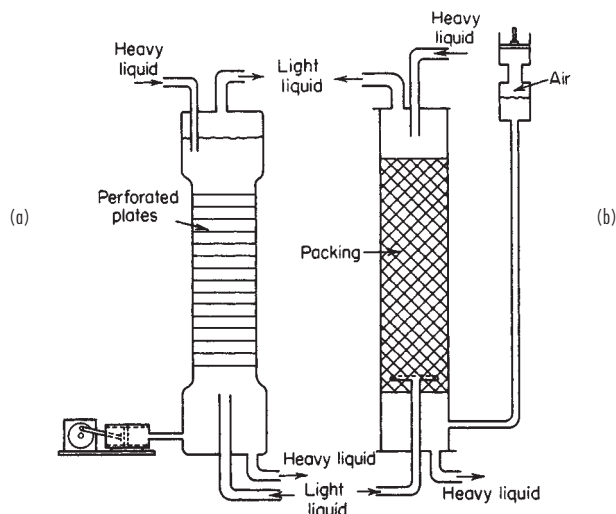


FIG. 15-52 Pulsed columns: (a) Perforated-plate column with pump pulse generator. (b) Packed column with air pulser.

tively, two columns could be pulsed 180° out of phase with one pulse generator (Griffith, Jasney, and Tupper, U.S. AEC AEC-3440, 1952). Irvine (U.S. AEC ORNL-2377, 1957) devised a pulse pump to utilize part of the pulse energy. Concatenated columns (long extractors built as several short columns, with liquids led from one to the other in strictly countercurrent fashion) may be pulsed by a single pulse generator to advantage, since less power is required owing to reduced static head [Jealous and Lieberman, *Chem. Eng. Prog.*, **52**, 366 (1956)].

The following terms are generally used to describe the pulse action: **Frequency** is the rate of application of the pulse action, cycles/time. **Amplitude** is the linear distance between extreme positions of the liquid in the column (not of the pulser) produced by pulsing. **Pulsed volume** = amplitude \times frequency \times column crosssectional area = volumetric rate of movement of liquid, expressed as volume/time or volume/(time-area).

Pulsed Spray Columns Billerbeck et al. [*Ind. Eng. Chem.*, **48**, 183 (1956)] applied pulsing to a laboratory [3.8-cm- (1.5-in-) diameter] column. At pulse amplitude 1.11 cm ($\frac{7}{16}$ in), rates of mass transfer improved slightly with increased frequency up to 400 cycles/min, but the effect was relatively small. Shirotuka [*Kagaku Kogaku*, **22**, 687 (1958)] provides additional data. There is not believed to be commercial application.

Pulsed Packed Columns Any of the ordinary packings may be used, although random packings tend to orient on pulsing, which may lead to channeling. For this reason, Thornton [*Chem. Eng. Prog.*, **50**, *Symp. Ser. 13*, 39 (1954); *Br. Chem. Eng.*, **3**, 247 (1958)] recommends fixed packing made from plates of corrugated expanded metal. Polyethylene packing, not wet by aqueous solutions, provides higher flow capacities and mass-transfer rates than ceramic (wetted) packing [Jackson, Holman, and Grove, *Am. Inst. Chem. Eng. J.*, **8**, 659 (1952)]. Pulsing reduces the size of dispersed-phase droplets, increases holdup, and increases interfacial area for mass transfer. There is a greater tendency toward emulsification, and maximum throughput is decreased, but HETS is reduced considerably, by the pulsing. Pulsing can be applied on existing nonpulsed packed towers to good mass-transfer advantage, provided limiting flow rates are not exceeded.

Figure 15-53 is perhaps typical of the results obtainable, although no generalizations have been devised for estimating the mass-transfer rates in the absence of experiment. For additional data, see Crico [*Genie Chim.*, **73**, 57 (1955)], Feich and Anderson [*Ind. Eng. Chem.*, **44**, 404 (1952)], Karpacheva et al. [*Khim. Masinostr.*, **1959**(3), 6; **1960**(2), 13; *Khim. Prom.*, **1960**, 469], Honda et al. [*Kagaku Kikai*, **21**, 645 (1957); *Kagaku Kogaku*, **22**, 97 (1958)], Oyama and Yam-

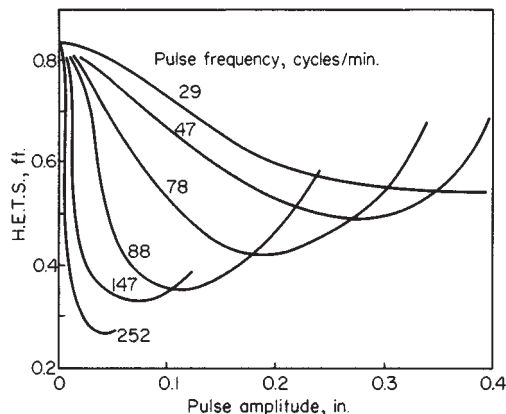


FIG. 15-53 Effect of pulsing on extraction in a packed column: methyl isobutyl ketone-acetic acid-water (continuous). Tower diameter = 1.58 in., 27-in depth of $\frac{1}{4}$ -in Raschig rings. $V_D = V_C = 7.5$ to 10. To convert inches to centimeters, multiply by 2.54. [Data of Chantry, von Berg, and Wiegandt, *Ind. Eng. Chem.*, **47**, 1153 (1955), with permission.]

aguchi [*Kagaku Kogaku*, **22**, 668 (1958)], Potnis et al. [*Ind. Eng. Chem.*, **51**, 645 (1959)], Widmer [*Chem. Ing. Tech.*, **39**, 900 (1967)]; Worall and Thwaites [*Br. Chem. Eng.*, **10**, 158 (1965)], Ziolkowski and Naumowicz [*Chem. Stosow.*, **2**, 457 (1958); **3**, 475 (1959); **5**, 363 (1961)].

A small perforated-plate column of conventional design was pulsed by Goldberger and Benenati [*Ind. Eng. Chem.*, **51**, 641 (1959)] with marked improvement in mass-transfer rates.

Pulsed Sieve-Plate Columns The standard arrangement (see Fig. 15-52a) consists of a tower fitted with horizontal sieve plates which occupy the entire cross section of the columns. There are no down spouts as in ordinary sieve-plate columns. Typical arrangements use 0.32-cm- ($\frac{1}{8}$ -in-) diameter perforations sufficient to provide 20 to 25 percent free space, with 5.08-cm (2-in) plate spacing, pulse amplitudes in the range 0.64 to 2.5 cm (0.25 to 1 in), and frequencies of 100 to 250 cycles/min, although the pulse characteristics will depend upon the system and flow rates under consideration. Plates are usually of metal, but Sobotik and Himmelblau [*Am. Inst. Chem. Eng. J.*, **6**, 619 (1960)] indicate that for certain services plates which are not wet by water (polyethylene) may be advantageous.

Sege and Woodfield [*Chem. Eng. Prog.*, **50**, *Symp. Ser. 13*, 179 (1954)] provide a good description of the operational characteristics. Refer to Fig. 15-54. Since in many cases the perforations are too small to permit flow owing to interfacial tension of the liquids, the total pulsed volume must ordinarily approximate the volumetric rate of flow of the liquids [Edwards and Beyer, *Am. Inst. Chem. Eng. J.*, **2**, 148 (1956), show that slightly higher rates than $V_d + V_c =$ pulsed volume may be obtained]. In region 1 of the figure, the column is flooded because of insufficient pulsed volume. In region 2, discrete layers of liquid appear between plates during the quiet portion of the pulse cycle. During upward pulsing, the light liquid is forced through the

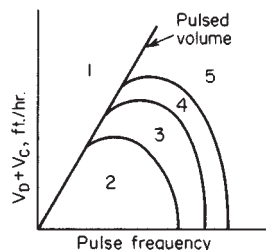


FIG. 15-54 Pulsed column characteristics. [Sege and Woodfield, *Chem. Eng. Prog.*, **50**, *Symp. Ser. 13*, 179 (1954).]

perforations and forms drops which rise to the plate above. During downward pulsing, the heavy liquid behaves similarly. Flow is stable, but mass-transfer rates are generally poor. In region 3 there is little change in phase dispersion throughout the pulse cycle, and a fairly uniform dispersion of small droplets persists throughout. This region provides the best mass-transfer rates. Region 4 is characterized by irregular coalescence into fairly large drops, and periodic reversal of the continuous phase (local flooding). Extraction rates are generally poor. Further increase in frequency results in flooding owing to emulsification, region 5. Transition between regions is gradual and continuous, not abrupt. Excellent photographs of these phenomena are provided by Defives, Durandet, and Gladel [*Rev. Inst. Fr. Pet. Ann. Combust. Liq.*, **11**, 231 (1956)].

The literature is unusually large. In view of the fact that application of these extractors is almost entirely confined to processes related to atomic energy, only a brief listing of sources of data is presented here.

Dispersed-phase holdup and flooding. Groenier, McAllister, and Ryon [U.S. AEC ORNL-3890, 1966; *Chem. Eng. Sci.*, **22**, 931 (1967)]; Babb et al. [*Ind. Eng. Chem.*, **51**, 1005 (1959); *Ind. Eng. Chem. Process Des. Dev.*, **2**, 38 (1963)]; Gelfer et al. [*Khim. Prom.*, **42**, 607 (1966)]; Thornton and Logsdail [*Trans. Inst. Chem. Eng. (London)*, **35**, 316, 331 (1957)].

Longitudinal mixing. Babb et al. [*Ind. Eng. Chem.*, **51**, 1011 (1959); *Ind. Eng. Chem. Process Des. Dev.*, **3**, 210 (1964)]; Burger and Swift (U.S. AEC HW-29010, 1953); Miyauchi et al. [*Am. Inst. Chem. Eng. J.*, **11**, 395 (1965); *Kagaku Kagaku*, **30**, 895 (1966)]; Otake and Komazawa [*ibid.*, **32**(6), 19 (1968)].

Mass-transfer rates. Correlations are offered by Smoot, Mar, and Babb [*Ind. Eng. Chem.*, **51**, 1005 (1959); *Ind. Eng. Chem. Fundam.*, **1**, 93 (1962)] and Zwolkowski and Kubica [*Chem. Stosow., Ser. B2*, 392 (1965)].

Controlled Cycling The compartmented character of sieve-plate columns described above lends itself particularly well to this technique, which is, however, not confined to these devices [Cannon, *Oil Gas J.*, **51**, 268 (1952); **55**, 68 (1956); Szabo et al., *Chem. Eng. Prog.*, **60**(1), 66 (1964); Belter and Speaker, *Ind. Eng. Chem. Process Des. Dev.*, **6**, 36 (1967); Horn, *ibid.*, **6**, 30 (1967); Robinson and Engel, *Ind. Eng. Chem.*, **59**(3), 22 (1967); and Löfstrand, *Ind. Eng. Chem. Process Des. Dev.*, **7**, 65 (1968)]. A cycle is completed by the following sequence of events: (1) a light-phase flow period, during which the heavy phase does not flow; (2) a coalescing period, during which neither phase flows; (3) a heavy-phase flow period, during which the light phase does not flow; and (4) a repeat of the coalescing period. The net result can be an increased flow capacity (in the case of sieve-plate pulsed columns) and stage efficiency, such that the effect of 2N stages may be obtained with a column of N stages, provided the total holdup of each phase is displaced during each cycle.

Centrifugal Extractors The force of gravity for counterflow of liquids of different density may be replaced and in effect increased (many thousandfold if desired) by centrifugal machines. These then become especially useful for handling liquids of low density difference and those with tendencies to form emulsions.

Podbielniak Extractor (Podbielniak, U.S. Patent 2,044,996, 1935, and other patents) This is the most important of the group. Refer to Fig. 15-55. Rotation is about a horizontal shaft. The body of the extractor is a cylindrical drum containing concentric perforate cylinders. The liquids are introduced through the rotating shaft with the help of special mechanical seals; the light liquid is led internally to the drum periphery and the heavy liquid to the axis of the drum. Rapid rotation (up to several thousand revolutions per minute,

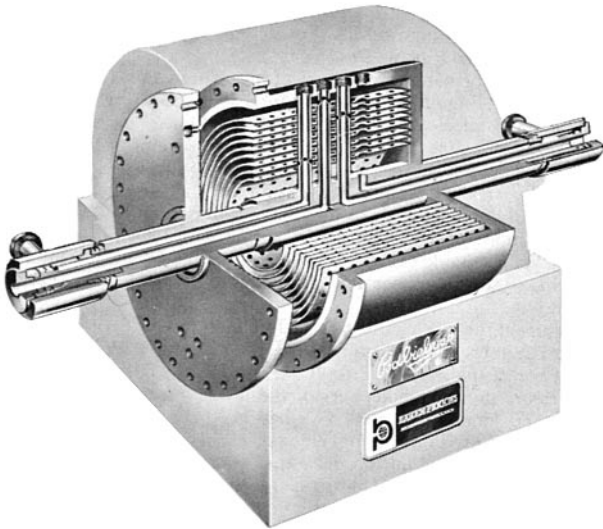


FIG. 15-55 Podbielniak centrifugal extractor. (Courtesy of Baker Perkins Inc.)

depending on size) causes radial counterflow of the liquids, which are then led out through the shaft. Materials of construction include steel, stainless steel, Hastelloy, and other corrosion-resistant alloys. The machines are particularly characterized by extremely low holdup of liquid per stage, and this led to their extensive use in the extraction of antibiotics, such as penicillin and the like, for which multistage extraction and phase separation must be done rapidly to avoid chemical destruction of the product under conditions of extraction. They have been used extensively in all phases of pharmaceutical manufacture and are increasingly being used in other fields: petroleum processing, both solvent refining and acid treating, dephenolization of wastewaters, extraction of uranium from ore leach liquors, as well as for clarification and phase-separation work. See Kaiser, *Sewage Ind. Wastes*, **27**, 311 (1955); Podbielniak, Gavin, and Kaiser, *J. Am. Oil Chem. Soc.*, **36**, 238 (1959); Doyle and Rauch, *Pet. Eng.*, **27**(5), C-49 (1955); Anderson and Lau, *Chem. Eng. Prog.*, **51**, 507 (1955); Todd and Podbielniak, *ibid.*, **61**(5), 69 (1965); and Todd, *ibid.*, **62**(8), 119 (1966). The last contains data on interstage back mixing. Table 15-11 lists some of the characteristics of the machines.

With a laboratory model [0.55 m (18 in) in diameter, 5.08 cm (2 in) wide, 18 concentric cylinders slotted at 180° intervals], Barson and Beyer [*Chem. Eng. Prog.*, **49**, 243 (1953)] obtained from two to eight ideal stages with isoamyl alcohol-boric acid-water at 5000 r/min. The number of stages increased with ratio of light-to-heavy-liquid flow but with varying position of the interface and consequently varying fraction of the machine devoted to light-liquid-dispersed. At constant flow rate, the number of stages was essentially independent of rotational speed. Jacobson and Beyer [*Am. Inst. Chem. Eng. J.*, **2**, 283 (1956)] obtained about the same results. Alexandre and Gentilini [*Rev. Inst. Fr. Pet. Ann. Combust. Liq.*, **11**, 389 (1956)] similarly obtained five

TABLE 15-11 Podbielniak Centrifugal Extractors*

Model number	Over-all dimensions, in.				Horsepower		Flow capacity, gal./min.	
	Width	Height	Length (incl. drive)	Total wt., lb.	Connected	Continuous	Multistage extraction	Neutralization, acid treating, extraction of fermentation broths
A-1	16	12	30	150	3.0	2.5	1.0	0.5
B-10	55.5	33	67.5	2,700	7.5	6.7	30	30
D-18	76	45	85	8,600	15	10	150	75
D-36	94	45	85	10,250	25	15	300	150
E-48	113	59	107	21,500	40	22	500	300

*Courtesy Baker Perkins Inc. To convert inches to centimeters, multiply by 2.54; to convert pounds to kilograms, multiply by 0.454; to convert horsepower to kilowatts, multiply by 0.746; and to convert gallons per minute to cubic meters per hour, multiply by 0.227.

ideal stages with benzene–acetic acid–water, and 3.4 to 12.5 ideal stages with methyl isobutyl ketone–acetic acid–water. Anderson and Lau [*Chem. Eng. Prog.*, **51**, 507 (1955)] describe a model handling 10 to 15 percent suspended solids in the liquids, and report a fraction to two ideal stages when extracting penicillin and chloromycetin, 7.04 to 8.71 m³/h (1860 to 2300 gal/h) total flow rate.

Quadronics (Liquid Dynamics) Extractor (Doyle et al., U.S. Patent 3,114,707, 1963, and others; paper at AIChE meeting, St. Louis, February 1968) This is a horizontally rotated device, a variant of the Podbielniak extractor, in which either fixed or adjustable orifices may be inserted as a package radially. These permit control of the mixing intensity as the liquids pass radially through the extractor. Flow capacities, depending on machine size, range from 0.34 to 340 m³/h (1.5 to 1500 gal/min).

Luvesta (Centriwesta) Extractor This is a development from

Coutor (U.S. Patent 2,036,924, 1936). See also Eisenlohr [*Ind. Chem.*, **27**, 271 (1951); *Chem. Ing. Tech.*, **23**, 12 (1951); *Pharm. Ind.*, **17**, 207 (1955); *Trans. Indian Inst. Chem. Eng.*, **3**, 7 (1949–1950)] and Husain et al. [*Chim. Ind. (Milan)*, **82**, 435 (1959)]. This centrifuge revolves about a vertical axis and contains three actual stages. It operates at 3800 r/min and handles approximately 4.92 m³/h (1300 gal/h) total liquid flow at 12-kW power requirement. Provision is made in the machine for the accumulation of solids separated from the liquids, for periodic removal. It is used, more extensively in Europe than in the United States, for the extraction of acetic acid, pharmaceuticals, and similar products.

De Laval Extractor (Palmqvist and Beskow, U.S. Patent 3,108,953, 1959) This machine contains a number of perforated cylinders revolving about a vertical shaft. The liquids follow a spiral path about 25 m (82 ft) long, in countercurrent fashion radially, and mix when passing through the perforations. There are no published performance data.